

DISSERTATION

Modelling of the fast fluidized combustion reactor of a dual fluidized bed biomass gasification system

Ausgeführt zum Zwecke der Erlangung des akademischen Grades eines
Doktors der technischen Wissenschaften unter der Leitung von

Univ.-Prof. Dipl.-Ing. Dr. Hermann Hofbauer

E 166

Institut für Verfahrenstechnik, Umwelttechnik und
Technische Biowissenschaften

eingereicht an der Technischen Universität Wien
Fakultät für Technische Chemie

von

Dipl.-Ing. Priyanka Kaushal

Matr.Nr.: 525672

Tendlergasse 12/112, 1090 Wien

3.Juli 2006

Priyanka Kaushal



"In the middle of difficulty lies opportunity..."

Albert Einstein

ACKNOWLEDGMENTS

First, I would like to extend my sincere thanks and gratitude to Univ.Prof. Dipl.-Ing. Dr. Hermann Hofbauer for accepting me as his Ph.D student at the Institute of Chemical Engineering, Technical University of Vienna and for his profound and persistent guidance, creative discussions and encouragement throughout the work.

I am also thankful to Dr. I Marini and Dr. F Winter, whose courses I attended during PhD to earn the necessary credits.

I wish to say many thanks to Dr. T Proell for his sustained guidance, help and discussions during my PhD work.

I wish to give a special thanks to Dr. G Loeffler for his help and fruitful discussions. I am also thankful to Dr. B Kronberger and Dr M. Luisser for their help on various occasions.

I render my thanks to Ms. G Bauer and Ms. E Haider for their cooperation.

Along with this I would also like to thank all fellow colleagues for their help which they provided me in some way or the other.

Last but not the least, I would like to pay my sincere thanks to the K_{net} program of Austrian government for the financial support for the project.

Abstract

Biomass is finding increasing use as a fuel for power generation because of the advantages associated with it, such as low sulphur and low ash contents, and zero net CO_2 release. Fluidized bed gasifiers impart excellent mixing and gas/solid contact, resulting in high reaction rates and conversion efficiency. Air gasification results in inferior quality gas (4-7 MJ/Nm³ LHV). Oxygen as gasification agent produces superior quality gas (10-16 MJ/Nm³ LHV) but implies additional costs for oxygen production. A similar high quality gas can be produced by using dual fluidized bed steam gasification systems. Here, the energy for the endothermic reactions in the gasifier is released by combustion of residual char in a second fluidized bed reactor called riser. The energy is transported by the hot circulating bed material. In the Dual Fluidized Bed (DFB) concept, the gasifier is a bubbling bed with steam as fluidizing agent and the combustion reactor is a fast fluidized bed (riser) with staged air introduction (bottom air, primary air, secondary air).

This work focuses on the modelling and simulation of the combustion reactor at the 8 MW fuel power DFB plant Guessing/Austria. Apart from residual char combustion, the riser serves as a sink for the small amounts of rich tar solvent and tar contaminated water occurring in the plant. The model is able to deal with highly volatile fuels and liquid water. The biomass char is considered to consist of C, H, and O. Within previous work, the net amount of char from gasifier to the combustion reactor could be determined as well as the composition (C, H and O) of this net char flux. The present work approaches the actual char that is transported from gasifier to combustion reactor and possibly partly returns to the gasifier due to incomplete conversion in the combustion reactor. The second aim is to focus on the CO concentration in the combustion exhaust gas.

With respect to the hydrodynamics, the riser is divided into two zones: dense zone and transport zone. The dense zone is modelled as bubbling bed assuming modified two phase theory, while the transport zone is modelled by a core-annulus approach. The transport zone is further divided into two sub zones: middle zone and upper zone. In middle zone evaporation and degasification of introduced secondary fuels occur, and in the upper zone heterogeneous gas-solid and homogeneous gas phase reactions take place. Gases are considered in perfect plug flow and the solids are assumed to be ideally mixed within each zone. Therefore, the solids mass balance and the energy balance are formulated not in every cell, but globally for each zone, i.e. dense zone, middle zone and upper zone.

Simulation results showed that the char from the gasifier is only partly converted in the riser and the remaining un-combusted char is circulated back to the gasifier together with the bed material. The temperature profile predicted by the model is in good agreement with the measured temperature. Sensitivity analysis of the model showed that the initial temperature and rate of the bed material circulating between the two fluidized bed (gasifier and combustion reactor) is the most sensitive parameter.

Kurzfassung

Ein qualitativ ähnliches Gas kann durch die Verwendung von Wasserdampf in einem Zweibett-Wirbelschichtsystem erzeugt werden. Hier wird die Energie für die endotherme Reaktion im Vergaser durch die Verbrennung von Restkoks in der zweiten Wirbelschicht (Riser) bereitgestellt. Die Wärme wird durch das zirkulierende heiße Bettmaterial transportiert. Im “Dual Fluidized Bed (DFB)“-Konzept ist der Vergaser eine blasenbildende Wirbelschicht mit Dampf als Fluidisierungsmittel und der Vergasungsreaktor eine schnell zirkulierende Wirbelschicht (Riser) mit stufenweiser Luftzufuhr (Bodenluft, Primärluft, Sekundärluft).

Die Arbeit fokussiert auf die Modellierung und Simulation des Vergasungsreaktors des 8 MW_{th} Biomassekraftwerks Güssing/Österreich. Neben der Restkoksverbrennung dient der Riser als Senke für kleine Mengen teerreicher Lösungsmittel und für durch Teer kontaminiertes Kondensat, welches in der Anlage anfällt. Das Modell ermöglicht die Beschreibung von hochflüchtigen Brennstoffen und Wasser. Der Biomassekoks wird als homogene Matrix aus C, H und O betrachtet. In der vorliegenden Arbeit kann die Nettomenge an Kohle vom Vergaser zum Verbrennungsreaktor, sowie die Zusammensetzung (C, H, O) dieses Nettokoksflusses bestimmt werden. Die tatsächliche Koks menge, die vom Vergaser zum Verbrennungsreaktor und teilweise, aufgrund des ebenfalls unvollständigen Umsatzes im Verbrennungsreaktor, zurück in den Vergaser gelangt. Ein weiteres Ziel der Arbeit ist die Beschreibung der CO-Konzentration im Abgas des Vergasers.

Im Bezug auf die Fluidodynamik ist der Riser in zwei Zonen unterteilt: eine dichte Zone und eine stark expandierte Transportzone. Die dichte Zone wird als blasenbildendes Bett modelliert, mit Annahme einer modifizierten Zweiphasentheorie, die Transportzone hingegen wird durch einen Kern-Ring-Ansatz beschrieben. Weiters kann die Transportzone in zwei Unterzonen unterteilt werden: die mittlere und die obere Zone. In der mittleren Zone erfolgt die Verdampfung und Entgasung der sekundär zugeführten Brennstoffe sowie des Wassers. In der oberen Zone treten heterogene Gas-Feststoffreaktionen und homogene Gasphasenreaktionen auf. Für die Kinetik der Koksverbrennung und Koksvergasung werden Literaturwerte verwendet. Die Kokspartikel während der Umsetzung werden durch Verringerung der Größe bei konstanter Zusammensetzung beschrieben. Für die Gase wird eine ideale Pfropfenströmung und für die Feststoffe eine ideale Durchmischung innerhalb jeder Zone angenommen. Aus diesem Grund werden die Massen- und Energiebilanz nicht in jeder Zelle, sondern global für jede Zone (dichte Zone, mittlere Zone, obere Zone) erstellt.

Die Ergebnisse der Simulation zeigen, dass die Kohle des Vergasers nur teilweise im Riser umgewandelt wird. Das Temperaturprofil des Modells steht in guter Übereinstimmung mit der gemessenen Temperatur. Genauere Analysen des Modells zeigen, dass die Eingangstemperatur und die Rate des zwischen den beiden Wirbelschichten (Vergaser –und Verbrennungsreaktor) zirkulierende Bettmaterials die kritischen Parameter sind.

Table of contents

Acknowledgement	
Abstract	i
Kurzfassung	ii
1 Introduction	1
1.1 Biomass	1
1.1.1 Types of biomass	1
1.1.2 Energy in biomass	1
1.1.3 Potential of biomass	2
1.1.4 Biomass properties	3
1.2 Thermochemical conversion	6
1.2.1 Pyrolysis	6
1.2.2 Combustion	6
1.2.3 Gasification	7
1.3 Types of gasifiers	8
1.3.1 Fixed bed	8
1.3.2 Fluidized bed	9
1.4 Steam gasification of biomass	10
1.5 Technologies using steam as gasification agent	11
1.5.1 Biomass gasification plant at Vermont/USA	12
1.5.2 Heat pipe reformer at TU Munich	13
1.5.3 Biomass gasification plant at Guessing/Austria	14
2 Fluidized bed technology	18
2.1 Onset of fluidization	18
2.2 Bubbling bed	21
2.3 Slugging bed	21
2.4 Turbulent bed	22
2.5 Fast fluidization	23
2.6 Regimes of fluidization	24
2.7 Geldart classification of particle	25
3 Model review	27
4 Char conversion model	33
4.1 Regimes of char conversion	33
4.1.1 Chemical reaction controlled	34
4.1.2 Pore diffusion controlled	34
4.1.3 Bulk diffusion controlled	35
4.1.4 Ash layer diffusion controlled	35
4.2 Modes of char conversion	35
4.2.1 Shrinking particle model	35
4.2.2 Shrinking core model	36
4.2.3 Progressive conversion model	38

5	Material classification and properties	39
5.1	Ideal gas properties	40
5.2	Water	44
5.3	Inorganic	44
5.4	Organic	47
6	Model development	50
6.1	Hydrodynamic sub model	54
6.1.1	Dense zone	55
6.1.2	Transport zone	62
6.2	Reaction sub model	69
6.2.1	Char combustion	69
6.2.2	Homogeneous reaction	72
7	Mass and energy balance	78
7.1	Mass balance	78
7.1.1	Gas balance	79
7.1.2	Liquid balance	80
7.1.3	Inert balance	84
7.1.4	Char balance	84
7.2	Energy balance	85
8	Results and discussions	87
8.1	Standard condition	87
8.2	Sensitivity analysis	100
8.3	Parameter variation	105
8.3.1	Temperature of bed material	105
8.3.2	Char composition	106
8.3.3	Char size	108
8.3.4	Char density	109
8.3.5	Producer gas	110
8.3.6	Bed circulation rate	114
8.3.7	Air distribution	115
8.3.8	Mixing pattern of spent scrubber liquid	117
	Summary and conclusions	119
	References	121
	Symbols and abbreviations	131
	Curriculum Vitae	

1 INTRODUCTION

1.1 Biomass

The definition of biomass is very diverse and broad. Biomass includes all water- and land-based vegetation and trees, and waste biomass such as, municipal sewage and animal wastes, forestry and agricultural residues. Categorically, biomass is the naturally-occurring carbon resource as a substitute for fossil fuels. IEA has defined biomass as “*A material originally produced by photosynthesis, such as wood or plant, or related municipal and agricultural waste*”. Bio energy technology uses these resources to produce heat, electricity or fuels that substitute petroleum. Unlike fossil fuels, biomass is renewable in the sense that only a short period of time is needed to replace what is used as an energy resource. Wood is the best option because it has ability to reduce or balance carbon in atmosphere as the process is cyclic [Kirschbaum, 2003]. Woody biomass, if properly managed does not contribute to climatic change through emissions of CO_2 to the atmosphere because it absorbs the same amount of carbon in growing as it releases when consumed as fuel.

1.1.1 Types of biomass

The types of biomass depend on the chemical and physical properties of the large molecules from which it is made. A simple way to categorise biomass is as follows

- woody plants
- herbaceous plants/grasses
- aquatic plants
- manures

Aquatic plants and manures are intrinsically high-moisture materials and are more suitable for 'wet' processing techniques. Apart from specific applications, most commercial activity for woody plants and herbaceous species has been directed towards the lower moisture-content types, woody plants are investigated in this study.

1.1.2 Energy in biomass

Sun is the primary source of energy for nearly all kinds of life on earth. The energy in sunlight is introduced into the biosphere by a physico-chemical process known as photosynthesis, Virtually all the energy available for the life in the Earth's biosphere, the zone in which life can

exists, is made available through photosynthesis. A generalised, unbalanced, chemical equation for photosynthesis is



Although seemingly simple in concept, the photosynthesis process is very complicated. Biomass is produced by green plants converting sunlight into plant material through photosynthesis and includes all land - and water-based vegetation. The biomass resource can be considered as organic matter, in which the energy of sunlight is stored in chemical bonds. For each gram mole of carbon fixed, about 470 KJ of energy is absorbed. The upper limit of the capture efficiency of the incident solar radiation in biomass has been estimated to range from about 8% to as high as 15%. When the bonds between the adjacent carbon, hydrogen and oxygen molecules are broken by digestion, combustion, or decomposition, these substances release their stored, chemical energy. Currently 15% of world's total primary energy comes from biomass fuel, making biomass world's fourth largest energy source after oil, coal and gas.

1.1.3 Potential of biomass

Since the past decades there has been renewed interest in biomass as an energy source. Primarily because of high emission level of greenhouse gases (CO_2 being the most important one) which in general is responsible for the shift toward the renewable energies. Other factors like, depleting fossil fuel, food surpluses and technological developments toward higher conversion efficiency makes biomass interesting as well. Biomass can be converted into three main types of products, heat/electricity, transport fuel and chemical feedstock. In 1992 the renewable intensive global energy scenario (RIGES) suggested that, by 2050, approximately half the world's current primary energy consumption of about 400 EJ/yr, could be met by biomass and that 60% of the world's electricity market could be supplied by renewables, of which biomass is a significant component [Price, 1998]. Numerous crops have been proposed for commercial energy farming. Potential energy crops include woody crops and grasses/herbaceous plants (all perennial crops), starch and sugar crops and oilseeds. In general, the ideal energy crop may be characterise as

- high yield (maximum production of dry matter per hectare)
- low energy input to produce
- low cost
- composition with the least contaminants
- low nutrient requirements.

1.1.4 Biomass properties

The inherent properties of the biomass influence the conversion process. Once the energy conversion process is selected, biomass properties become important for subsequent processing. The main material properties of interest (for dry biomass conversion) are moisture content, heating value, elemental composition and ash content.

Moisture content

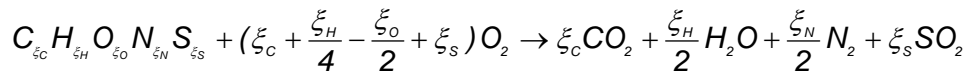
Moisture content in biomass can be described in two ways:

- Intrinsic : The bound moisture content in the biomass
- Extrinsic : Overall moisture present in biomass (including weather effect)

In practical terms, it is the extrinsic moisture content that is of concern, as the intrinsic moisture content is usually only achieved, under laboratory conditions. For the production of ethanol by biochemical (fermentation) conversion, high moisture plant species, such as sugarcane, are more suited where as thermal conversion requires low moisture content feedstock (typically <50%). However thermal conversion technologies can also use feedstocks with high moisture content but then the overall energy balance for the conversion process is adversely effected.

Heating value

Heating value is the amount of heat produced by complete combustion of a unit quantity of fuel to the products CO_2 , H_2O , SO_2 , and N_2 , represented as



The heating value is dependent on the phase of H_2O (water/steam) in the combustion products. Heating value is expressed in two forms, the higher heating value (HHV) and the lower heating value (LHV). HHV is also known as gross heating value (GHV) or the calorific value (CV). If H_2O in the combustion product is in the liquid form, heating value is called HHV. HHV is obtained when all of the products of combustion are cooled to the temperature existing before combustion, the water vapour formed during combustion is condensed, and all the necessary corrections have been made. So HHV represents the maximum amount of energy potentially recoverable from a biomass source. Various correlations are proposed in literature to calculate HHV. HHV based on proximate analysis of biomass (dry basis) is given in Eq. 1-1 [Jimenez & Gonzalez, 1991].

$$HHV = -1.081E^{10} + 3.13E^8 (VM + FC) \quad \text{Eq. 1-1}$$

The use of proximate analysis of fuel for calculating heating value has limited application. The correlations based on the proximate data have low accuracy because the proximate analysis provides only an empirical composition of the biomass. In present time when ultimate analysis can be done, it is wise to use ultimate analysis of fuel because the error in calculation is smaller. Based on ultimate analysis HHV [Annamalai et al., 1987] is

$$HHV = (34835 w_C + 115853 w_H - 1080 w_O + 6280 w_N + 10465 w_S) 10^3 \text{ J} \quad \text{Eq. 1-2}$$

When H_2O is in vapour form, heating value is called LHV (Lower Heating Value). Based on ultimate analysis LHV is

$$LHV = (34835 w_C + 93870 w_H - 1080 w_O + 6280 w_N + 10465 w_S) 10^3 \quad \text{Eq. 1-3}$$

LHV is also obtained by subtracting the latent heat of vaporization of the water vapour formed by the combustion from the HHV

$$LHV = HHV - w_H \cdot \frac{M_{H_2O}}{2 \cdot M_H} \cdot \Delta h_{vap} \quad \text{Eq. 1-4}$$

In reality the actual amount of energy recovered varies with the conversion technology. Practically, the latent heat contained in the water vapour cannot be used effectively and therefore, LHV is the appropriate value to use for the energy available for subsequent use for most applications. All calculations in the present model is based on lower heating value. It was found that the correlations based on ultimate analysis are the most accurate.

Elemental composition

It is customary to analyse solid fuel as fraction of fixed carbon to volatiles. Volatile matter (VM) of a solid fuel is the portion that is driven-off as a gas (including moisture) by heating. The fixed carbon content (FC), is the mass remaining after the releases of volatiles, excluding the ash and moisture contents. It is internationally standardized to analyse a solid fuel on two basis:

^Π Boie Formula

Proximate analysis: The “Proximate analysis”, is the weight fraction of moisture, volatile matter, fixed carbon and ash present in the fuel when heated to a temperature of 950°C for seven minutes [McKendry, 2002].

Ultimate analysis: The “ultimate analysis” is the weight fraction of carbon, hydrogen and oxygen (the major components) as well as sulphur and nitrogen present in the fuel.

The alkali metal content of biomass i.e. Na, K, Mg, P and Ca, is especially important for any thermo-chemical conversion processes. The reaction of alkali metals with silica present in the ash produces a sticky phase, which can block the airways of the reactor. Compared with coal, biomass has a high content of chlorine and alkali metals (potassium). During biomass thermal utilization, gaseous alkali metals may result in slagging, fouling and corrosion on the heat transfer surfaces.

Table 1-1: Proximate and ultimate analyses of some common wood.

Name (wood)	Proximate analysis (wt %)			Ultimate analysis (wt %)					Lower heating value (KJ/g)
	FC	VM	Ash	C	H	O	N	S	
Beech	-	-	0.65	51.6	6.2	41.4	0.00	0.00	19.11
Douglas Fir	17.7	81.5	0.8	50.7	5.7	41.9	0.5	0.01	19.89
Poplar	-	-	0.6	51.6	6.3	41.4	0.00	0.00	19.46
White Oak	17.2	81.2	1.5	49.5	5.4	43.1	0.35	0.01	18.32
Yellow Pine	-	-	1.3	52.6	7.0	40.1	0.00	0.00	20.87

Ash content

Solid fuel (coal/biomass) does not contain ash but it contains minerals and other inorganic components that upon combustion or gasification form ash [Benson, 1993]. The conditions that the fuel and the inorganic components present in it are exposed to during the process of combustion result in complex chemical and physical transformations to produce vapour liquid and solid (residue). The residue produced by combustion is called ‘ash’. The ash content of biomass affects both the handling and processing costs of the overall biomass energy conversion cost.

1.2 Thermochemical conversion

Apart from combustion (that directly transforms biomass into energy) there are other possible routes of biomass up gradation producing different kinds of compounds that can be used as chemical commodities or for energy production.

1.2.1 Pyrolysis

Pyrolysis is the thermal decomposition of materials in the absence of oxygen. It is important to differentiate pyrolysis from gasification. Gasification decomposes biomass to producer gas by carefully controlling the amount of oxygen present. Pyrolysis often describes processes in which oils are the preferred products. Over the last two decades, research on fast pyrolysis has shown that high yields of liquids and gases (including valuable chemicals, chemical intermediates, petrochemicals, and fuels) can be obtained from carbonaceous feedstocks [Bridgwater, 2001]. The pyrolytic breakdown of wood produces a large number of chemical substances. Some of these chemicals can be used as substitutes for conventional fuels. Fast pyrolysis is a high-temperature process in which biomass is rapidly heated in the absence of oxygen to generate vapors and char. After cooling a gas and a dark brown liquid are formed. In slow pyrolysis, biomass is heated to 500°C. The heating rate in conventional/slow pyrolysis is typically much slower than that used in fast pyrolysis [Pyne, 2006].

1.2.2 Combustion

Combustion is a chemical process in which an exothermic reaction between a substance (the fuel) and a gas (the oxidizer), usually O_2 , takes place to release heat. The prime requirement for combustion is a high temperature and enough air or O_2 (air ratio, $\lambda > 1$). The combustion of biomass is used over a wide range of outputs to convert the chemical energy stored in biomass to heat and subsequently to mechanical power and electricity.

The burning of biomass in air is the oldest and most widely used method to convert the chemical energy stored in biomass into heat. Combustion of biomass produces hot gases at temperatures around 800–1000°C. It is possible to burn any type of biomass but in practice combustion is feasible only for biomass with a moisture content <50%. The scale of combustion plants ranges from very small scale (e.g. for domestic heating) up to large-scale industrial plants in the range 100–300 MW. Co-combustion of biomass in coal-fired power plants is an attractive option because of the high electrical efficiency of these plants. Fluidized bed combustion (FBC) is a combustion technology extensively used in power plants. FBC plants are more flexible than conventional plants as they can be fired with coal, biomass, sludge and waste among other fuels. Commercial FBC units operate at competitive

efficiencies, and are cost effective, and have NO_x and SO_2 emissions below mandated levels.

1.2.3 Gasification

Gasification can be broadly defined as the thermochemical conversion of a solid or liquid carbon-based material (feedstock) into a combustible gaseous product (combustible gas) by the supply of a gasification agent (oxygen containing gaseous compound). The thermochemical conversion changes the chemical structure of the biomass. The gasification agent allows the feedstock to be quickly converted into gas by means of different heterogeneous reaction shown in Table 1-2. The producer gas mainly contains, CO_2 , CO , H_2 , CH_4 , H_2O , inert gases (if present in the gasification agent), various contaminants such as small char particles, ash and tars. Unlike combustion where oxidation is substantially complete in one process, gasification converts the intrinsic chemical energy of the biomass into a combustible gas. The gas produced is good has easy transportability and more versatile to use than the original biomass.

Direct/autothermal gasification occurs when an oxidant gasification agent is used to partially oxidise (combustion) the feedstock in the same reactor where the gasification takes place. The oxidation reactions supply the energy to keep the temperature of the process up. A major disadvantage of autothermal gasification process is the dilution of producer gas with the flue gas of combustion process. This dilution effect is because both the gasification process and combustion process takes place simultaneously in same reactor. If the gasification and combustion processes are not taking place in the same reactor, it is called indirect/ allothermal gasification and needs an external supply of energy. Steam is the most commonly used indirect gasification agent, because it is easily produced and increases the hydrogen content of the producer gas [Belgiorno et al., 2003].

Allothermal gasification systems are usually bubbling or circulating fluidized bed gasification systems. The main technical challenge for allothermal gasifiers is the heat transfer into the fluidized bed. Especially steam reforming requires large heat fluxes at high temperatures. The main disadvantage of an allothermal gasifier is its efficiency, which are lower than the efficiency of autothermal gasifiers.

A new concept is the biomass integrated gasification/combined cycle (BIG/CC), where gas turbines converts the gaseous fuel to electricity. In BIG/CC the product gas is cleaned before being combusted in the turbine. The exhaust gas is further used in a steam cycle. An advantage of BIG/CC systems is high overall conversion efficiency nearly 40–50%. The overview of what has been achieved so far in this area of biomass gasification shows that there is a lack of scientific knowledge of process and the gas cleaning technology.

Nevertheless several developments have resulted in successful pilot plants and demonstrations that work. Gasification processes offer technically more pleasant options for medium to large scale applications. It is a relatively clean path for extracting energy from biomass, since in the presence of non-oxidation conditions, the pollutant emissions are much lower [Franco et al., 2003].

1.3 Types of gasifier

In the recent years a range of reactor configuration have been designed for the gasification process. Two major types of gasifiers currently available for commercial use are: Vertical fixed bed reactors (VFB) and fluidized bed reactor (FBR). The fixed bed gasifiers can further be subdivided as counter current (updraft) and co-current (downdraft) gasifier. This section briefly discusses these gasification types.

1.3.1 Fixed bed

Vertical fixed bed reactors (VFB) are the most competitive fixed bed gasifiers. They are further subdivided into updraft and downdraft gasifiers.

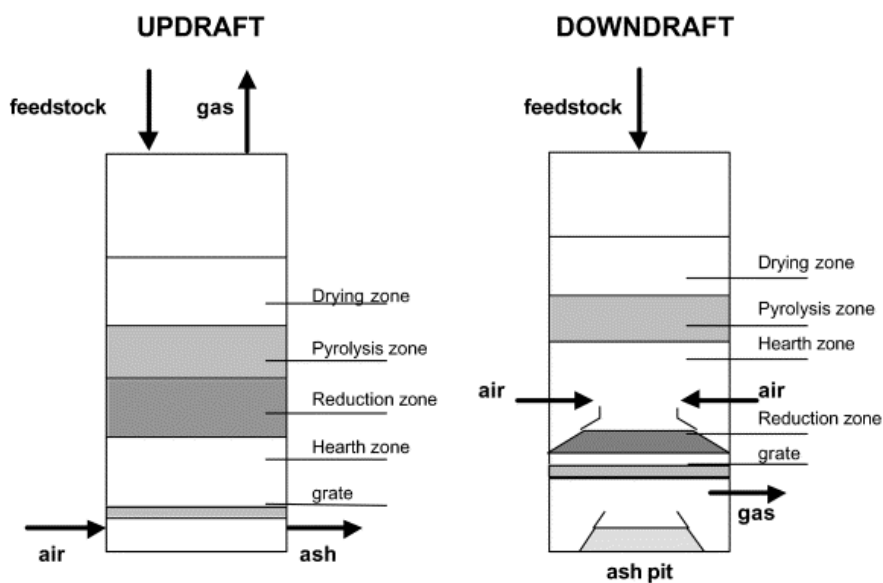


Figure 1-1: Schematic updraft and downdraft gasifier.

Updraft

Updraft is a counter-current gasifier, where the feedstock is loaded from the top while air is introduced from the bottom of the reactor. During its downward journey in the reactor the solid material is converted into combustible gas. As the feed moves down it undergoes the following process in sequence, drying, pyrolysis, reduction and combustion (Hearth zone). In the combustion/hearth zone, the highest temperature of the reactor is greater than $\sim 1200^{\circ}\text{C}$.

As a consequence of the updraft configuration, the tar coming from the pyrolysis zone is carried upward by the flowing hot gas. The result is the production of a gas with high tar content. Typically, the sensible heat of the producer gas is recovered by means of a direct heat exchange with incoming feedstock. Major drawback in this reactor type is the "channelling" in the equipment.

Downdraft

In a downdraft reactor there is a co-current flow of solid and gas. The solid feed is introduced in the reactor from the top, the air is introduced at the sides above the grate. Grate is a region of high temperature and high turbulence. Near the grate the reaction products are intimately mixed and tar is cracked. The combustible gas is withdrawn under the grate. As a consequence of the downdraft configuration, pyrolysis vapours allow an effective tar thermal cracking. However, the internal heat exchange is not as efficient as in the updraft gasifier. Downdraft gasifiers also suffer from the problems associated with high ash content fuels (slagging) to a larger extent than updraft gasifiers.

1.3.2 Fluidized bed

Fluidization is the term applied to the process whereby a fixed bed of fine solids, typically silica sand, is transformed into a liquid-like state by contact with an upward flowing gas (gasification agent). Fluidized bed gasification was originally developed to solve the operational problems of fixed bed gasification related to feedstocks with high ash content and principally to increase the efficiency. Fluidized bed reactors are the only gasifier with almost isothermal bed operation. They have the advantage of easy and reliable scale up. However, fluidized beds are not economical for small scale application due to high investment and operating cost.

Bubbling fluidized bed

In a BFB reactor, the velocity of the upward flowing gasification agent is around 1-3 m/s and the expansion of the bed limits only in the lower part of the gasifier. Generally bed material and char do not come out of the reactor because of the low velocity. Most of the conversion of the solid feed takes place within the bed, however some solid conversion do take place in freeboard because of the entrained small particle. The homogeneous gas phase reaction continues in the freeboard too. The bubbling fluidized gasifier produces gas with tar content between that of the updraft and the downdraft gasifiers.

Circulating fluidized bed

The velocity of the upward flowing gasification agent in a CFB reactor is around 5–10 m/s. Consequently, the expanded bed occupies the entire reactor and a fraction of bed material

and char is carried out of the reactor together with the gas stream. That fraction is captured and recycled in the reactor using a cyclone that intercepts the gas stream to increase the efficiency of the process. Circulating beds give an improved carbon conversion efficiency compared with the bubbling bed.

1.4 Steam gasification of biomass

Steam gasification of biomass is a promising technology for thermochemical hydrogen production from biomass. In the conventional biomass gasification process large amount of tar is produced which reduces thermal efficiency, interrupt fluidization and plugs pipeline. So, it is necessary to convert tar into gaseous products such as H_2 and CO during gasification for easy controllability and higher efficiency of gasifiers. In present time steam gasification has become an area of interest because it produces a gaseous fuel with relatively higher H_2 content which could be used in fuel cells. Steam gasification, has advantages of producing a gas with higher heating value with no dilution effect (N_2 from air) and it also eliminates the need of expensive oxygen plant installation. Unlike air or oxygen gasification, steam gasification is a more complex process. In steam gasification process the heat required for the gasification reaction has to be supplied externally whereas in air or oxygen gasification the heat for gasification is directly supplied by partial combustion of feedstock during gasification.

The catalytic activity of the ash plays an important role in steam gasification reaction. It is also a complicated reaction system because all the gaseous species present participate in consecutive reactions. Carbon dioxide gasification reaction has been studied most extensive of all gasification reactions because of its simplicity, since the products do not enter into side reactions. However, the activation energy of this reaction is strongly influenced by the type of the carbon. [Dutta et al., 1987] [Reed, 1981]. Methane formation by the hydrogasification reaction is important especially for air and oxygen gasification for two reasons. Firstly, the energy content of the synthesis gas is increased due to the presence of methane and secondly, the oxygen necessary for gasification is reduced because of the heat released in methane formation.

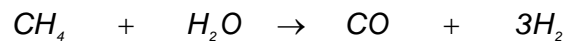
Antal [1981] studied the effect of temperature, residence time, and pressure on producer gas composition during the steam gasification reaction of biomass in a fixed-bed reactor in the temperature range of 500-750°C. He found that increasing temperatures and residence times resulted in increased CH_4 formation while maximum H_2 production (18 mol %) was observed at 750 °C. It was also observed that increased pressure inhibited the gasification process.

In the past, steam gasification of biomass has been mainly studied with or without catalyst in fluidized bed reactors.

Table 1-2: Basic heterogeneous steam gasification reactions.

Steam gasification	$C + H_2O \Leftrightarrow CO + H_2$
Carbon dioxide gasification (Boudouard reaction)	$C + CO_2 \Leftrightarrow 2CO$
Hydrogasification reaction	$C + 2H_2 \Leftrightarrow CH_4$
Water gas shift reaction	$CO + H_2O \Leftrightarrow CO_2 + H_2$
Methane decomposition	$CH_4 + H_2O \Leftrightarrow CO + 3H_2$

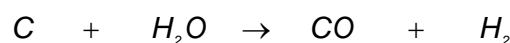
Corella et al. [1988] made possible improvements of steam gasification of biomass using two reactors in series, where the first reactor was a simple fluidized reactor and the second reactor was a fixed or fluidized catalytic bed reactor. They observed that high H_2 and CO were produced using dolomite as a catalyst. During investigation Prasad et al.[1988] found that the H-O ratio in the biomass is the most important parameter that affected the product distribution. Baker et al. [1987] and Pfeifer et al. [2004] found that Ni catalysts are effective for increasing the gas yield from steam gasification of biomass (wood, bagasse) by converting tars and other hydrocarbons to gas.



1.5 Technologies using steam as gasification agent

The gasification process requires an oxidising agent that provides oxygen for the formation of CO from solid fuel. Commonly used oxidising agent or gasifying agents are air, oxygen and steam. Air is most often used because of its availability at zero cost. Air, though cheap, is not a perfect agent because of its nitrogen content. Oxygen gasification produces a higher heating value producer gas ($10-18 \text{ MJ} / \text{Nm}^3$) but has a drawback of high production cost of oxygen.

Steam is another alternative. It also generates a medium calorific value gas ($10-14 \text{ MJ} / \text{Nm}^3$) and increases the hydrogen content of the product gas. The presence of steam is important in case of further catalytic upgrading of the product gas [Gil et al., 1997]. Steam gasification is however a highly endothermic reaction. The overall steam gasification reaction can be represented as:



Steam gasification of solid biomass is extensively. A lot of references are available in the paper by Barrio et al. [2000]

1.5.1 Biomass gasification plant at Vermont USA

Battelle has developed an indirect gasification process which utilizes two different circulating fluid-bed loops to pyrolyze and steam-gasify the injected biomass. The remaining char is captured in the cyclone of the first fluidized bed and sent to the second circulating fluidized bed where it is combusted with air to increase the bed material temperature and burn out the residual char. The heating of the bed material in the second fluid bed allows the endothermic pyrolysis and steam gasification reactions to continue in the first bed without having to add oxygen and dilute the syngas with nitrogen by adding air to the gasifier.

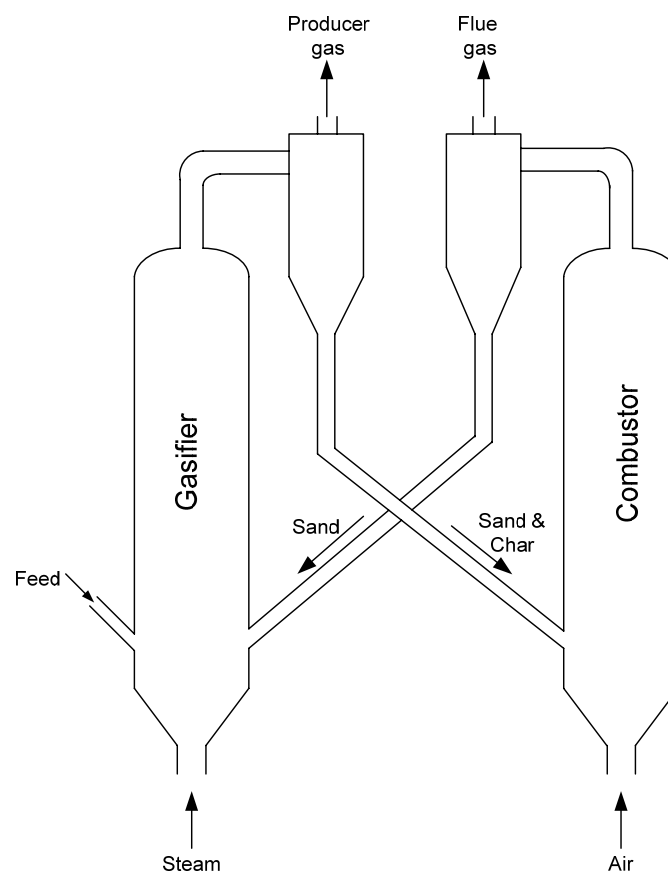


Figure 1-2: The Battelle gasification process at Vermont/USA.

This generates a medium heating value gas ($11\text{--}14\text{ MJ}/\text{Nm}^3$). Sand is used as the heat transfer medium that circulates between the gasifier and the combustion reactor. The process operates at atmospheric pressure. The reactivity of biomass is such that throughputs in excess of $14,600\text{ Kg}/\text{hr}\cdot\text{m}^2$ can be achieved and is designed for a feed rate of 182 dry tonnes of wood per day [Farris et al., 1998].

1.5.2 Heat pipe reformer at TU Munich

The Heat pipe reformer consists of three main parts -Reformer (a bubbling fluidized bed gasifier), integrated sand filter, and combustion reactor (bubbling fluidized bed). Gasifier and sand filter are integrated in the combustion chamber. Liquid metal heat pipes, transfer heat from the combustion reactor into the reformer. A siphon system separates the gasifier and the combustion reactor in order to allow steam gasification with pressures above 5 bars. The sand filter separates dust and coke particles.

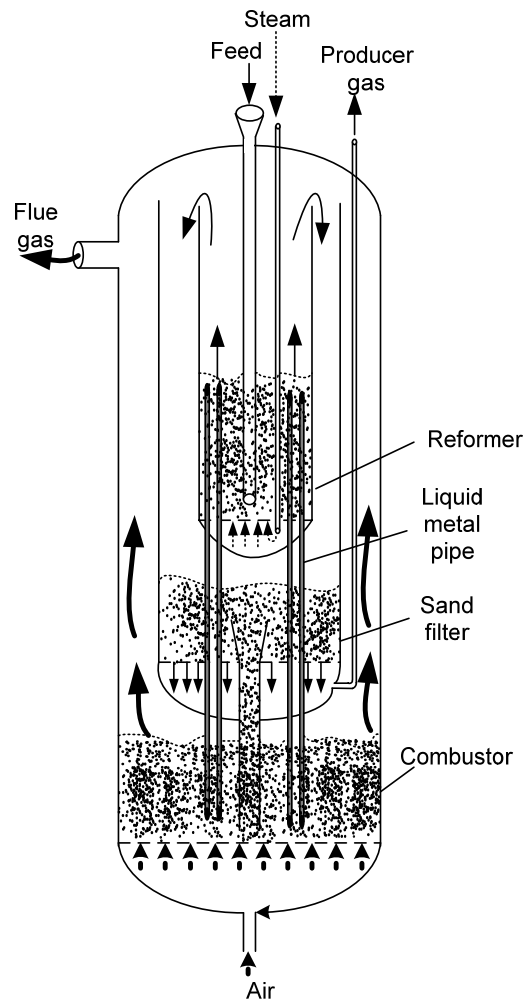


Figure 1-3: Heat pipe reformer (BioHPR) at TU Munich.

External sand filters cause tar condensation and requires regeneration systems. The integration of the filter into the hot reactor solves this problem. A siphon system transfers the ashes and the unconverted coke particles into the combustion chamber in order to provide the necessary heat-of-reaction. The integration of the components into a single pressure vessel reduces heat losses, operational cost, investment cost and increases safety from leakages.

1.5.3 Biomass gasification plant at Guessing/ Austria

The fluidized bed gasifier, developed at Vienna university of Technology, consist of two zones, a gasification zone and a combustion zone

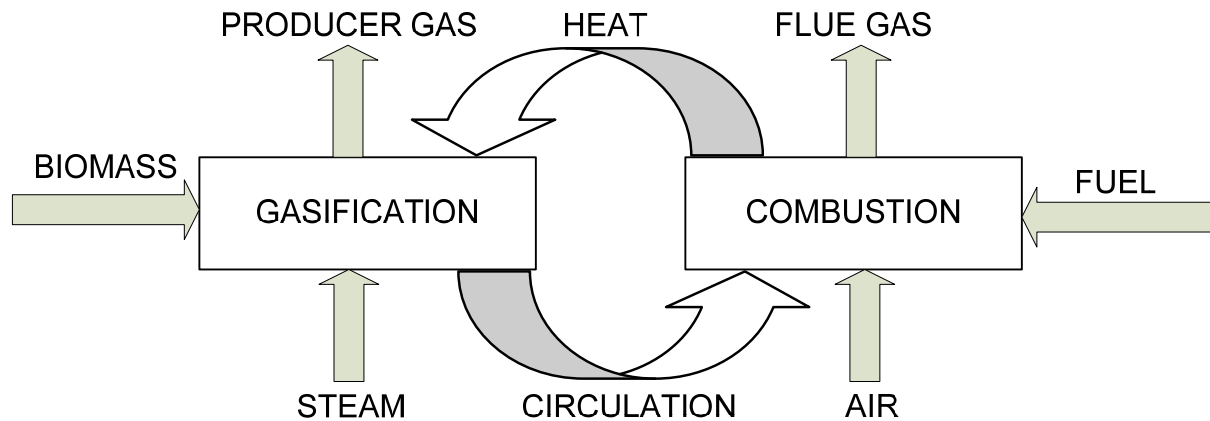


Figure 1-4: Schematic representation of the dual fluidized bed gasification system at Guessing/Austria [Hofbauer et al., 1995].

The wood trunks are dried naturally by storage of six months in the forest before they are delivered to the CHP-plant and chipped. The actual biomass water content is about 25-35 wt-%. Biomass chips are transported from a daily hopper to a metering bin and fed into the fluidized bed reactor via a rotary valve system and a screw feeder (Figure 1-6). The gasification zone is fluidized by steam and hence produces nitrogen free producer gas. Steam is produced by the waste heat of the process. The combustion zone is fluidized by air, where exothermic reactions take place. The heat released is carried by the circulating bed material to the gasification zone where endothermic reactions take place. The raw producer gas is cooled and cleaned by a two stage cleaning. A water cooled heat exchanger reduces the temperature from 850° C-950° C to about 160° C-180° C. The first stage of the cleaning system is a fabric filter to remove particulates and some of the tar from the producer gas. Approximately 99.8% of the dust and fly ash and 10-30% of tar are separated in fabric filter [Hofbauer et al., 1997]. So a second stage of gas cleaning (scrubber) is implemented to remove tar compounds. The scrubber uses rape oil methyl ester (RME) as solvent and reaches high tar separation efficiencies of about 98 % for tars detectable with gravimetric methods.

The scrubber also reduces the temperature of the clean producer gas to about 40° C, which is necessary for the gas engine. Condensation of water occurs in the scrubber and this increases the heating value of producer gas and also removes some of the water-soluble trace components like NH_3 . The clean producer gas is finally fed into a gas engine to produce electricity and heat. A GE Jenbacher J620 gas engine is used for power generation.

An oxidation catalyst minimizes the emissions from the engine. The only streams exiting the plant are the clean stack gas and the ash from the flue gas filter. Heat for the local district heating grid is extracted by cooling producer gas, flue gas cooling and engine exhaust. Alternatively to the gas engine, a conventional gas boiler for heat generation is available. The design data of the plant are summarized below. A gas filter separates the particles before the flue gas is released via a stack to the environment.

Table 1-3: Design data of the CHP plant in Guessing/Austria.

Thermal fuel power (LHV)	8000	KW
Net Chemical producer gas power(LHV)	5600	KW
Generator output	2000	KW
Electric consumption of plant	200	KW
Net electric output	1800	KW
Net heat production	4500	KW

Operational performance of CHP plant Guessing

The Guessing plant is in continuous operation since the middle of the year 2002, except few periods of maintenance and design improvement. Since the beginning of operation of the demonstration plant the improvement and optimisation of the operation performance is a permanent task. The process optimisation work is carried out by Renet-Austria. Figure 1-5 highlights the optimization work over the past years (2003, 2004 and 2005).

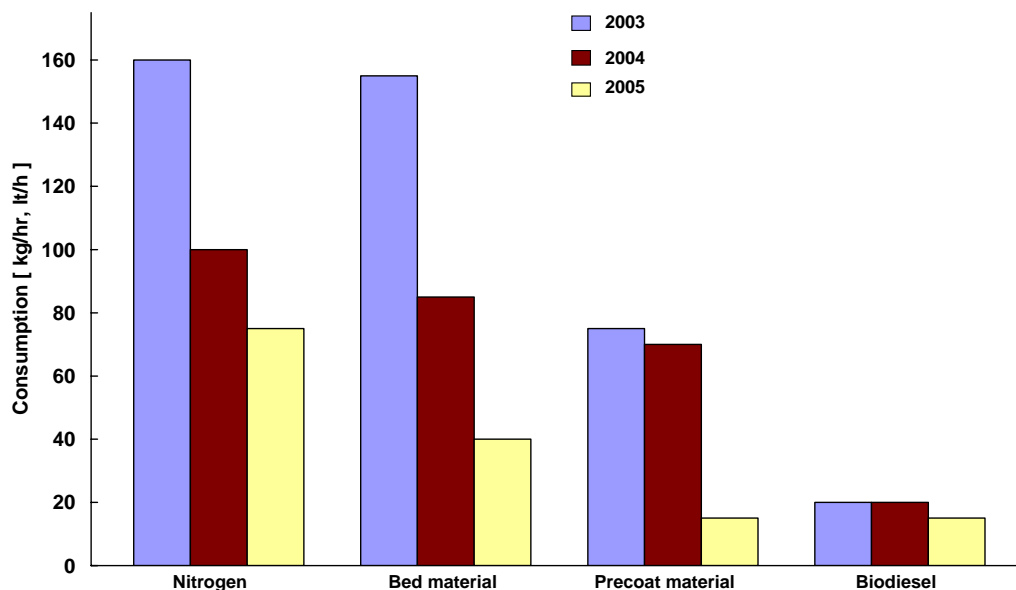


Figure 1-5: Operational cost optimisation over the past few year[Hofbauer, 2005]

Nitrogen is used as purge gas at all entrances to or exits from the plant. Furthermore, nitrogen is used also for removing the dust from the fabric filter in the producer gas line. From 2003 to 2005 the nitrogen consumption is reduced to about 50 % of the original amount.

The bed material that is circulating in the dual fluidized bed gasifier has a certain attrition rate during operation. This attrition rate and therefore the loss of the bed material depend mainly on the kind of the bed material, the velocities of the riser, and also on the separation efficiency of the cyclone. On the basis of the operation experience, some simulation work, and optimisation of these parameters a reduction of the bed material loss by more than 70 % is obtained.

Precoat material is necessary to avoid the condensation of tar compounds directly on the filter bag which could lead to plugging or even to damage of the filter cloth. At the beginning a swing operation with two filters (one in operation mode, on-line, another in pre-coating mode, off-line) were applied. Now this operation mode has been change to an online operation. This leads to a reduction in the need of the precoat material down to about 20 % of the original amount and also to a reduction in the nitrogen consumption.

The scrubber for the tar separation is operated with biodiesel. The spent biodiesel together with some condensate is fed into the combustion chamber of the gasifier. With this scrubber the overall tar in the producer gas can be removed over 90 %. The operation experience leads to a slight reduction of the biodiesel of about 25 %.

To agree with the government policies, the plant economy suggests operating the plant at maximum electricity production limit. The maximum possible power output for the engine used is 1960 kW which approximately is reached now.

Table 1-4: Typical producer gas composition from technologies using steam (dry basis).

[vol%]	Vermont /USA [Paisley et al., 2000]	Guessing/Austria [Proell, 2004]
H_2	18	39.21
CO	47	23.58
CO_2	14.3	22.74
CH_4	14.9	11.08
C_2H_4	4.7	2.45
C_2H_6	1.1	0.94
Heating value MJ / Nm^3	16.8(HHV)	11.97 (LHV)

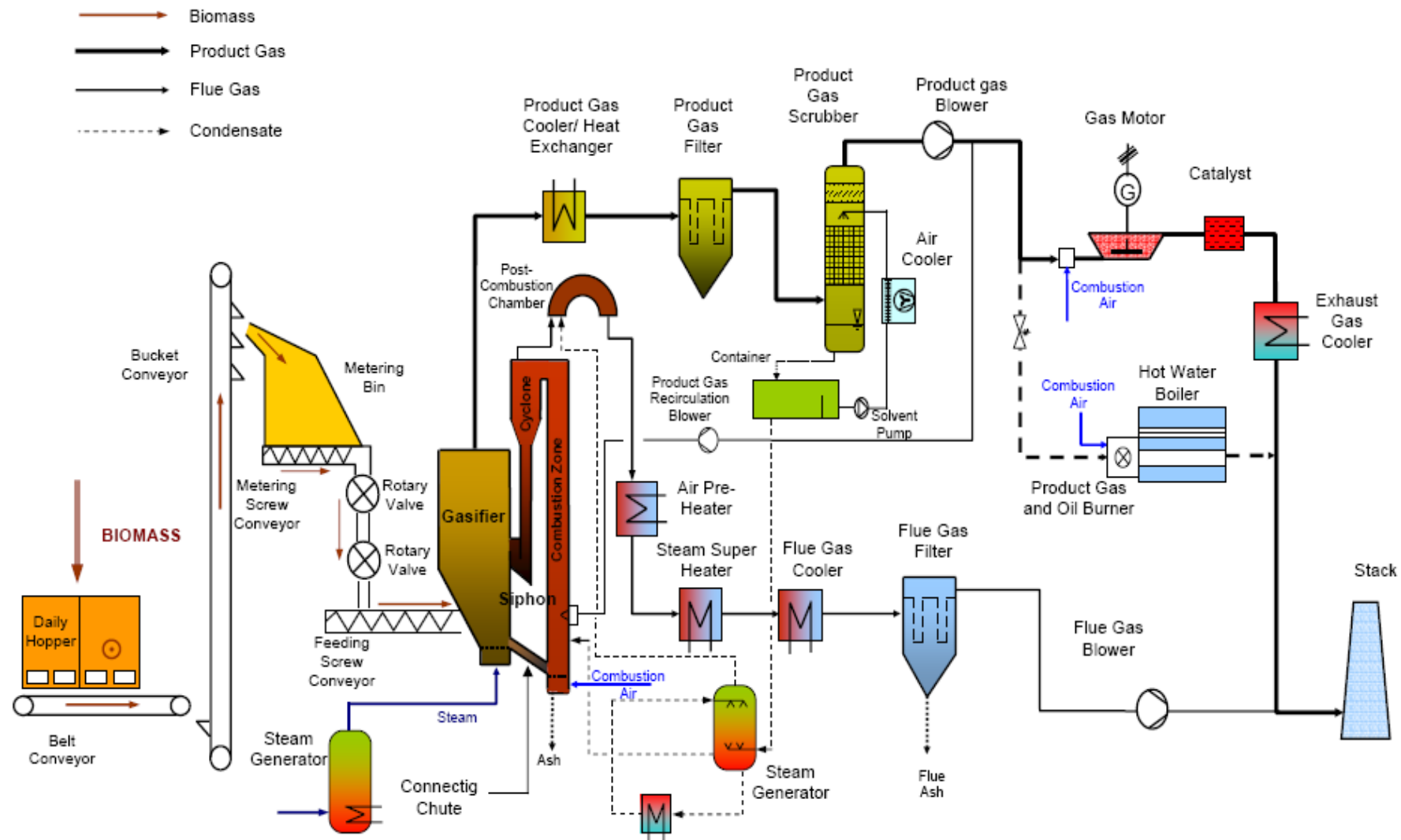


Figure 1-6: Process flow diagram of CHP(Combined Heat and Power) plant at Guessing/Austria.

2 FLUIDIZED BED TECHNOLOGY

Fluidization is commonly defined as the operation by which the fine solids are transformed into a fluid-like state through contact with an up flowing gas or liquid. Fluidized beds are characterised for their high heat and mass transfer coefficients, due to the high surface area-to-volume ratio of fine particles. When the velocity of the gas flowing upward over a bed of fine solids resting on a perforated plate is increased the system undergoes different characteristic flow patterns/regimes (Figure 2.1). As the velocity increases the system transforms as fixed bed, homogeneous fluidization, bubbling fluidization, slugging fluidization, turbulent fluidization, fast fluidization and dilute pneumatic conveying, respectively. Sometimes not all regimes exist in a particular system while on the other hand regimes can co-exist in different parts of the same system [Gogolek et al., 1995].

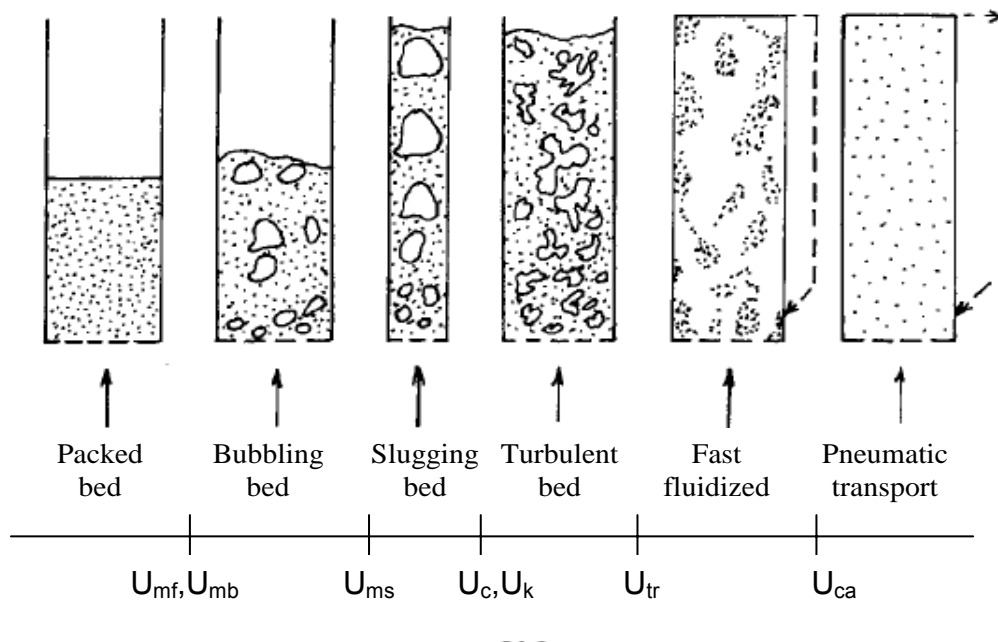


Figure 2.1: Flow patterns in gas-solids fluidized beds.

2.1 Onset of fluidization

The onset of fluidization occurs with a relatively sharp transition when the velocity exceeds the minimum fluidization velocity U_{mf} , defined as the superficial fluid velocity at which the upward drag force exerted by the fluid is equal to the weight of the particles in the bed.

$$\text{drag force by upward moving gas} = \text{weight of particles}$$

or,

$$\Delta p_{bed} A = AH_{mf}(1-\varepsilon_{mf})(\rho_s - \rho_g)g \quad \text{Eq. 2-1}$$

Rearranging Eq. 2-1 gives,

$$\frac{\Delta p_{bed}}{H_{mf}} = (1 - \varepsilon_{mf})(\rho_s - \rho_g)g \quad \text{Eq. 2-2}$$

Using the equation of *Ergun (1952)* for the pressure drop due to friction for a fluid flowing through a fixed bed gives

$$\frac{\Delta p}{H} = 150 \frac{(1 - \varepsilon)^2}{\varepsilon^3} \frac{\mu_g U}{(\varphi_p d_p)^2} + 1.75 \frac{(1 - \varepsilon)}{\varepsilon^3} \frac{\rho_g U^2}{\varphi_p d_p} \quad \text{Eq. 2-3}$$

Comparing Eq. 2-2 and Eq. 2-3 it is possible to calculate minimum fluidization velocity. It was shown that the solution is very sensitive towards the particle sphericity φ_p and the voidage at minimum fluidization ε_{mf} . Thus, it is preferred to use an equation for the Reynolds number at minimum fluidization conditions of the following form.

$$Re_{mf} = \sqrt{C_1^2 + C_2 - Ar} - C_1 \quad \text{Eq. 2-4}$$

$$Ar = \frac{d_p^3 \rho_g (\rho_s - \rho_g) g}{\mu^2} \quad \text{Eq. 2-5}$$

$$Re_{mf} = \frac{U_{mf} d_p \rho}{\mu} \quad \text{Eq. 2-6}$$

The value of constants in Eq. 2-4 are

$$C_1 = \frac{150(1 - \varepsilon_{mf})}{2 * 1.75 \varphi_p} \quad \text{Eq. 2-7}$$

$$C_2 = \frac{\varphi_p \varepsilon_{mf}^3}{1.75} \quad \text{Eq. 2-8}$$

Eq. 2-4 can be fitted to experimental data to find the values of constant C_1 and C_2 . In Figure 2.2, various correlations from literature are compared. It can be seen at higher Ar number the discrepancy is usually below 40%, however for fine particles there can be a difference of more than a factor of 2 [Yang, 1998].

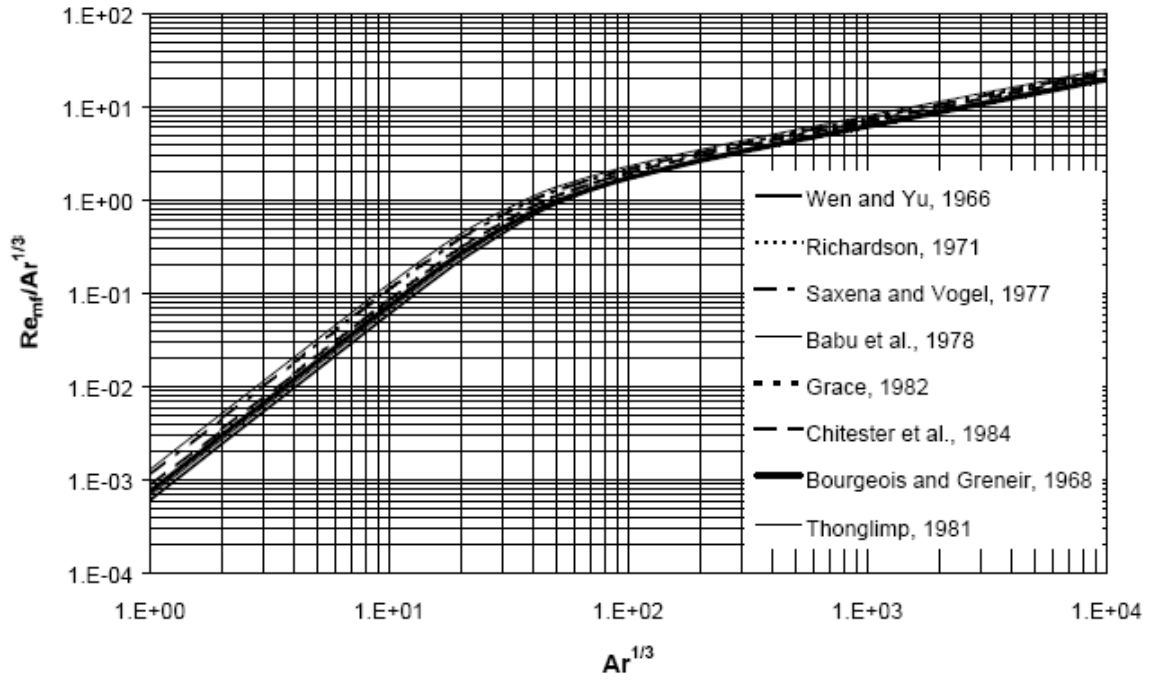


Figure 2.2: Comparison of minimum fluidization condition from literature[Yang, 1998].

Numerous correlations have been proposed for the prediction of U_{mf} [Loeffler, 2001]. These correlations should of course be used in the range of conditions in which they were obtained. Grace [1982] proposed Eq. 2-9 for minimum fluidization condition.

$$U_{mf} = \frac{\mu_g}{\rho_g d_p} \left(\sqrt{27.2^2 + 0.0408 Ar} - 27.2 \right) \quad \text{Eq. 2-9}$$

Once the minimum fluidization velocity is determined, the voidage at minimum fluidization conditions can be calculated using Eq. 2-3.

$$\varepsilon_{mf}^3 - \frac{150 Re_{mf}}{\phi_p^2 Ar} (1 - \varepsilon_{mf}) - \frac{1.75 Re_{mf}^2}{\phi_p Ar} = 0 \quad \text{Eq. 2-10}$$

For $177 < Ar < 4030$ Doichev et al. [1977] suggested

$$\varepsilon_{mf} = 0.478 Ar^{-0.018} \quad \text{Eq. 2-11}$$

2.2 Bubbling bed

When the gas velocity is increased above that of the incipient fluidization the bed expands. When this happens uniformly, it is called homogeneous or particulate fluidization but when this happens with appearance of bubbles than it is called bubbling, aggregated or heterogeneous fluidization. The velocity at onset of bubbling is called U_{mb} . Geldart et al. [1978] proposed the following equation for the minimum bubbling velocity in the bed.

$$U_{mb} = 33d_p \left(\frac{\mu_g}{\rho_g} \right)^{-0.1} \quad \text{Eq. 2-12}$$

For coarse particles, U_{mb} and U_{mf} are essentially the same, whereas for fine particles or for a low density ratio of solid to fluid, there is a range of velocities between U_{mb} and U_{mf} where the bed expands uniformly. In bubbling regime the bed appears to be divided into two phases, the bubble phase and the emulsion phase. The formation, properties and movement of bubbles (heterogeneities, gas pockets, and voids) are dominant factors that determine the overall behaviour of a fluidized bed. The emulsion phase (dense or particulate phase) consists of all bed particles that are fluidized by interstitial gas. It is a characteristic feature of the bubbling bed regime that the emulsion phase forms a continuous medium between discrete gas bubbles. The ascending bubbles bring about motion of the emulsion phase which is the main cause of solids mixing in bubbling fluidized beds. The bubbles coalesce to form bigger bubbles and when they become too large, they split. The average bubble size equilibrates at about the maximum stable size. The location in the bed where the equilibrium size is attained depends on the kind of particles. For the Geldart group A particles the maximum stable diameter is relatively small, therefore the average bubble size stabilizes close to the distributor plate and remains constant through the rest of the bed. The maximum stable diameter for the Geldart group B particles is larger and the equilibrium is reached typically only in the upper levels of the bed. The movement of particles in fluidized beds depends largely on the bubble properties.

2.3 Slugging bed

In deeper fluidized beds of smaller diameter, the process of bubble coalescence can result in the formation of bubbles the size of which is close or even equal to the bed diameter. Such a situation corresponds to the onset of slugging and the formed voids are called slugs. In contrast to normal bubbles, the slugs rise more slowly than bubbles of similar size. Slugging is a special case of bubbling fluidization. Slugging behaviour is strongly affected by the type

of particle for example, coarse, very angular, or cohesive particles gives “plug flow” type of slug, where the bed is occupied by series of dense and lean phase, separated by sharp horizontal interfaces [Geldart et al., 1978]. For large ratio of the particle diameter d_p to the bed diameter D , angular particles and rough bed walls, slugs tend to adhere to the wall. Slugging brings large pressure fluctuations and also reduces gas-solid mixing. Slugging is unlikely to occur in shallow bed. Onset of slug flow is highly dependent on the gas velocity and the bed dimensions. Stewart et al. [1967] proposed the following equation for the minimum slugging velocity in the bed U_{ms} .

$$U_{ms} = U_{mf} 0.07 \sqrt{gD} \quad \text{Eq. 2-13}$$

2.4 Turbulent bed

As the gas velocity is increased, the amplitude of pressure fluctuations as well as the void fraction increases in the slugging or bubbling bed. At a certain superficial gas velocity, which is often called U_c [Yerushalmi et al., 1979], the amplitude of pressure fluctuations reaches a maximum. U_c is marked by the beginning of the breakdown of bubbles and decrease of the amplitude of pressure fluctuations. Above U_c , the fluidized bed gradually gives way to a condition of increasing uniformity. Complete transition to the turbulent regime occurs at a superficial velocity U_k , where large discrete voids are absent and the amplitude of pressure fluctuations has levelled off [Yerushalmi et al., 1979], [Bi et al., 1992]. The two superficial velocities U_c and U_k increase with increasing particle size and particle density.

$$U_c = (3 \sqrt{\rho_p d_p}) - 0.17 \quad \text{Eq. 2-14}$$

$$U_k = (7 \sqrt{\rho_p d_p}) - 0.77 \quad \text{Eq. 2-15}$$

Different investigators had different opinions about turbulent fluidization. The phenomenon is not well understood. Some investigators [Geldart et al., 1986] argue that turbulent regime does not really exist, and is a transition from bubbling to fast fluidization.

Turbulent fluidization is characterised with vigorous gas-solid contacting, good mixing, high heat and mass transfer rates, high solids hold-up (typically 25-35% by volume) and relatively low axial mixing of the gas. The surface of a turbulent bed is much more diffusive than that of freely bubbling bed because of considerable entrainment of particles.

2.5 Fast fluidization

While the lower bound of the turbulent regime is represented by the characteristic velocities U_c and/or U_k , the upper limit is defined by the transport velocity U_{tr} .

$$\begin{aligned} U_{tr} &= 5.5U_t & (\text{Geldart group A}) \\ U_{tr} &= 1.7U_t & (\text{Geldart group B}) \end{aligned} \quad \text{Eq. 2-16}$$

$$U_t = \sqrt{\frac{4}{3} \left(\frac{\rho_p - \rho_g}{\rho_g} \right) \frac{d_p g}{C_w}}$$

$$C_w = \begin{cases} \frac{24}{Re_t} & \text{for } Re_t < 1 \\ \frac{24}{Re_t} + \frac{4}{\sqrt{Re_t}} + 0.4 & \text{for } 1 < Re_t < 3000 \\ 0.43 & \text{for } Re_t > 3000 \end{cases} \quad \text{Eq. 2-17}$$

$$Re_t = \frac{\rho_p U_t d_p}{\mu_g}$$

Transition from turbulent to fast fluidization is suggested to occur at the transport velocity U_{tr} . In general a fast fluidized bed is characterized by two different coexisting regions [Berruti et al., 1995], a bottom dense (bubbling region) and a dilute region (dispersed flow with a core annulus flow). As the gas flow rate is approaching this velocity, the rate of entrainment from the top of the vessel markedly increases so that it becomes essential to capture and return the entrained solids (circulating beds) or to feed fresh solids to the bottom of the column (pneumatic transport). Such a situation occurs when the gas superficial velocity is greater than the terminal velocity of a considerable fraction of the particle clusters. The transport velocity in the systems with small particles is often by an order of magnitude greater than the terminal velocity corresponding to the mean particle size. In the systems with larger particles, the transport velocity is close to the terminal velocity of an average single particle. The regime of fast fluidization is most often considered as a mode of fluidization where there is no longer a distinct interface between a dense bed and a diluted freeboard region. While the fast fluidized bed contains typically 2 to 15% by volume solids, the flow in transport bed reactor is more dilute usually with 1 to 5% by volume solids [Staub et al., 1978]. The regime of fast fluidization is characterized by a high degree of particle turbulence. Advantages of the regime of fast fluidization with respect to the bubbling and turbulent beds include higher gas throughput, control of residence time of particles, reduced tendency of particles to agglomerate, and possibility of staged addition of gaseous reactants at different levels. Erosion appears to be a serious problem in some of the circulating fluidized beds.

At the onset of pneumatic transport, the dense phase disappears in the bottom section of the riser. This region is characterized by a relatively high density and pressure fluctuations of high amplitude [Bi et al., 1992].

2.6 Regimes of fluidization

Various investigators have constructed charts to map the regimes of fluidization. The one prepared by Grace [1986] seems to be most useful for engineering applications. The axes of the Figure 2.3 represent the dimensionless variable d_p^* and U^* . Figure 2.3 shows information from Grace's original diagram plus information from other sources [Catipovic et al., 1978], [Deemter, 1980] and [Horio et al., 1986].

$$d_p^* = d_p \left(\frac{\rho_g (\rho_s - \rho_g) g}{\mu^2} \right)^{1/3} = Ar^{1/3} \quad \text{Eq. 2-18}$$

$$U^* = U \left(\frac{\rho_g^2}{\mu (\rho_s - \rho_g) g} \right)^{1/3} = \frac{Re_p}{Ar^{1/3}} \quad \text{Eq. 2-19}$$

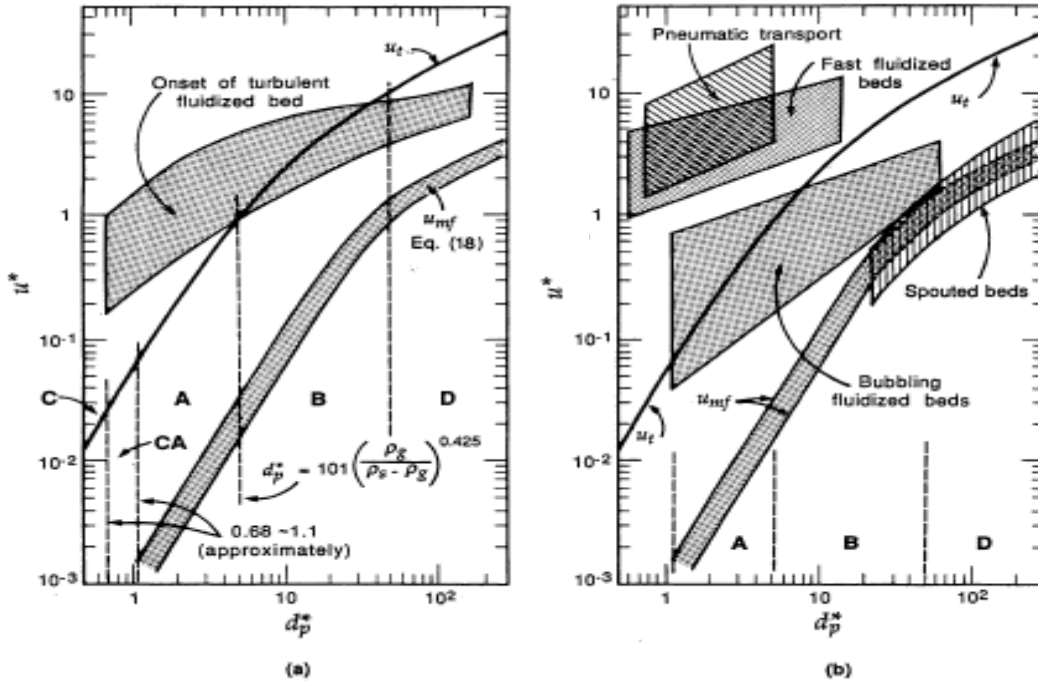


Figure 2.3: General flow regime diagram for the whole range of gas-solid contacting, from percolating packed beds to lean pneumatic transport of solids; letters C, A, B, and D refer to the Geldart classification of solids; adapted from Grace [1986], but also including information from van Deemter [1980], and Catipovic et al. [1978].

These authors showed the onset of fluidization and the terminal velocity in beds of single-size particles. They locate the modified boundaries for the Geldart classification of solids. The C-A boundary is uncertain and is affected by cohesive forces between particles. Stronger surface forces will shift the boundary to the right, and increased humidity of the

gases will shift the boundary to the left. They showed that spouting is characteristic of Geldart D solids and can occur at gas velocities lower than U_{mf} . Bubbling beds are seen to operate stably over a wide range of conditions and particle size, for Geldart A and B particles. For larger particles, these beds only operate over a relatively narrow range of gas velocities. For smaller particles, the bed can be in bubbling regime even when the gas velocity is beyond the terminal velocity of the particles. The onset of turbulent flow is gradual, and is not clearly shown on this graph, but it can be seen to occur beyond U_t for very small particle systems. For larger particles, it occurs close to U_{mf} . Fast fluidization is only practical for very small particles and at very high gas velocities, as high as approximately $1000 U_{mf}$.

2.7 Geldart classification of particles

Not every particle can be fluidized. The behaviour of solid particles in fluidized beds depends mostly on their size and the density difference. Geldart [1972, 1973] was the first to classify the behaviour of solids fluidized by gases into four clearly recognizable groups (Groups C, A, B and D) characterized by the density difference between the particles and the fluidizing medium and by the mean particle size. Geldart's classification has since become the standard to demarcate the types of gas fluidization. Geldart's classification of particle is shown in Figure 2.4. He identified four regions in which the fluidization characteristics can be distinctly defined. The Geldart Classification of particle is now widely used.

Group C materials are 'cohesive' and very fine powders. Their sizes are usually less than $30 \mu m$ and they are extremely difficult to fluidize because interparticle forces are relatively large, compared to those resulting from the action of gas. In small diameter columns, Group C particles tend to rise as a plug of solids, whereas in deep beds channelling occurs. Examples for group C particles are talc, flour and starch.

Group A is designated as 'aeratable' particles. These materials have small mean particle size ($d_p < 100 \mu m$) and these particles are larger than Group C solids. Fluid cracking catalysts typically are in this category. These solids fluidize easily, with smooth fluidization at low gas velocities without the formation of bubbles. At higher gas velocities, a point is eventually reached when bubbles start to form and the minimum bubbling velocity U_{mb} is around 2 or 3 times U_{mf} [Botterill, 1989].

Group B means intermediate size materials (sand like), usually larger and denser than Group A. Most particles of this group have size d_p , less than $1000 \mu m$. These particles are characterized by the existence of bubbles as soon as they are fluidized, i.e. $U_{mb} = U_{mf}$. Bubbles in a bed of group B particles can grow to a large size. Their growth is roughly linearly with distance from distributor and excess gas velocity $U - U_{mf}$. The bubble size is roughly independent of mean particle size and most of the bubbles rise faster than the emulsion gas. Typically used group B materials are glass beads and coarse sand.

Group D is called 'spoutable' and the materials are either very large or very dense. They are difficult to fluidize in deep beds. Unlike group B particles, as velocity increases, a jet can be formed in the bed and material may then be blown out with the jet in a spouting motion. If the gas distribution is uneven, spouting behaviour and severe channelling can be expected. Roasting coffee beans and roasting metal ores are examples of group D materials.

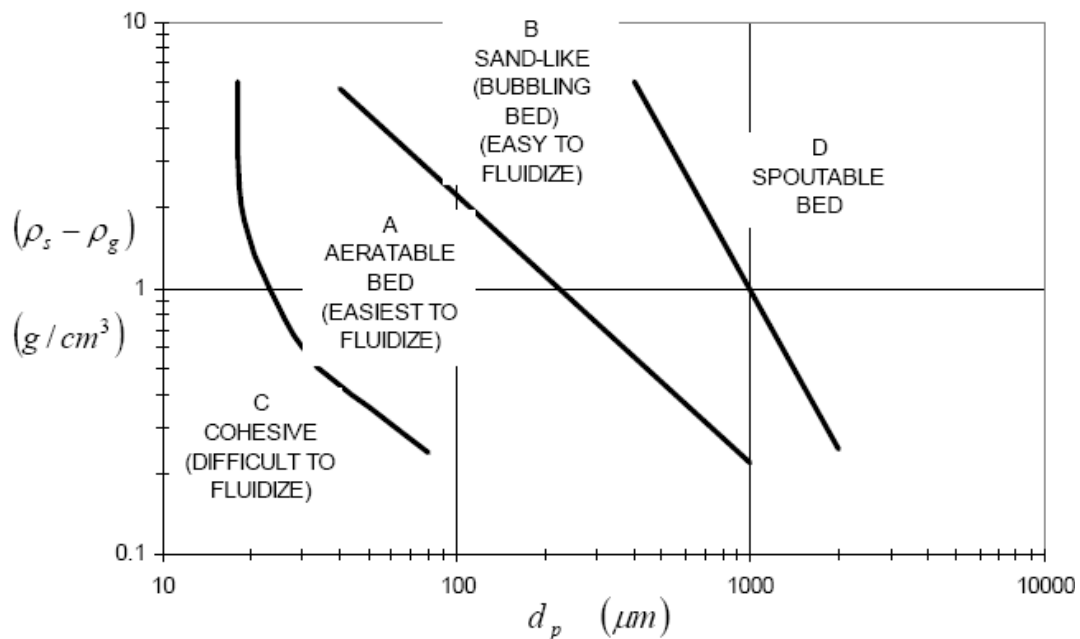


Figure 2.4: Particle classification by Geldart.

3 MODEL REVIEW

Fluidized beds are characterized by exceptional temperature uniformity, favourable heat transfer, and solids mobility, which make it attractive for different applications. In case of combustion in fluidization, the complex phenomenon requires individual modelling of the individual cases. The purpose of modelling is vast and wide. It could be optimization of process parameters, design improvement, control strategies etc.

The first attempts in fluidized bed reactor modelling were based on single-phase models neglecting the segregation of gas and solids by the presence of voids. These models tried to predict catalytic fluidized bed reactor performance solely by residence time distribution [Reman, 1955]. The inability of the single-phase model to describe fluidized bed behaviour led to the consideration of two phases [Toomey and Johnstone, 1952] and later this concept was worked out by May [1959] and van Deemter [1961]. Several modelling approaches were published in the decade of 70s [Horio et al., 1977 & 1978] and [Chen et al., 1978].

A very comprehensive model for bubbling bed combustion that couples fluid dynamic and combustion together was introduced by Horio et al. [1977]. The one dimensional bubbling fluidized bed model was also pioneered by him. The model assumed two phases (complete gas phase and a solid rich emulsion phase) in both bubbling bed as well as in free board above. The model used discrete cells to calculate the gradient of temperature and concentration of gas and solids. The above mentioned models of bubbling beds assume that nearly all material is held in the dense bed with no essential elutriation of solids into the freeboard region. Heterogeneous reactions are therefore negligible in the freeboard. This approach of modelling was adopted by many investigators [Preto, 1986], [Louis et al., 1982], [Wells et al., 1981] and Hartleben [1983]. The model proposed by Orcutt et al. [1962], later reproduced by Davidson and Harrison (1963), was one of the first, where the parameters were related to bubble dynamics. Their works have been the lighthouse for many models to follow afterwards, from bubbling to circulating fluidized beds with lean core to denser annulus approach. Yates [1983] suggests that it is convenient to divide the models into models based on empirical correlations and models based on bubble dynamics which describe reactor behaviour in terms of the known physics and hydrodynamics of fluidized beds. On the other hand, van Swaaij [1985] categorizes the models by three different levels as originally proposed by Horio [1977]:

- Level I: parameters not related to bubble size constant along the bed.
- Level II: parameters related to characteristic bubble size constant along the bed.
- Level III: parameters related to bubble size, which varies with bed height.

Table 3-1 reference to some of the outstanding models of bubbling fluidized bed. The table highlights the phases, gas flow, flow behaviour and interphase transfer considered by different authors.

Table 3-1: Models on fluidized bed operated in bubbling regime.

Reference	Phases	Gas Flow	Interphase transfer	Flow bubble	Flow emulsion
Shen & Johnstone [1955]	2-Phase Theory	2-Phase Theory	Reaction dependent	Plug flow	Plug flow, Ideally mixed
Mathis & Watson [1956]	2-Phase Theory [solids in bubbles]	2-Phase Theory	Reaction dependent	Plug flow	Plug flow
Lewis et al. [1959]	2-Phase Theory [solids in bubble]	All gas in bubble	Reaction dependent	Plug flow	Plug flow, Ideally mixed
Orcutt et al. [1962]	2-Phase Theory	2-Phase Theory	Diffusion, No resistance	Plug flow	Plug flow, Ideally mixed
Davidson & Harrison[1963]	2-Phase Theory	2-Phase Theory	Diffusion, No resistance	Plug flow	Plug flow, Ideally mixed
Rowe [1963]	2-Phase Theory [cloud, bubble, wake, emulsion]	2-Phase Theory	No resistance, No cloud-emulsion transfer	Plug flow	Plug flow
van Deemter [1967]	2-Phase Theory	Fitted	Gas mixing	Plug flow	Plug flow, Down flow
Kunii & Levenspiel [1969]	Three phases [bubble, cloud, emulsion]	2-Phase Theory, down flow of gas	Diffusion	Plug flow	Plug flow, Down flow, Stagnant
Darton [1979]	2-Phase Theory	2-Phase Theory	Diffusion, No resistance	Plug flow	Ideally mixed
Werther [1980a,b]	2-Phase Theory	2-Phase Theory	Gas mixing	Plug flow	Plug flow
Grace [1984]	2-Phase Theory [solids in bubbles]	2-Phase Theory	Diffusion, No resistance	Plug flow	Stagnant

An overview on bubbling bed and some circulating bed models can be found in Braun [1997]. Lim et al. [1995] reviewed gas-solid fluidization for hydrodynamic ranging from bubbling to fast fluidization. They gave special attention to the mixing phenomena and circulating

fluidized beds. An unconventional and interesting approach to model fluidized bed was put forward by authors like Fitzgerald et al. [1983], Glicksman [1984] and Horio et al. [1986b] who scaled fluidized bed with a set of dimensionless numbers to combine the micro scale particle behaviour with the plant dimensions. Kehlenbeck et al. [2001] developed a one-fifth scale cold flow model of a circulating fluidized-bed pilot plant for biomass gasification. Results revealed that the solid circulation rate is a function of the superficial gas velocity in the riser and the total mass load in the system.

With the work of Yerushalmi et al., 1979] there has been an increased interest in the characteristics of fast fluidization regime. Table 3-2 summarises recent studies on the fast fluidization regime. Most of the investigator agreed that they found an S-shaped solid fraction curve. This S-shaped curve moved up or down the column, depending on the solid and gas flow rates. This behaviour was found in both large-diameter (e.g. $d_p = 0.4$ m) and small-diameter (e.g. $d_p = 0.09$ m) columns.

Table 3-2: Studies on the fast fluidization regime [Kunii & Levenspiel, 1991].

Investigator	$D(cm)$	Particles	$\rho_s (kg / m^3)$	$d_p (\mu m)$
Kehoe & Davidson [1971]	5 - 10	Glass	1100	22 - 55
Massimilla [1973]	15.6	Catalyst	1000	50
Yemshdmi et al. [1976]	15.2	Alumina	1170-1470	49
Canada et al. [1976]	30	Glass	2480	650
Thiel & Potter [1977]	5	Catalyst	930	60
Crescitelli et al. [1978]	15.2	Cat.	940-1550	60-95
Kwauk et al. [1988]	9	Iron Catalyst	1780-4510	54-105
Abed [1985]	15.5	Catalyst	850	55
Zhang et al. [1985]	11.5	Glass	2130	68
Arena et al. [1988]	4.1	Glass	2600	88
Brereton & Stromberg [1986]	20	Sand	2500	170-550
Wisecarver et al. [1986]	10.2	Glass	2300-2500	65-155
Hartge & Werther [1986]	5	Quartz	-	56
Monceaux et al. [1986]	14.4	Catalyst	Bulk 900	59
Rhodes & Geldart [1987]	15.2	Alumina	1200-1800	38-64
Weinstein et al. [1986]	15.2	Catalyst	1400	59
Fusey et al. [1986]	9	Sand	2520	130
Horio et al. [1986, 88]	5	Glass	1000	60
Takeuchi et al. [1986]	10	Catalyst	1080	57
Schnitzlein [1987]	15.2	Catalyst	1070	49

The injection of secondary air few meter above the bottom air has been modelled by few investigators only [Kaiser et al., 2000, Breault et al., 1989 and Bai et al., 1997] and they all agree that it significantly affects the hydrodynamics of the gas–solid flow in the riser.

A number of circulating fluidized bed (CFB) models have been developed and reviewed by Grace et al. [1997] and Basu [1999]. However, most of the CFB models developed focus on coal combustion while biomass processing in CFBs has received less attention so far [Adanez et al., 2003], [Drift et al., 2001], [Jennen et al., 1999] and [Yin et al., 1996].

The simplest approach is for predicting gas mixing in riser operating in the fast fluidization regime is to ignore lateral or radial gradients, thereby treating the entire cross-section of the riser as if it were uniform. Such approach were modelled by Ouyang et al.[1993], Hastaoglu et al. [1988], Arena et al. [1995]

The findings of Grace [1982] and Hartge [1986] confirmed a laterally distinct zone in the freeboard of a circulating fluidized bed. The laterally distinct zones were a dilute core and a denser annulus at the wall. Most of the circulating fluidized bed operated in fast fluidization regimes are subject to predominantly down flow of relatively dense stream along the outer wall (annulus) while there is a net dilute upflow in the core. Experiment by Pugsley et al. [1995] and Bader et al. [1988] confirm the core-annulus flow, hence they modelled transport zone as a lean core and denser annulus. The core-annulus approach was also modelled by Talukdar et al. [1993], Haider [1993], Hiller [1995], Lei et al. [1998] and in this work. The axial voidage profile in the transport zone is modelled as exponential function of height as proposed by Zenz and Weil [1958], Johnsson [1991] and Wein [1992].

Table 3-3 lists some of the fast fluidized bed modelled as core-annulus flow. Most of the authors divide the bed into two zones bottom zone and freeboard zone. The bottom zone is either modelled as 'dense zone' or 'accelerated zone'. Some investigators (Rhodes [1990], Talukdar [1996]) had not considered this division of zone and assume a single zone throughout the bed. For the model that assumes two zones in the bed (Gupta & Berruti [2000], Park & Basu [1997], Hannes [1996]) the voidage in the dense zone is either dependent or are kept constant. It is conventional to assume that the cross sectional area of the core increases with the height of the fluidized bed. Different researchers use different techniques to define this relation between the core area and the height. Some models (Namkung & Kim [1998]) assume that the core area is independent of height and is a function of the cross-sectional area of the bed. The mean porosity of the bed also changes with height. Most of the authors modelled the mean voidage as an exponential decay function. Some modeled it as constant or dependent, while some assign this value from experiment (Berruti and Kalogerakis [1989]). The core voidage as seen in table is a dependent value. It depends on other variables like the core area and the mean voidage. Similarly in most of model reported (Table 3-3), the annulus voidage is also dependent on other variables. Some investigator assumes the annulus to be at minimum fluidizations condition (Berruti and Kalogerakis [1989], Hannes [1996]).

Table 3-3: Models on core annulus structure.

Reference	Zone Division	Voidage in dense zone	Core area	Mean voidage	Core voidage	Annulus voidage	Solid exchange (Core-Ann.)
Berruti and Kalogerakis [1989]	No	-	Depend	Experiment	Depend	ε_{mf}	Depend
Rhodes [1990]	No	-	Depend	Depend	Depend	Depend	MT coeff
Pugsley, et al. [1994a]	Accelerated & transport	-	$\frac{A_c}{A} = f\left(\frac{Fr}{G_s}, U\right)$	-	Depend	Depend	No
Gupta & Berruti [2000]	Dense & transport	0.82	Depend	Exp. decay	Depend	Depend	MT coeff
Harris & Davidson [1994]	No	-	Depend	Dependent	Depend	Depend	MT coeff
Park & Basu [1997]	Dense & transport	-	-	Exp. decay	-	-	-
Talukdar [1996]	No	-	Depend	Exp. decay	Depend	Depend	MT coeff
Hannes [1996]	Dense & transport	M2P T^ϕ	Depend	Exp. decay	Depend	ε_{mf}	Depend
Namkung & Kim [1998]	No	-	$\frac{A_c}{A} = Constant$	Constant	Mean porosity	Mean porosity	Depend
Talukdar & Basu [1995,1997]	No	-	Depend	Exp. decay	Depend	Depend	Depend
Rhodes, Zhou & Benkreira [1992]	No	-	Depend	Constant	Depend	Depend	No

In order to predict the combustion performance of a fluidized bed, it is necessary to combine the models for devolatilization and char combustion with expressions of overall system mass and heat balances. In Table 3-4 different fluidized bed combustion model are summarized. The table gives an overview of fluidized bed combustion models for coal and biomass (wood). Though the references are given in the table, the detailed mathematical descriptions of drying, devolatilization and char combustion are not presented here. It can be seen, most of the authors preferred the two-phase theory as suggested by Davidson and Harrison [1963]. The gas flow pattern in the fluidized bed is mainly assumed perfectly mixed in the particulate phase and plug flow in the bubble phase. Plug flow in both phases is also investigated [Horio & Wen, 1978.] In fluidized beds, the most common assumption for solid fuel particles is that they are well mixed in the bed. The combustion efficiency is influenced by the rate of char elutriation. Zhang et al. [1987] and Goel et al. [1995] considered the char particle elutriation in their model. The combustion in the freeboard depends on the operating conditions, the design, coal properties etc. The influences of the operating parameter on

^{ϕ} Modified two phase theory

freeboard combustion are only little known. Nevertheless some authors, (Zhang et al. [1987], Goel et al. [1995] etc) modelled combustion in the free board too.

Table 3-4: Models on combustion in fluidized bed.

Reference	Model	Gas	solid	Elutriation	Freeboard Rx.
Avedesian & Davidson [1973]	2 phase bubbling	Plug in bubble, mixed in emulsion	Well mixed	No	No
Campbell & Davidson [1975]	2 phase bubbling	Plug in bubble, mixed in emulsion	Well mixed	No	No
Chen & Saxena [1977]	3 phase bubbling (bubble, cloud and emulsion)	Plug in both,gas exchange	Well mixed	Yes	No
Horio & Wen [1978]	2 phase bubbling	Mixed in both phase	Well mixed	Yes	No
Gibbs et al. [1980]	2 phase bubbling	Plug in both,gas exchange	Well mixed	-	No
Zhang et al. [1987]	2 phase bubbling	Plug in bubble, mixed in emulsion	Well mixed with RTD	Yes	Yes
Goel et al. [1995]	2 phase bubbling	Plug in both,gas exchange	Well mixed	Yes	Yes
Kulasekaran et al. [1999]	3 phase bubbling (bubble, cloud and emulsion)	Plug in all phase	-	No	Yes
Hannes & Renz [1995]	Core -annulus	Plug flow	Well mixed	Yes	Yes
Sriramulu et al. [1996]	3 phase bubbling (bubble, cloud and emulsion)	Plug flow	Well mixed	-	-
Yan et al.[1998]	3 phase bubbling (bubble, cloud and emulsion)	Plug flow	Well mixed	-	Yes
Ducarne et al. [1998]	2 phase Exponential decay	Plug flow	Well mixed	-	Yes

4 CHAR CONVERSION MODEL

The combustion of char generally starts after the release of the volatiles, sometime there is an overlap of these two processes. Devolatilization is a fast process, typical time scale is 10 to 100 s for a fuel particle of 10 mm diameter). Char combustion is an order of magnitude slower (100 to 1000s).

4.1 Regimes of char conversion

The combustion of a single char particle is a combination of physical and chemical mechanisms. There are a series of steps taking place [Winter, 1995]

- The transfer of oxygen from the bulk gas to the surface of char (bulk diffusion),
- Then, if the char particle is surrounded by an inert ash layer, the oxygen must diffuse through the ash layer to the char core (ash diffusion),
- Then, if the char core is a porous system, oxygen reacts only partly at the core surface and diffuses into the pores (pore diffusion, chemical kinetics),
- Then diffusion of the product gas (CO and CO_2) through the ash layer,
- Then diffusion of the product gas (CO and CO_2) through the gas film back to the bulk gas.

Due to combustion operating conditions (temperature, pressure, mixing, fluid dynamics, mode of fluidization) and fuel characteristics (reactivity, pore structure, size, ash content, chemical composition) it is likely that the rate of a certain mechanism becomes the slowest in this consecutive scheme. Then this mechanism is controlling the char combustion process i.e. *the slowest step is the rate determining step*. This assumption simplifies the experimental and the theoretical procedure toward determining the char combustion rates.

If the rates of these mechanisms are of the same order of magnitude then the char combustion rates will be controlled by combined effects of mechanisms. As the char conversion progresses the relative importance of bulk diffusion, ash diffusion, pore diffusion and chemical reaction changes. Hence during the life time of a char particle's combustion the controlling mechanisms may change.

4.1.1 Chemical reaction controlled

If the chemical reaction rate is much slower than the mass transfer rates, the combustion process is controlled by chemical kinetics. This occurs mainly at low particle temperatures where chemical reaction rates are either slow, with fuels of low reactivity or with fine particle where there is small diffusion resistance. For non porous char particle without ash layers the combustion occurs at the external surface and as reaction progress the char shrinks with constant density (shrinking particle model). If the particle forms an ash layer, combustion occurs at the core surface and the core shrinks with constant density (shrinking core model). For macro-porous char the combustion occurs throughout the particles and consequently the char particle density decreases but the size remains constant (progressive conversion model).

The observed activation energies and reaction orders are the same as their actual value. For coarse non porous char particles in a fluidized bed reactor, this regime (chemical reaction controlled) exists at temperature around 900°C. For a fine porous char particle (where mass transfer is high) this regime (chemical reaction controlled) may exist at temperature around 800°C [Halder & Basu, 1987], [Basu & Fraser, 1991].

4.1.2 Pore diffusion controlled

The pore diffusion regime is an intermediate regime between bulk diffusion and chemical reaction regime. In this regime oxygen penetrates to a limited depth into the porous char and reacts at the pore wall. Pore diffusion and chemical reaction rate are comparable with each other. The observed activation energy is half the true value and the apparent reaction order (n) is related to the true order (m), according to the following relation.

$$n = \frac{m + 1}{2} \quad \text{Eq. 4-1}$$

Pore diffusion often controls in the circulating fluidized bed combustion with medium sized char particle [Basu & Fraser, 1991].

If the chemical reaction rate is faster than the pore diffusion rate then all the incoming oxygen will be used up at the surface and the penetration of oxygen into the pores will be small and the density of the core can be assumed to be constant. Then the burning particle can be described with a shrinking particle model, or, if an ash layer exists, with a shrinking core model.

If the chemical reaction is slow, the oxygen will penetrate deep into the pore system and its concentration profile will be similar to the porous particle controlled by chemical kinetics. In the same way it can be described with a progressive conversion model.

4.1.3 Bulk diffusion controlled

This is called diffusion controlled combustion and occurs when the mass transfer rate is very slow compared to the kinetic rate. For both porous and non porous char particles reaction takes place on their external surfaces and hence, the carbon burns with constant density. A shrinking particle or a shrinking core model can be applied.

The observed activation energy is small because the temperature dependence of the diffusivity of oxygen through the surrounding gas film is proportional $T_g^{1.5}$ to $T_g^{1.75}$ [Fuller et al., 1966], [Field et al., 1967] and the reaction order is 1. When the char particle size is big, then the combustion is often controlled by this mechanism.

4.1.4 Ash layer diffusion controlled

If the pore structure of the inert ash layer is very fine, ash layer diffusion can become the controlling mechanism. Due to relatively slow mass transfer rates compared to the reaction rates, the oxygen is consumed at core's surface before it might enter the pores. Similar to the bulk diffusion controlled regime the density of the carbon core remains constant and a shrinking core model can be applied. The observed activation energy is small and the reaction order is 1.

4.2 Modes of char conversion

The combustion regimes mentioned in previous chapter are related to different modes of char Combustion modes. These basic modes are, The Shrinking Particle Model (SPM), The Shrinking Core Model (SCM) and The Progressive Conversion Model (PCM). The main objective of all these modes is to simplify the description of the fuel particle combustion process.

4.2.1 The shrinking particle model (SPM)

The char combustion is modelled as shrinking particle model* [Figure 4-1] and it is assumed that the diameter of the char particle decreases while the density of the char remains constant. Oxidation occurs at the thin layer close to the particle surface and no ash layer is formed.

* Explained in detail in chapter 6

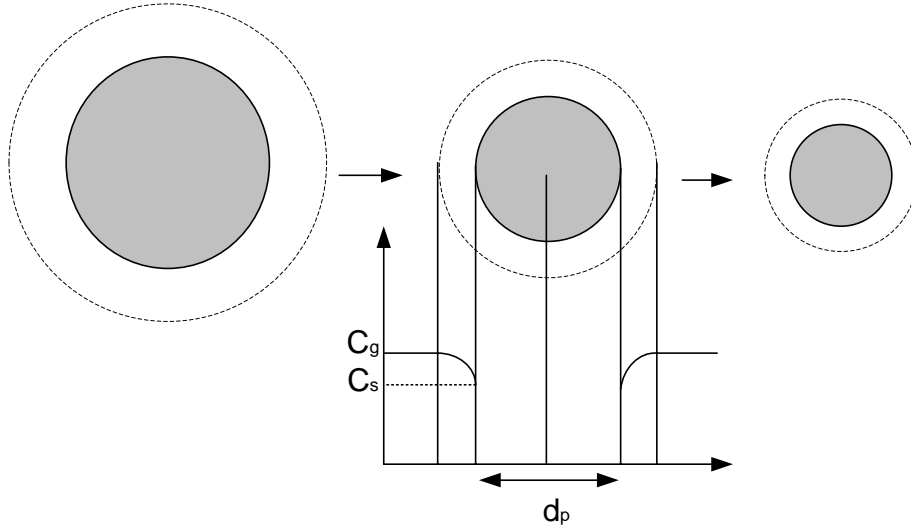


Figure 4-1: Char conversion model with the shrinking particle model.

The combustion rate in term of mass transfer through the gas film can be described as

$$q = h_m (C_g - C_s) \quad \text{Eq. 4-2}$$

C_g is the partial pressure of oxygen in bulk gas. h_m is the mass transfer coefficient. The chemical reaction rate of carbon with oxygen per unit time per unit external surface area of the particle may be written as

$$q = k_{char,s} C_s^n \quad \text{Eq. 4-3}$$

Since both diffusion limit and the chemical reaction limit are comparable to each other [Winter et al., 1995], therefore both rates are considered. For 1st order reaction ($n=1$) the combustion rate can be simplified as

$$q = \frac{1}{\frac{1}{h_m} + \frac{1}{k_{char,s}}} C_g \quad \text{Eq. 4-4}$$

4.2.2 The shrinking core model (SCM)

When it is assumed that the char particle follows the shrinking core mode mass transfer to the particle surface, mass transfer through the ash layer and chemical reaction at core surface have to be investigated. The outer diameter of the char particle stays constant, but inside the particle, the reactive core decreases continuously (and ash layer thickness increases). The density of this reactive core and ash layer is constant as shown in following Figure 4-2.

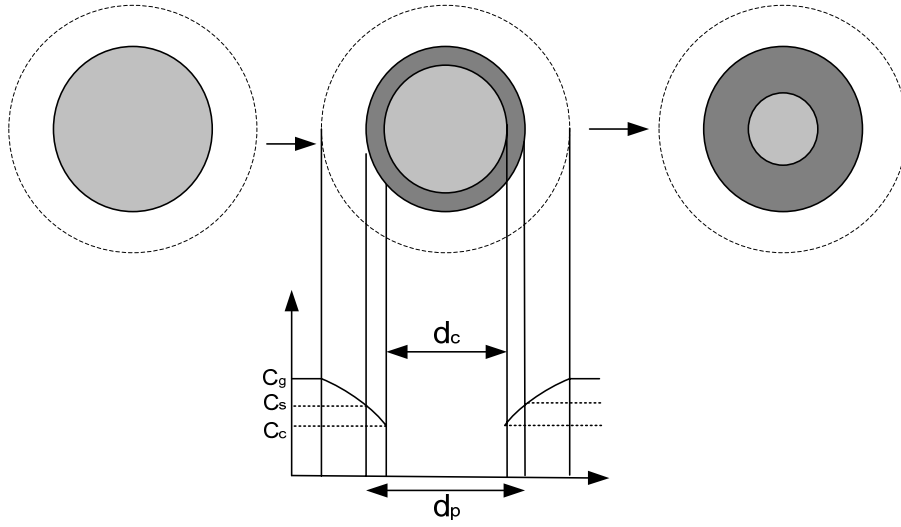


Figure 4-2: Char conversion model with the shrinking core model.

The combustion rate (Q , kg/s) in terms of the mass transfer to the particle surface is described as

$$Q = \pi d_p^2 h_m (C_g - C_s) \quad \text{Eq. 4-5}$$

To obtain the combustion rate in terms of the mass transfer through the ash film it is necessary to integrate Fick's law for diffusion from the core radius to the particle surface

$$Q = 2\pi \frac{d_p d_c}{d_p - d_c} D_{eff} (C_s - C_c) \quad \text{Eq. 4-6}$$

The chemical reaction is expressed as following n^{th} order kinetics

$$Q = \pi d_c^2 k_{char,c} C_c^n \quad \text{Eq. 4-7}$$

Equating these three cases for steady state,

$$Q = \pi d_c^2 k_{char,c} \left(C_g - \frac{Q}{\pi d_p^2 h_m} - \frac{Q}{2\pi \frac{d_p d_c}{d_p - d_c} D_{eff}} \right)^n \quad \text{Eq. 4-8}$$

The shrinking core model is frequently used in the literature especially for large, ash rich fuel [Pillai, 1981], [Andrei et al., 1983], [Abdel-Hafez, 1988], [Durao et al., 1989], [Durao et al., 1990].

4.2.3 The progressive conversion model (PCM)

In the progressive conversion model it is assumed that the diameter of the particle stays constant whereas its density is continuously decreasing throughout the particle [Figure 4-3].

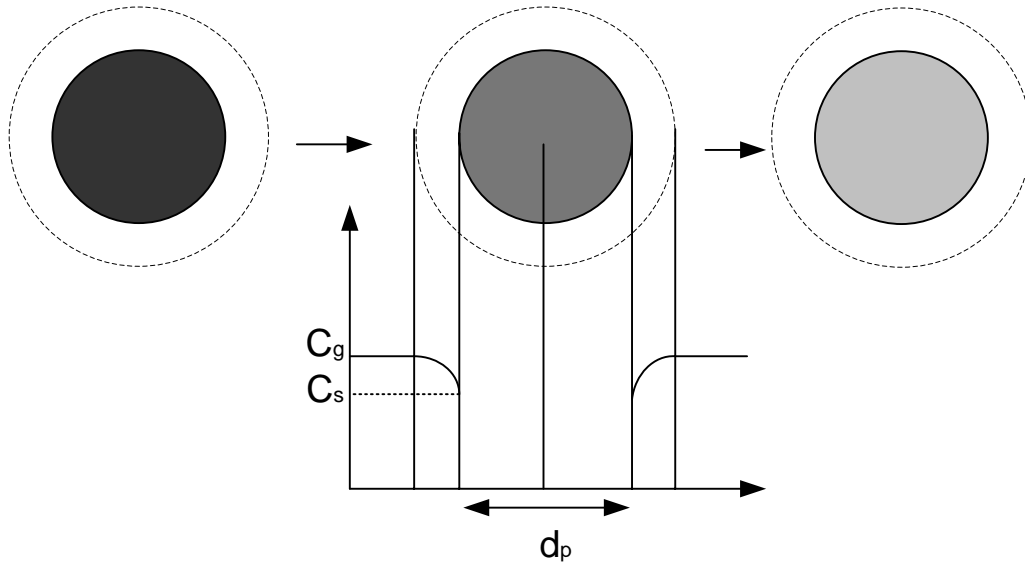


Figure 4-3: Char conversion model with the progressive conversion model.

Similar to the shrinking particle and the shrinking core model the combustion rate (Q , kg/s) in terms of the mass transfer to the particle surface is

$$Q = \pi d_p^2 h_m (C_g - C_s) \quad \text{Eq. 4-9}$$

The combustion rate (Q) based on the particle volume is

$$Q = \frac{\pi}{6} d_p^3 k_{char,p} C_s^n \quad \text{Eq. 4-10}$$

Equating these two cases for steady state, we obtain

$$Q = \frac{\pi}{6} d_p^3 k_{char,p} \left(C_g - \frac{Q}{\pi d_p^2 h_m} \right)^n \quad \text{Eq. 4-11}$$

The progressive conversion model is mainly used for small, porous char particles with low reactivity combusting in the chemical reaction and pore diffusion regimes.

5. MATERIAL CLASSIFICATION AND PROPERTIES

In the model as shown in Figure 6-1, all materials that are flowing inside or across the system boundary are levelled as any of the following classes. Each class has got its own members. Members of a class have similar properties. The objective behind the material classes is to collectively define the physical, chemical and thermodynamic properties of their members. Table 5.1 shows the classes and its members.

Table 5-1: Material classes and its member.

Class	Ideal gas	Water	Inorganic	Organic	
members	CO, CO ₂ , CH ₄ , C ₂ H ₄ , C ₂ H ₆ , H ₂ C ₃ H ₈ , H ₂ O, O ₂ , N ₂	(Liquid) H ₂ O	Bed material SiO ₂ , Fe ₂ SiO ₄ CaO, Mg ₂ SiO ₄	(Liquid) RME Fuel oil	(Solid) Char

All pure gas species (CO, CO₂) and gas mixture ('gas-stream') are members of class 'Ideal Gas'. Members of class 'Ideal gas' are defined as percentage (Vol. %) of gaseous species. (eg. bubbles in the dense bottom zone is a mixture of pure gases. The composition of bubble is defined as the volume percentage of CO, CO₂, CH₄, H₂, C₂H₄, C₂H₆, C₃H₈, H₂O, O₂ and N₂).

'Water' is a class that has pure liquid water as its member. Water at the system boundary is in liquid phase. Once it enters the system it evaporates and changes its phase from liquid to gas (Figure 6-1). When water changes its phase from liquid to gas it also changes its class from "water" to 'Ideal Gas.'

Bed material that is circulating between gasifier and combustion reactor is a member of class 'Inorganic.' Inorganic class members are defined as percentage (wt. %) of different materials. (eg. the bed material circulating may be a mixture of 50% SiO₂ and 50% CaO).

The class 'Organic' has two sub-classes as 'organic liquid' and 'organic solid'. Spent scrubber liquid and heating oil are members of sub-class 'organic liquid' where as char is a member of sub-class 'organic solid'. The chemical composition of both the sub-classes of class organic are not clear, hence the member of this class are defined in percentage (wt %) of C, H, O, N and S. Table 5-2 shows the elements and chemical species (compounds) that are present in different model classes.

Table 5-2: Table of elements.

ELEMENT	Ideal Gas (Vol %)	Water	Inorganic (wt%)	Organic (wt%)	
				Liquid	Solid
C	Y			Y	Y
H	Y	Y		Y	Y
O	Y	Y	Y	Y	Y
N	Y				
Fe			Y		
Si			Y		
Ca			Y		
Mg			Y		
Species	CO, CO ₂ , CH ₄ , C ₂ H ₄ , C ₂ H ₆ , H ₂ , H ₂ O, O ₂ , N ₂ , C ₃ H ₈	H ₂ O			

5.1 Ideal gas properties

An ideal gas is a special case of a pure substance in the vapor phase. Since the gases and gas mixture are assumed to be ideal in behaviour, therefore it follows the ideal gas law i.e.

$$PV_{\text{gas}} = n_{\text{gas}} RT \quad \text{Eq. 5-1}$$

The average molecular weight of the gas mixture is

$$M_{\text{gas}} = \sum_{i=1}^N y_i M_i \quad \text{Eq. 5-2}$$

$$m_{\text{gas}} = M_{\text{gas}} n_{\text{gas}} \quad \text{Eq. 5-3}$$

5.1.1 Molecular diffusion coefficient

The calculation uses the method of Fuller, Schettler and Giddings, described in ' Properties of Gases and Liquids ' [Reid et al., 1986]. The correlation of Fuller et al. is recommended because it has been found that this correlation yield the smallest average error of the methods discussed there [Reid et al., 1986]. $D_{A,B}$ is the diffusivity of component A in component B. The unit of $D_{A,B}$ is m^2 / s and p is pressure in bar in Eq. 5-4.

$$D_{A,B} = \frac{1.43 T^{1.75} \times 10^{-7}}{p \sqrt{M_{A,B}} \left(\left(\sum_{\nu} \right)_A^{\frac{1}{3}} + \left(\sum_{\nu} \right)_B^{\frac{1}{3}} \right)^2} \quad \text{Eq. 5-4}$$

$$M_{A,B} = 2 \left(M_A^{-1} + M_B^{-1} \right)^{-1} \quad \text{Eq. 5-5}$$

The term $(\sum_v)_A$ is calculated by summing the atomic diffusion volumes of element present in component A. In Table 5-3 the atomic diffusion volume of some common elements and compounds are tabulated.

Table 5-3: Atomic diffusion volume [Reid et al., 1986].

Atom	Diffusion volume	Atom	Diffusion volume increment
C	15.9	Cl	21.0
H	2.31	Br	21.9
O	6.11	I	29.8
N	4.54	S	22.9
F	14.7		
Diffusion volume for some simple molecule			
Molecule	Diffusion volume \sum_v	Molecule	Diffusion volume \sum_v
He	2.67	CO	18.0
Ne	5.98	CO ₂	26.9
Ar	16.2	N ₂ O	35.9
Kr	24.5	NH ₃	20.7
Xe	32.7	H ₂ O	13.1
H ₂	6.12	SF ₆	71.3
N ₂	18.5	Cl ₂	38.4
O ₂	16.3	Br ₂	69.0
Air	19.7	SO ₂	41.8

5.1.2 Viscosity

If a shearing stress is applied to a fluid, the fluid will move with velocity gradient, and the maximum velocity is the point where stress is applied. If the local stress per unit area at any point is divided by velocity gradient, the ratio obtained is called viscosity of the medium. Thus viscosity is the measure of internal fluid friction that tends to oppose any dynamic change in fluid motion. The rigorous kinetic theory of Chapman and Enskog can be extended to determine the viscosity of a low pressure multicomponent mixture. The final expression are complicated and rarely used [Reid et al., 1986]. A simplification of the kinetic theory approach was done by Wilke [1950] that neglects 2nd order effect. Wilke's method is widely accepted as it is very accurate in predicting viscosity of mixture. Reported average deviation is less than 1%. Wilke's method is interpolative in nature and need the viscosity of pure

components. The viscosity of the pure species is calculated using 3rd order polynomial correlation described in Table 5-4. The correlations for CO₂, CH₄, H₂, H₂O and N₂ are based on a table out of 'VDI-Wärmeatlas' [VDI-GVC 1997]. The correlations for CO and O₂ are according to the 'Handbook of Chemistry and Physics' [The Chemical Rubber Co. 1977]. The correlations for C₂H₄, C₂H₆ and C₃H₈ are according to Todd & Young [2002].

Table 5-4 : Viscosity of pure species [Pas].

Species	dynamic viscosity [Pas]
CO	$(6.12430\text{E} - 08 * T^3 - 9.58389\text{E} - 05 * T^2 + 8.48528\text{E} - 02 * T - 6.97080\text{E} - 01) * 10^{-6}$
CO ₂	$(4.87022\text{E} - 09 * T^3 - 2.34095\text{E} - 05 * T^2 + 6.11504\text{E} - 02 * T - 1.33587\text{E} + 00) * 10^{-6}$
CH ₄	$(9.83710\text{E} - 10 * T^3 - 1.82433\text{E} - 05 * T^2 + 4.28954\text{E} - 02 * T - 2.00742\text{E} - 01) * 10^{-6}$
C ₂ H ₄	$(0.00000\text{E} - 00 * T^3 + 1.28439\text{E} - 05 * T^2 + 1.86644\text{E} - 03 * T + 9.892789\text{E} - 01) * 10^{-6}$
C ₂ H ₆	$(1.41977\text{E} - 09 * T^3 - 7.410209\text{E} - 6 * T^2 + 2.70827\text{E} - 02 * T + 1.297213\text{E} + 01) * 10^{-6}$
C ₃ H ₈	$(7.90416\text{E} - 10 * T^3 - 5.60498\text{E} - 06 * T^2 + 2.47048\text{E} - 02 * T + 8.54300\text{E} - 00) * 10^{-6}$
H ₂	$(4.58331\text{E} - 09 * T^3 - 1.37650\text{E} - 05 * T^2 + 2.73110\text{E} - 02 * T + 1.88272\text{E} + 00) * 10^{-6}$
H ₂ O	$(-5.9916\text{E} - 09 * T^3 + 1.15667\text{E} - 05 * T^2 + 3.37086\text{E} - 02 * T - 1.677664\text{E} + 00) * 10^{-6}$
O ₂	$(1.39088\text{E} - 08 * T^3 - 4.49772\text{E} - 05 * T^2 + 7.72693\text{E} - 02 * T + 9.85268\text{E} - 01) * 10^{-6}$
N ₂	$(1.89696\text{E} - 08 * T^3 - 4.99074\text{E} - 05 * T^2 + 7.22905\text{E} - 02 * T + 1.66136\text{E} - 01) * 10^{-6}$

Viscosity for a mixture (μ_m) of n species is

$$\mu_m = \sum_{i=1}^n \frac{y_i \mu_i}{\sum_{j=1}^n y_j \phi_{ij}} \quad \text{Eq. 5-6}$$

$$\phi_{ij} = \frac{\left[1 + \left(\frac{\mu_i}{\mu_j} \right)^{1/2} \left(\frac{M_j}{M_i} \right)^{1/4} \right]^2}{\left[8 \left(1 + \frac{M_j}{M_i} \right) \right]^{1/2}} \quad \text{Eq. 5-7}$$

5.1.3 Enthalpy and entropy

Enthalpy and entropy of pure component for isobaric condition is defined in Eq. 5-8 and Eq. 5-9 respectively.

$$H_i(T) = \Delta H_{f,298,i}^0 + \int_{298.15}^T C_{P,i}(T) \cdot dT \quad \text{Eq. 5-8}$$

$$S_i^0(T) = S_{298,i}^0 + \int_{298.15}^T \frac{C_{P,i}(T)}{T} \cdot dT \quad \text{Eq. 5-9}$$

The temperature dependence heat capacity at constant pressure C_p is described in Eq. 5-10 in terms of 4th order NASA polynomial [Gordon & McBride, 1971].

$$\frac{C_p(T)}{R} = a_1 + a_2 \cdot T + a_3 \cdot T^2 + a_4 \cdot T^3 + a_5 \cdot T^4 \quad \text{Eq. 5-10}$$

Integrating Eq. 5-10 and substituting the integral in Eq. 5-8 and Eq. 5-9 gives the enthalpy and standard state entropy respectively.

$$\frac{H(T)}{R \cdot T} = a_1 + \frac{a_2}{2} \cdot T + \frac{a_3}{3} \cdot T^2 + \frac{a_4}{4} \cdot T^3 + \frac{a_5}{5} \cdot T^4 + \frac{a_6}{T} \quad \text{Eq. 5-11}$$

$$\frac{S^0(T)}{R} = a_1 \cdot \ln T + a_2 \cdot T + \frac{a_3}{2} \cdot T^2 + \frac{a_4}{3} \cdot T^3 + \frac{a_5}{4} \cdot T^4 + a_7 \quad \text{Eq. 5-12}$$

The coefficient a_6 and a_7 is also provided in the table. Burcat & McBride [1997] summarized the coefficients a_1 to a_7 for a variety of materials, in two sets of temperature one set for ($T \leq 1000$ K) and other set for ($T > 1000$ K). The JANAF table (Table 5-5) [Chase et al., 1985] supplies the basis for the data needed in this work. The enthalpy of ideal gases mixtures is linear with the composition [Baehr, 2000]. The enthalpy of a gas mixture can be computed as

$$H_{\text{gas}}(T) = \sum_{i=1}^N y_i H_i(T) \quad \text{Eq. 5-13}$$

Table 5-5: Properties of ideal gas species (standard enthalpy of formation, standard entropy and heating value).

Gas	M	$\Delta H_{f,298}^0$	S_{298}^0	H_u
	g/mol	J/mol	J/(mol·K)	J/mol
CO	28.010	-1.10E+05	197.657	2.829E+05
CO ₂	44.010	-3.93E+05	213.787	0.000E+00
CH ₄	16.043	-7.48E+04	186.167	8.022E+05
C ₂ H ₄	28.054	5.22 E+04	219.18	1.322E+06
C ₂ H ₆	30.069	-8.48E+04	229.08	1.427E+06
C ₃ H ₈	44.096	-1.03E+05	270.182	2.043E+06
H ₂	2.016	0.00 E+00	130.679	2.410E+05
H ₂ O(g)	18.015	-2.41E+05	188.829	0.0E+00
O ₂	31.999	0.00 E+00	205.149	0.0E+00
N ₂	28.013	0.00 E+00	191.607	0.0E+00

5.2 Water

Water is modelled as material fluid, which is present as liquid at the system boundary, but inside the system it is in gaseous state. So water in its liquid form is encountered only when the energy balance is implemented. The standard values for liquid water are $\Delta H_{f,298,H_2O(l)}^0 = 2.85E+05$ J/mol and $\Delta S_{298,H_2O(l)}^0 = 69.939$ J/(mol.K) [Burcat & McBride, 1997], the molar mass of H_2O amounts to 18.015 g/mol. Similar to the ideal gas, the temperature dependence of the enthalpy of water is described in terms of 4th order NASA polynomial

5.3 Inorganic

Inorganic are very much like ideal gas i.e. mixture of chemically defined component. The composition of the solid stream is described in weight fraction of the bed materials. The bed materials that are present in the databank of the model are shown in Table 5-6. From the thermodynamic point of view only the temperature dependence is considered. The enthalpy of a pure solid species as a function of temperature is described in terms of 4th order NASA polynomial.

For a solid mixture

$$H_{bed}(T) = \sum_{i=1}^N w_i H_i(T) \quad \text{Eq. 5-14}$$

$$h_{bed}(T) = \sum_{i=1}^N \frac{w_i H_i(T)}{M_i} \quad \text{Eq. 5-15}$$

Table 5-6: Types of bed material and their standard enthalpy of formation and entropy.

Bed material	w	M (g/mol)	$\Delta H_{f,298}^0$ (J/mol)	S_{298}^0 (J/mol·K)
CaO	w_{CaO}	56.077	-6.35 E+05	38.07
SiO ₂	w_{SiO_2}	60.084	-9.10 E+05	41.46
Mg ₂ SiO ₄	$w_{Mg_2SiO_4}$	140.693	-2.17E+06	95.14
Fe ₂ SiO ₄	$w_{Fe_2SiO_4}$	203.777	-1.47 E+06	145.20
Σ	1	-	-	-

The coefficients for the solids (Table 5-7) are tabulated by Ihsan Barin [Barin, 1995].Like the ideal gas, for inorganic solids too, there are two sets of coefficients, one for the lower temperature range and other for the upper temperature range.

Table 5-7: Coefficient for calculation of the thermodynamic properties using the NASA polynomial approach [Barin,1995].

	T_{min} (K)	T_{max} (K)	a_1	a_2	a_3	a_4	a_5	a_6	a_7
Gas									
CO	200	1000	3.048486E+00	1.351728E-03	-4.857941E-07	7.885364E-11	-4.698075E-15	-1.426612E+04	6.017098E+00
	1000	6000	3.579534E+00	-6.103537E-04	1.016814E-06	9.070059E-10	-9.044245E-13	-1.434409E+04	3.508409E+00
CO ₂	200	1000	4.636511E+00	2.741457E-03	-9.958976E-07	1.603867E-10	-9.161986E-15	-4.902490E+04	-1.934896E+00
	1000	6000	2.356813E+00	8.984130E-03	-7.122063E-06	2.457301E-09	-1.428855E-13	-4.837197E+04	9.900904E+00
CH ₄	300	1000	2.359405E+00	8.730941E-03	-2.839705E-06	4.045984E-10	-2.052710E-14	-1.028882E+04	6.029001E+00
	1000	5000	2.928396E+00	2.569109E-03	7.843706E-06	-4.910298E-09	2.038003E-13	-1.005417E+04	4.634222E+00
C ₂ H ₄	300	1000	4.398545E+00	9.622861E-03	-3.166378E-06	4.574763E-10	-2.365941E-14	4.115320E+03	-2.462744E+00
	1000	5000	1.217660E+00	1.300268E-02	3.503745E-06	-1.115551E-08	4.720322E-12	5.337383E+03	1.548017E+01
C ₂ H ₆	300	1000	4.702885E+00	1.404264E-02	-4.646938E-06	6.747374E-10	-3.508931E-14	-1.267199E+04	-4.543395E+00
	1000	5000	1.539526E+00	1.504084E-02	6.684712E-06	-1.338295E-08	4.856140E-12	-1.124877E+04	1.410738E+01
C ₃ H ₈	300	1000	7.534137E+00	1.887224E-02	-6.271849E-06	9.147565E-10	-4.783807E-14	-1.646752E+04	-1.789235E+01
	1000	5000	9.335538E-01	2.642458E-02	6.105973E-06	-2.197750E-08	9.514925E-12	-1.395852E+04	1.920169E+01
H ₂	200	1000	2.932831E+00	8.265980E-04	-1.464006E-07	1.540985E-11	-6.887962E-16	-8.130558E+02	-1.024316E+00
	1000	6000	2.344303E+00	7.980425E-03	-1.947792E-05	2.015697E-08	-7.376029E-12	-9.179241E+02	6.830022E-01
H ₂ O	200	1000	2.677039E+00	2.973182E-03	-7.737689E-07	9.443351E-11	-4.268999E-15	-2.988589E+04	6.882550E+00
	1000	6000	4.198635E+00	-2.036402E-03	6.520342E-06	-5.487927E-09	1.771968E-12	-3.029373E+04	-8.490090E-01
O ₂	200	1000	3.660961E+00	6.563655E-04	-1.411495E-07	2.057977E-11	-1.299132E-15	-1.215977E+03	3.415362E+00
	1000	6000	3.782456E+00	-2.996734E-03	9.847302E-06	-9.681295E-09	3.243728E-12	-1.063944E+03	3.657676E+00
N ₂	200	1000	2.952541E+00	1.396884E-03	-4.926258E-07	7.860009E-11	-4.607498E-15	-9.239375E+02	5.871822E+00
	1000	6000	3.530963E+00	-1.236595E-04	-5.029934E-07	2.435277E-09	-1.408795E-12	-1.046964E+03	2.967439E+00
Inorganic									
SiO ₂	300	1000	5.591942E+01	-1.448622E-01	1.619612E-04	-7.894187E-08	1.4279731E-11	-1.247154E+05	-2.857243E+02
	1000	1700	6.860991E+00	-2.473208E-02	9.592132E-05	-1.110188E-07	4.1324849E-11	-1.110985E+05	-3.001988E+01
Mg ₂ SiO ₄	300	1000	1.061837E+01	2.087193E-02	-1.575732E-05	6.182795E-09	-9.270436E-13	-2.658377E+05	-5.480953E+01
	1000	2171	3.362243E-01	7.351565E-02	-1.119956E-04	8.185677E-08	-2.272431E-11	-2.643570E+05	-8.082881E+00
Fe ₂ SiO ₄	300	1000	-2.525026E+01	1.4744929E-01	-1.7586684E-04	9.5931433E-08	-1.9499119E-11	-1.736847E+05	1.2907704E+02
	1000	1490	1.3952594E+00	8.0312963E-02	-1.34331E-04	1.0768664E-07	-3.2299364E-11	-1.809861E+05	-9.333655E+00
CaO	300	1000	5.1451406E+00	2.1137313E-03	-1.0915919E-06	3.2412832E-10	-3.5547897E-14	-7.805970E+04	-2.517389E+01
	1000	3200	1.5783523E+00	1.8815154E-02	-2.9795129E-05	2.1894089E-08	-6.0366053E-12	-7.746806E+04	-8.574768E+00

5.4 Organic

The class 'organic' is different from other classes because the members (RME, char, biomass) of this class are not very clearly chemically defined. Elemental analysis reveals that they are complex chemically-bonded mixtures of elements like C,H,O,N,S,Cl etc. The enthalpy of an organic specie can be expressed by

$$h(T) = \Delta h_{f,298}^0 + \int_{298.15}^T c_p(T) dT \quad \text{Eq. 5-16}$$

The standard enthalpy of formation is calculated from the heating value. The heat capacity C_p is calculated from empirical equation. C_p as a function of temperature can be mathematically formulated as

$$c_p(T) = kT + d \quad \text{Eq. 5-17}$$

Integrating Eq. 5-17 in Eq. 5-16 gives enthalpy of the liquid organic species

$$h(T) = \Delta h_{f,298}^0 + \frac{k}{2}(T^2 - T_0^2) + d(T - T_0) \quad \text{Eq. 5-18}$$

Rapeseed oil methyl ester (RME), and liquid fuel (heating oil) enters at a temperature approximately near $\sim 80^\circ\text{C}$ in the process. The coefficient 'k' and 'd' for the above equation for different organic species is given in Table 5-8. These data are valid for temperature as high as 300°C . For heat capacity and enthalpy of solid organic (char) the following relations are taken from the literature [Merrick, 1988].

$$c_p(T) = \frac{R}{M_{wt}} \left\{ \exp\left(\frac{380}{T}\right) \left[\frac{\exp\left(\frac{380}{T}\right) - 1}{\frac{380}{T}} \right]^{-2} + 2 \exp\left(\frac{1800}{T}\right) \left[\frac{\exp\left(\frac{1800}{T}\right) - 1}{\frac{1800}{T}} \right]^{-2} \right\} \quad \text{Eq. 5-19}$$

The average molecular weight M_{wt} of the char in above equation is calculated according to Eq. 5-20.

$$M_{wt} = \left[\sum_i \left(\frac{w_i}{M_i} \right) \right]^{-1} \quad \text{Eq. 5-20}$$

Integrating Eq. 5-19 in Eq. 5-21 gives enthalpy of the char (Eq. 5-22).

$$h(T) = \Delta h_{f,298}^0 + \int_{298.15}^T c_p(T) dT \quad \text{Eq. 5-21}$$

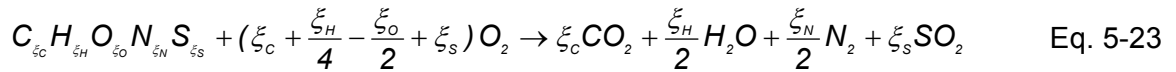
$$h(T) = \Delta h_{f,298}^0 + \frac{R}{M_{waf}} \left[\left[\frac{380}{\exp\left(\frac{380}{T}\right) - 1} + \frac{2(1800)}{\exp\left(\frac{1800}{T}\right) - 1} \right] - \left[\frac{380}{\exp\left(\frac{380}{T_o}\right) - 1} + \frac{2(1800)}{\exp\left(\frac{1800}{T_o}\right) - 1} \right] \right] \quad \text{Eq. 5-22}$$

The enthalpy of formation at standard state is calculated from the heating value Eq. 5-24.

Table 5-8: Coefficient k and d for RME.

Organic	$k \text{ [J/kg K}^2\text{]}$	$d \text{ [J/kg K]}$	$T \text{ [K]}$	Reference
RME	3.35	850	298-423	[Goodrum & Eiteman, 1996]
Heating oil	-	2000	298	-

In energy engineering the energy chemically bound in a fuel is expressed traditionally by the heat value H_u . The heating value is defined as the energy released during the complete combustion of a unit quantity of fuel with O_2 to produce CO_2 , H_2O , SO_2 , and N_2 . In general the complete combustion reaction can be formulated as



The temperature of combustion is the standard temperature of 298.15 K. H_2O present in the exhaust gas is in gaseous state

For chemically defined species (e.g. CH_4 , C_2H_4 or gas mixture) the heating value can be computed directly as difference of the standard enthalpies of formation of fuel (reactant) and the products.

$$H_u = \Delta H_{f,298}^0 - \xi_C \cdot \Delta H_{f,298,CO_2}^0 - \frac{\xi_H}{2} \cdot \Delta H_{f,298,H_2O(g)}^0 - \xi_S \cdot \Delta H_{f,298,SO_2}^0 \quad \text{Eq. 5-24}$$

For ideal gas mixtures the enthalpy of mixing is zero and the resulting heating value is a linear combination of the heating value of individual gases.

$$H_{U, gas} = \sum_{i=1}^N (y_i H_{U,i}) \quad \text{Eq. 5-25}$$

The molecular structure of the organic is not known clearly, therefore for the computation of the heating values of organic fuels empirical correlations based on the elementary composition are used. For the class 'organic' (solid and liquid) the formula of Boie[†] (Eq.1.3) is implemented Comparing Eq. 5-24 and Eq. 1.3 the standard enthalpy of formation for organic material mixtures can be calculated from the heating values and elementary analysis [Schuster et al., 2001].

[†] Eq.1.3 : $H_U = 34835 w_c + 93870 w_H - 10800 w_O + 6280 w_N + 10465 w_S$

6. MODEL DEVELOPMENT

The fundamental idea of the Dual Fluidized Bed (DFB)¹ concept is to divide the gasification process into two fluidized bed reactors, a gasifier and a combustion reactor (riser). The energy needed for the endothermic gasification reactions in the gasifier is generated by combustion of residual char in the riser and is transported to the gasification reactor by circulating bed material [Proell et al., 2005]. Since a longer residence time is required in the gasifier, so it is designed as a bubbling bed while the riser is designed as fast fluidized bed.

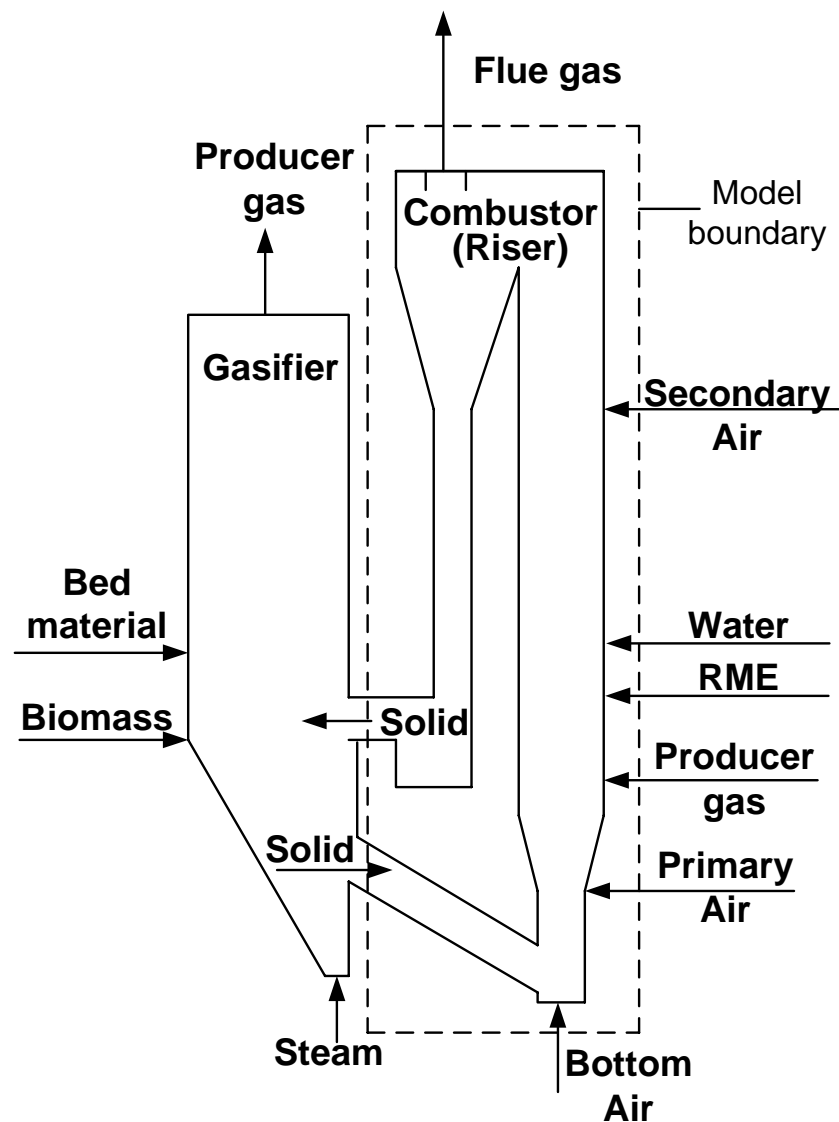


Figure 6-1: Modelling boundary of the DFB gasification plant.

¹ The gasification reactor of the DFB is named gasifier, while combustion reactor is named riser

The boundaries of the investigated system are the connecting chute at the bottom of the riser where the bed material enters together with the residual biomass char from the gasifier and the cyclone at the top of the riser where the hot solids (bed material and spent char) are separated from the flue gas stream. Fluidization and combustion air is introduced at three points into the riser as bottom air, primary air and secondary air. In the region where the primary air enters, low amount of clean producer gas is recycled into the riser. Additional fuel (producer gas) is introduced in riser in order to control the gasification temperature. A fraction of the spent scrubber solvent i.e. tar-loaded bio diesel (rapeseed oil methyl ester – RME) emulsified in water (separated in an equalization tank) (Figure 1- 4) and is continuously introduced in the riser while the remaining is partially evaporated and sent to the hot flue gas line. So the riser is also modelled to serve as a sink for spent scrubber solvent. This emulsion (RME + water) is also introduced as in the region of primary air introduction.

The primary aim of this study is to develop a model for the combustion of char in order to predict the gas phase concentration and temperature profile along the height axis of the riser. Directly measured validation data from the 8 MW (fuel power) gasification plant in Guessing/Austria is limited to several temperatures along the height of the riser and the final flue gas composition only.

To handle the geometry of the riser in the mathematical model, it is simplified in a reasonable way. Figure 6-2 shows the simplified geometry used for the simulation of the demonstration plant. The upper part of the riser is assumed to be a perfect cylinder of 8 meters height. For the initial two meters of height the diameter of the riser is 0.61 meter, for the next 2 meters (i.e. from 2 meter to 4 meter height) the diameter increases with an angel of 3° up to a height of 4 meters. Finally from a height of four meters the diameter becomes constant at 0.66 meter. Primary air, producer gas, RME emulsion and secondary air enter the riser at heights of 2, 3, 3.5 and 4 meters respectively. There are five active thermocouples and pressure gauges in the riser along the height of the riser. The bed material and residual char from the gasifier enters the riser at reference level (0 meter). Present work focuses on the mathematical modelling of the riser according to Figure 6-3.

Model Assumptions

To model the combustion rector (riser) of the dual fluidized bed gasification system the following assumption are made

- The model is one dimensional, in steady state and isothermal in each zone.
- Gases are ideal and are in plug flow regime. [Caram & Amundson, 1979] [Gururajan et al., 1992] [Chatterjee et al., 1995] [Purdy et al., 1984].

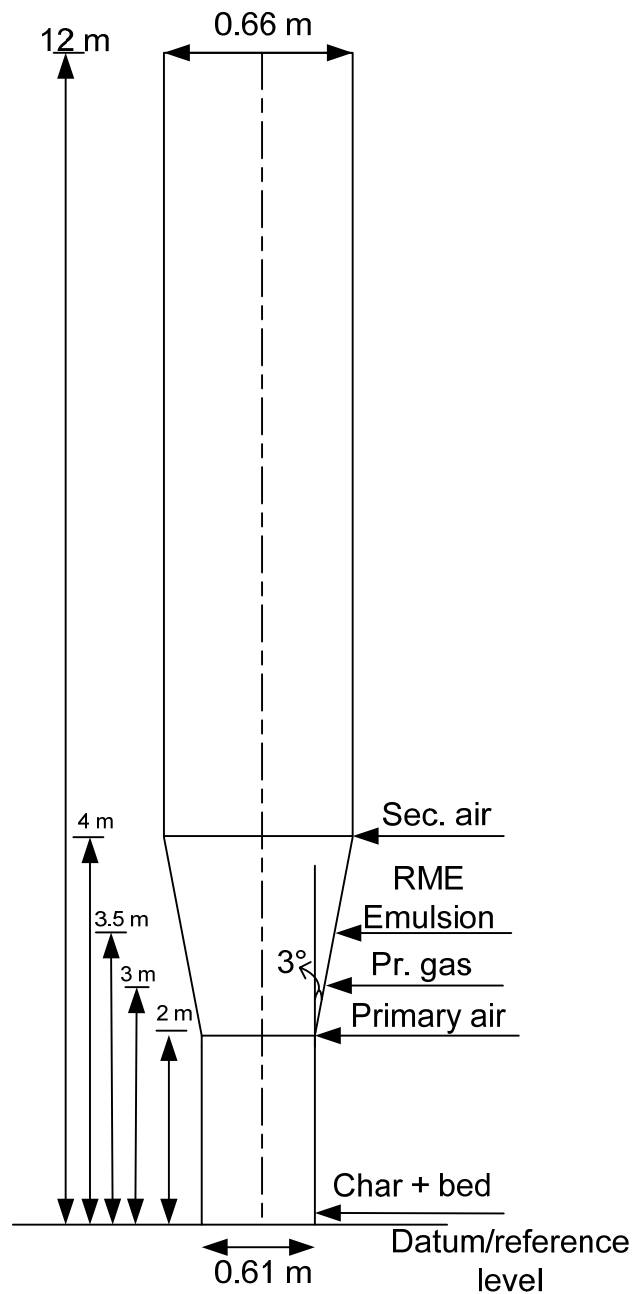


Figure 6-2: Simplified geometry of the riser.

- The mass transfer between bubble and emulsion is modelled with mass transfer coefficient.
- Axial diffusivity of gas is assumed to be zero.
- Solids are uniform in size, perfectly mixed with no attrition and are classified as Geldart type "B". Inorganic bed materials are chemically inert.
- The fluid dynamic parameters are evaluated with the material properties of the inert bed.

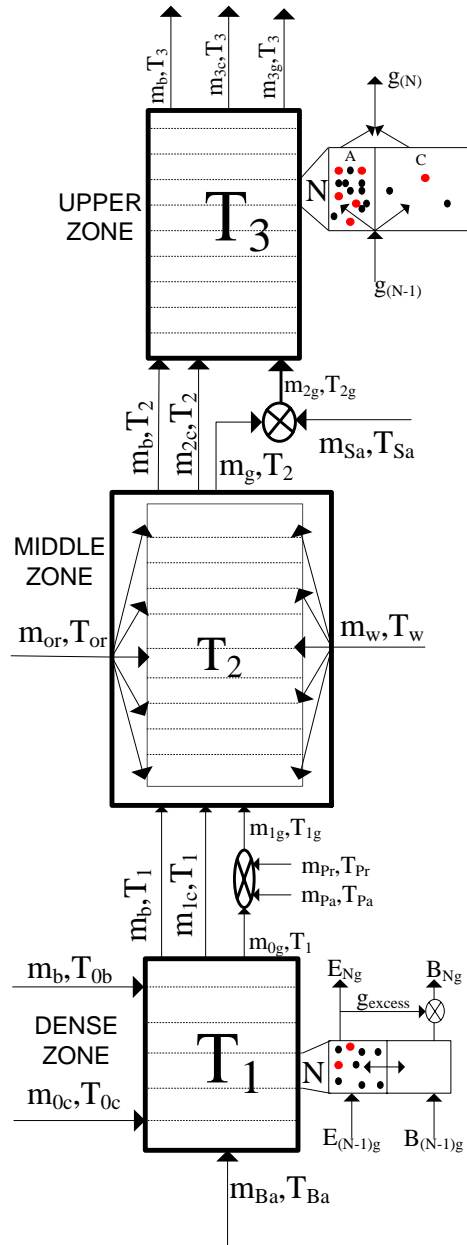


Figure 6-3: Structure of the riser model.

- Char is spherical and is a homogeneous matrix of carbon, hydrogen and oxygen, and its composition is described by ultimate analysis.
- Composition of char is a model parameter.
- Bubbles are solid free.
- Through flow in bubble is lumped with bubble flow (Table 6-1, 2)
- Dense bed is assumed to follow the modified two phase theory.
- Transport zone is assumed to have a core-annulus structure.
- No heat loss in the process.

The riser is divided into two zones, dense zone and transport zone. The transport zone is further sub-divided into a middle zone and upper zone as seen in Figure 6-3. Preheated bottom air, residual char and bed material (from gasifier) is introduced in the dense bed where combustion takes place. At the exit of dense zone the flow rate, composition and temperature of coke and gas phase is changed to a new value (Figure 6-3). The char and bed material then goes to the middle zone while the exiting gas (dense zone) is introduced to a mixer, where the preheated primary air and producer gas are also introduced. This mixer adiabatically mixes these three gas stream to form a homogeneous gas phase and is then introduced in the middle zone. In the middle zone combustion of char and producer gas takes place. At the outer boundary of this zone the temperature, composition and flow rate of gas phase and char is changed to a new value. The exiting gas phase is then mixed with the preheated secondary air in the adiabatic mixer to a new composition and temperature and is introduced in the upper zone. In the upper zone char is further combusted. The exiting stream from upper zone goes to the cyclone, where the gas phase (flue gas) is separated from the solid phase. Solid exiting from the cyclone consists of inert bed material and unburnt char. The blow down from cyclone is recycled back into the gasifier. The middle zone is a special case. In the middle zone the evaporation and gasification of the introduced emulsion take place. Each zone is further divided into cells. Each cell calculates its local kinetic, hydrodynamic and thermodynamic state based on theoretical principles. The cells are solved sequentially from bottom to top with the output of each cell considered as input for the next cell. The conservation equations for carbon, bed material, and energy are not evaluated in each cell, but across the entire zone. Therefore, each zone shows a homogeneous char concentration. The code for the model is written in a Microsoft visual C++ environment.

6.1 Hydrodynamic sub-model

The riser is a very complex part of dual fluidized bed assembly. Therefore a reasonable description of the phenomenon occurring here must be focused while modelling. The riser is a fast fluidized bed often seen as intermediate state between bubbling bed and pneumatic transport, and a dense bed in the bottom with small axial expansion is observed [Johnsson et al., 1991].

Hence the Riser is divided into two zones with different hydrodynamic characteristics

- dense zone
- transport zone

6.1.1 Dense zone

Dense zone, in most cases is in bubbling regime and is hence modelled as bubbling fluidized bed. A number of reviews of bubbling fluidized bed models is provided in literature [Pyle, 1970], [Grace, 1971], [Rowe, 1972], [Yates, 1975], [van Swaaij, 1978], [Yates, 1983], [van Swaaij, 1985] and [Grace, 1986a,b]. Numerous different models have been based on the concept of phase division as indicated below

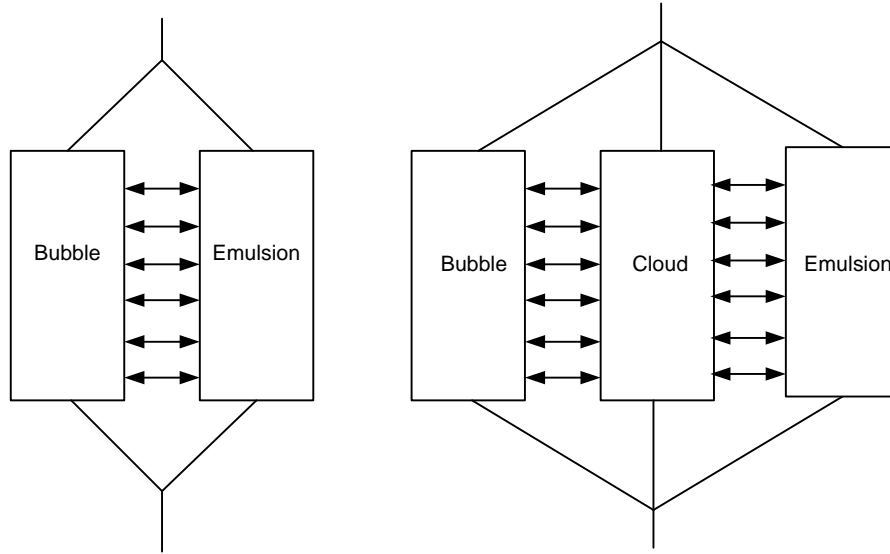


Figure 6-4: Typical models of bubbling bed.

The description of the expansion of a bubbling fluidized bed is derived from the Two-Phase Theory of fluidization by Toomey et al. [1952]. According to two phase theory the bubbling fluidized bed is composed of two phases; the bubbling phase (the gas bubbles) and the emulsion phase (the fluidized solids around the bubbles). The theory states that any gas in excess of that required at minimum fluidization will pass through the bed as bubbles. Thus, in bubbling fluidization, bed expansion at velocities beyond minimum bubbling velocity is due to the presence of bubbles.

If Q is actual gas flow and Q_{mf} is the gas flow for minimum fluidization condition then the amount of gas passing through the bed as bubbles is

$$Q_B = Q - Q_{mf} = (U - U_{mf}) A \quad \text{Eq. 6-1}$$

Modified two phase theory

In practicality two phase theory overestimate the amount of gas flowing through the bed as bubble. So to correct this overestimation two phase theory is modified by many authors [Pyle

et al., 1967], [Grace et al., 1969] and [Chavarie, 1973] etc. A generalised representation for the visible bubble flow rate is

$$Q_B = Y(U - U_{mf})A \quad \text{Eq. 6-2}$$

Y is always below unity and usually in the range from 0.7 to 0.8, but can also be 0.3 for coarse particles [Hilligardt et al., 1986]. As can be seen in Figure 6-5 the value of Y quoted by various investigators varies reasonably. Nevertheless a general behaviour of Y as a function of Ar number is presented by [Baeyens, 1981] [Figure 6-5]

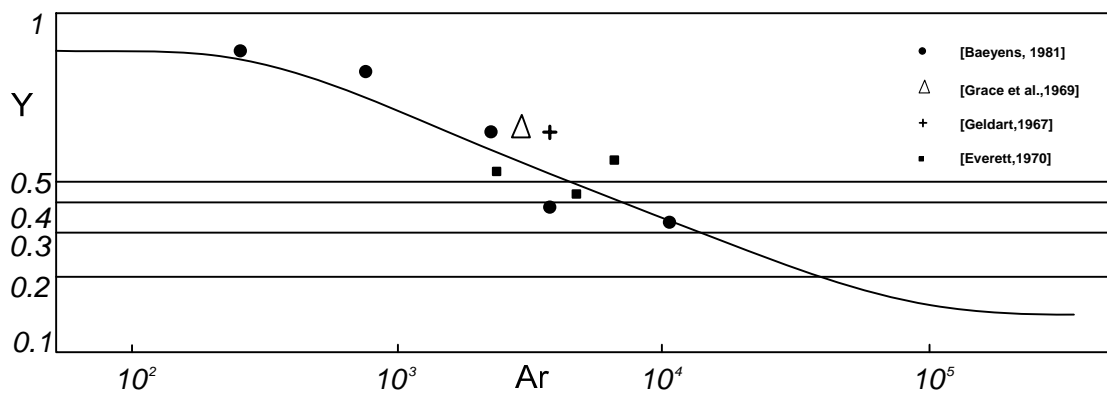


Figure 6-5: A generalised behaviour of Y as a function of Ar Number.

$$Y = \frac{0.26 + 0.7 \exp(-0.0033 d_p)}{[0.15 + (U - U_{mf})]^{0.33}} \left(z + 4 \sqrt{\frac{A}{N_{or}}} \right)^{0.4} \quad \text{Eq. 6-3}$$

Investigators [Pyle et al., 1967], [Godard et al., 1968], [Rowe et al., 1972] have attributed this deficit in bubble phase to an increase in interstitial gas velocity in emulsion phase above that required for incipient fluidization. This modified division of gas flow between phases is more favourable for gas solid reaction than predicted by Toomey et al. [1952]. The flows assumed for each phases by different versions of the modified two phase theory are listed in Table 6-1.

It is clear from Table 6-1 that the fraction of the total flow in the dense phase varies considerably according to the interpretation adopted by different workers. The range of dense phase flow is between 14% and 59% of the total gas flow. It would be even greater if recent work [Kunii & Levenspiel, 1991], which assumes net downflow in the dense phase were considered.

The original two phase theory postulate provides one estimate for the total flows in each phase, (though the visible bubble flow is overestimated). To overcome this limitation of original two phase theory, other approaches (Table 6-1 (2, 3, 4) etc) were put forward.

The modified two phase theory (Table 6-1 (2)), assumes that the visible bubble flow is less than what is predicted by original two phase theory. The visible bubble flow (G_B) according to modified two phase theory is $Y(U - U_{mf})A$. The value of Y is less than 1.

The n-type theory, on the other hand, can be regarded as a conservative estimate in reactor modelling since all the invisible flow except for $A(U_{mf}(1 - \delta_B))$ is assigned to the bubble phase.

Unfortunately, satisfactory means for measuring the actual invisible flow have not yet been found.

Table 6-1: Flow assumed in various version of two phase theory [Grace&Clift, 1974].

		Visible flow in bubble phase	Invisible flow in bubble phase Through flow	Total flow in bubble phase	Flow in dense phase	Total flow
1	Original two phase theory	$(U - U_{mf})A$	0	$(U - U_{mf})A$	$U_{mf}A$	UA
2	Total deficit between actual G_B and that predicted by above ascribed to interstitial flow	G_B	0	G_B	$UA - G_B$	UA
3	Throughflow velocity of U_{mf}	G_B	$U_{mf}\delta_B A$	$G_B + U_{mf}\delta_B A$	$A(U - U_{mf}\delta_B) - G_B$	UA
4	n – type theory	G_B	$U_{mf}(1+n)\delta_B A$	$A(U - U_{mf}(1 - \delta_B))$	$A(U_{mf}(1 - \delta_B))$	UA

Bubble properties

The phenomenon of bubbling is an obvious feature of gas-solid fluidization. Bubbles are responsible for features that differentiate fixed bed from fluidized bed (in gas–solid fluidization). They modify the gas flow in the system and cause particle movement which result in rapid and extensive particle mixing and high heat transfer coefficient. The extent and vigour of bubbling increases with increasing gas velocity. As the gas velocity is increased, more and more particles are transported from the top of the bed and when the terminal falling velocity of the largest particle is approached, the whole bed is carried over. Gas fluidized beds are difficult to observe as it is not transparent and bubbles can not be normally seen within bed. Nevertheless, the behaviour of bubbles are studied with special kind of

observation like digital image analysis, acoustic characteristic etc and some information is also obtained from the analogy with the liquid boiling.

Bubble size

Figure 6-6 illustrates the growth of a typical bubble at a hole in the grid plate supporting a fluidized bed. Normally the operating superficial velocity U is an order of magnitude greater than the systems U_{mf} and the velocity through the grid holes is considerably greater than U . Therefore, the local gas velocity at the exit of the hole is much higher than U_{mf} , so the interface is lifted to a new stable position shown in Figure 6-6 (b). In b the average velocity through the gas solids interface has decreased by a factor equal to

$$\frac{\text{Orifice area}}{\text{area of gas to solid interface}} \quad \text{Eq. 6-4}$$

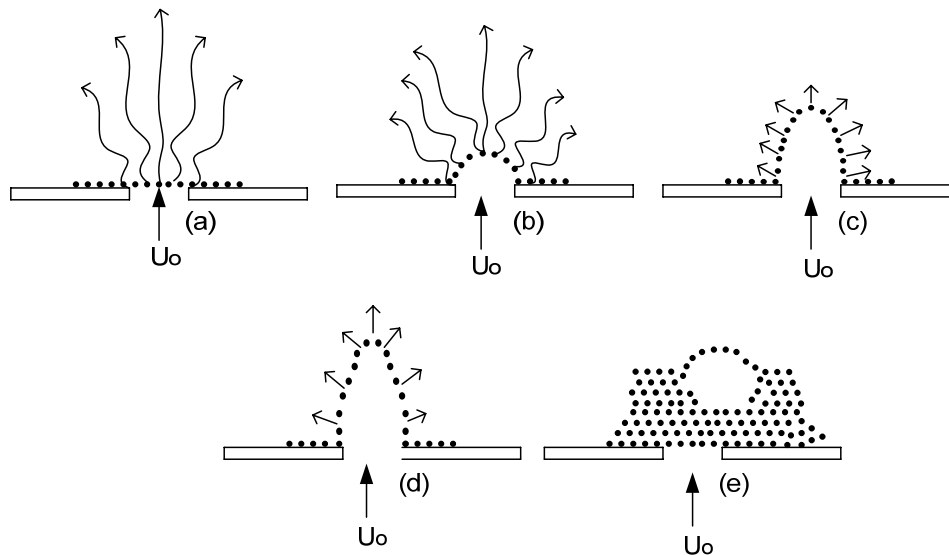


Figure 6-6: Growth of a bubble.

If this factor multiplied by the hole velocity still exceeds U_{mf} than the interface remains stable and the void grows further (Figure 6-6 (c)). Eventually the void above the hole grows so large that the velocity through the gas solid interface decreases to a value of U_{mf} and there after if the void were to grow larger its surface would no longer be stable. The volumetric flow of gas from a grid hole and the system's U_{mf} there gives the first approximation to the size of the void or 'bubble's initial size'. The shape and size of bubble varies roughly from a shallow spherical to an almost complete sphere [Huttenhuis et al., 1996].

Bubbles have a precise boundary which is in agreement with two phase theory, i.e. concentrated particle in emulsion and particle free in bubble. Detailed knowledge of gas flow

is of considerable interest whenever mass transfer or chemical reaction between gas and particle takes place. The ideal bubble is largely defined by a spherical diameter of d_B .

The bubble formation is of course strictly dependent on the gas distributor as indicated in Figure 6-6. For the initial bubble diameter $d_{B,\infty}$ different correlations were proposed in literature [Davidson & Schuler, 1960]. Darton et al. [1977] have suggested a correlation (Eq. 6-5) for bubble size as a function of bed height

$$d_B = 0.54 (U - U_{mf})^{0.4} \left(z + 4 \sqrt{\frac{A}{N_{gr}}} \right)^{0.8} g^{-0.2} \quad \text{Eq. 6-5}$$

The initial bubble size is calculated from Eq. 6-5 ($z = 0$). The bubble growth is limited by different mechanisms. Davidson and Harrison [1963] proposed that bubbles are filled by particles supplied from their wake and for this reason bubbles are not stable if their rising velocity exceeds the terminal velocity of the bed particles. Based on this postulation Davidson and Harrison [1963] suggest the concept of a maximum stable bubble size with a theoretical correlation.

$$d_{B,max} = \frac{2U_t^2}{g} \quad \text{Eq. 6-6}$$

Bubble velocity

Bubble velocity is mainly dependent on the size of the bubble. Once detached from the grid, observation [Davidson & Harrison, 1971] shows that the velocity of a given sized bubble depends on the properties of the bed material, it also depends on the concentration of the bubbles and increase with increasing bubble fraction. The analogy between gas-liquid and gas-solid systems has often been exploited to describe the behaviour of bubbles in fluidized beds [Davidson et al., 1977]. Davies et al., [1950] showed that the rise velocity $U_{B,\infty}$ of an isolated spherical bubble of radius r_b in liquid is given by Eq. 6-7.

$$U_{B,\infty} = \frac{2}{3} \sqrt{gr_B} \quad \text{Eq. 6-7}$$

Clift et al. [1978] demonstrate that Eq. 6-7 is reliable for bubbles with, $Re_b > 40$.

In terms of equivalent diameter Eq. 6-7 can be written as

$$U_{B,\infty} = \left(\frac{2}{3} \sqrt{\frac{r_B}{d_{B,eq}}} \right) \sqrt{g d_{B,eq}} \quad \text{Eq. 6-8}$$

If it is assumed that the base of the bubble is flat, then the factor $\left(\frac{2}{3} \sqrt{\frac{r_B}{d_{B,eq}}} \right)$ in Eq. 6-8 becomes a weak function of bubble's Reynolds number. For $Re_B > 100$ it becomes constant at 0.71. Hence the rise velocity of a single isolated bubble is

$$U_{B,\infty} = 0.71 \sqrt{g d_{B,eq}} \quad \text{Eq. 6-9}$$

Fluidizing a bed of particles at a gas velocity exceeding the minimum bubbling velocity, bubbles are formed continuously at the distributor and rise through the bed called freely bubbling bed. The coalescence also causes a decrease in bubble frequency and an increase in diameter. However, it was found [Clift et al., 1985] that the volume of the combined bubble exceeds 10-20% the volume of the original bubbles.

More is the gas passing from the bed larger is the number of bubbles formed in the bed and faster should be the velocity of a gas bubble as it rises through the bed.

When many bubbles are present, their velocity would be affected by other factors. More bubbles mean less drag on an individual bubble, and the bubbles would carry each other up through the bed. Other factors that affect the velocity of the bubble are the viscosity of the gas and the size and density of the solid particles (Both of these terms also affect the minimum fluidization velocity). The higher the minimum fluidization velocity, the lower will be the velocity of the rising bubble. Accordingly, a common used adaptation is given by Davidson & Harrison [1963] as

$$U_B = U_{B,\infty} + (U_o - U_{mf}) \quad \text{Eq. 6-10}$$

In small diameter beds the walls friction suppress the solids flow pattern and thus the bubble rise velocity reduces. Therefore, Werther [1978] proposed following correlations as shown in Table 6-2.

Table 6-2: Empirical correlation for the bubble velocity.

$U_B = 3.2 D^{\frac{1}{3}} U_{B,\infty} + Y(U_0 - U_{mf})$	Group A, $0.05 < D < 1$
$U_B = 2 D^{\frac{1}{3}} U_{B,\infty} + Y(U_0 - U_{mf})$	Group B, $0.1 < D < 1$
$U_B = 0.87 U_{B,\infty} + Y(U_0 - U_{mf})$	Group D, $0.1 < D < 1$

Bubble fraction

The height of the bed increases due to the presence of bubbles. Applying the original two-phase theory (Toomey & Johnstone, 1952) and assuming that the bubbles are free of solids and the voidage in the emulsion phase remains at ε_{mf} then bubble fraction δ_B is

$$\delta_B = \frac{U - U_{mf}}{U_B} \quad \text{Eq. 6-11}$$

But for modified two phase theory

$$\delta_B = \frac{Y(U_0 - U_{mf})}{U_B} \quad \text{Eq. 6-12}$$

Mean voidage of the bed, ε_z in dense zone is

$$\varepsilon_z = 1 - (1 - \delta_B)(1 - \varepsilon_{mf}) \quad \text{Eq. 6-13}$$

Gas exchange between bubbles and emulsion

Form two-phase theory it is evident, that a significant part of the gas flows in the bubble phase. Thus, the interphase mass transfer between bubble- and emulsion phase is essential for each gas-solid reaction.

The bubble-to-emulsion transfer was studies by Zenz and Othmer [1960] and Davidson and Harrison [1963]. The exchange of gas between bubble and emulsion depends on the ratio of bubble rising velocity and the gas velocity in the emulsion. Ratios higher than unity characterize fast bubble and ratio lower than unity represent slow bubble. Slow bubble enables a sufficient gas exchange with the emulsion, so that no real gradient in gas concentration between bubble and emulsion appears. Fast bubbles cause a bypassing of gas. Thus it is very important for the understanding of the process to know about the gas exchange taking place. In fast fluidized beds with typically high gas velocities and smaller particles, there is very high probability of bypassing of gas.

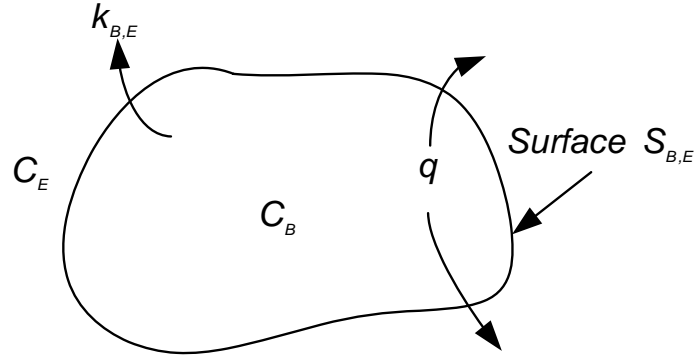


Figure 6-7: Bubble to emulsion mass exchange.

The interchange coefficient $K_{B,E}$ is defined as

$$-\frac{1}{V_B} \frac{dN_{A,B}}{dt} = -U_B \frac{dC_{A,B}}{dx} = K_{B,E} (C_{A,B} - C_{A,E}) \quad \text{Eq. 6-14}$$

The gas exchange based on the interphase surface area $S_{B,E}$ is defined by

$$\frac{S_{B,E}}{V_B} = \frac{a}{\delta_B} = \frac{6}{d_B} \quad \text{Eq. 6-15}$$

With 'a' being the bubble-emulsion interfacial area per unit bed volume and assuming a spherical bubble it can be written

$$K_{B,E} = \frac{S_{B,E}}{V_B} k_{B,E} = \frac{a}{\delta_B} k_{B,E} = \frac{6}{d_B} k_{B,E} \quad \text{Eq. 6-16}$$

Sit and Grace (1978) proposed a model with additive convective and diffusive mass transfer and obtained an expression for the overall mass-transfer coefficient for a spherical bubble

$$K_{BE} = \frac{U_{mf}}{4} + \sqrt{\frac{4\varepsilon_{mf} D U_B}{\pi d_B}} \quad \text{Eq. 6-17}$$

6.1.2 Transport zone

A fluidization vessel typically has two zones, a dense bubbling phase with a distinct upper surface and an upper lean phase where the density of solid decreases with height. The section of bed between the surface of dense bed and the exit of the gas stream is called the freeboard and its height is called the freeboard height. Entrainment or carryover is the

transport of particles from the bed into the freeboard. An important term in describing entrainment is the transport disengaging height (TDH). TDH is the height above which the elutriation rate remains constant [Wen et al., 1982]. Geldart [1985] defined TDH as the height where the solids flux is within 1% of the equilibrium flux.

After the injection of primary air into the combustion reactor (Figure 6-3), the superficial gas velocity is increased and the reactor operates in fast fluidization regime. When the bed is operated in fast fluidization regime the carryover of solid is very large and fresh solid has to be supplied to makeup for the loss. The importance of the freeboard increases with decreasing conversion in the bed and increasing particle entrainment. Since there is a favourable contact between the gas and the entrained solids in the freeboard, this region has a significant influence on the overall performance of the fluidized bed reactor.

With the work of Yerushalmi et al. [1976] there has been an increased interest in the characteristics of fast fluidization regime. Kwauk [1988], Weinstein et al. [1986], Hartge et al. [1986], all found an S-shaped solid fraction curve, as shown in Figure 6-8.

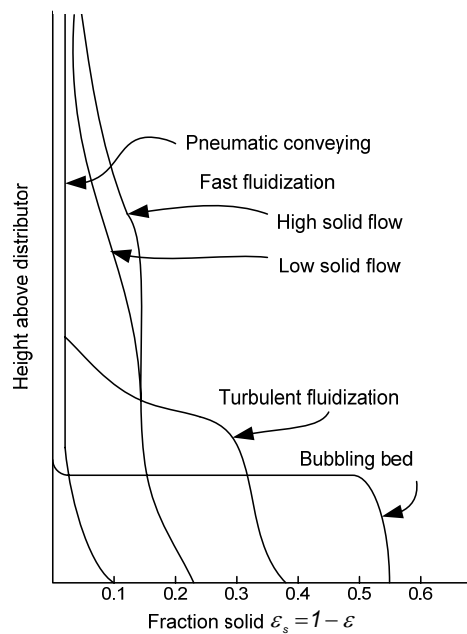


Figure 6-8: Axial voidage profile as a function of height.

This S shape curve moves up or down in the column depending on the solid and gas flow rate as shown in Figure 6-8. Different approaches are proposed to describe fast fluidized bed reactors [Fane et al., 1982], [Grace, 1986], [Van Swaaij, 1978]. The axial mean voidage is calculated using an exponential decay function as proposed by Zenz and Weil [1958]

$$\frac{\varepsilon_z - \varepsilon_\infty}{\varepsilon_0 - \varepsilon_\infty} = \exp[-a(z - z_0)] \quad \text{Eq. 6-18}$$

The two critical parameters in (Eq. 6-18) are, the decay factors 'a' and the porosity above transport disengaging height ' ε_∞ '. ε_0 is the porosity at height z_0 . The decay factor 'a' in Eq. 6-18 is a parameter to express the decay of the solids fraction along the height. In literature the values of the decay constant vary widely

Table 6-3: Table for proposed values of decay constant.

Author	Decay constant [m^{-1}]
[Large et al.,1976]	2 – 3
Wen and Chen [1982]	3.5 - 6.4
Anderson and Leckner [1989]	1.3 - 2.5 m^{-1} for a FBC

It has been concluded [Kunii & Levenspiel, 1990], [Walsh et al., 1984] that the product of 'a' and 'U' is a function of particle size.

$$aU = \text{const} = \begin{cases} 2 - 5 \text{ s}^{-1} & \text{for } d_p \leq 70 \mu m \\ 4 - 12 \text{ s}^{-1} & \text{for } d_p \geq 88 \mu m \end{cases} \quad \text{Eq. 6-19}$$

Based on our experiments it was found that the decay constant depends on the fluidizing velocity to a higher power than one [Löffler et al., 2003]. Thus, the correlation proposed by Adanez et al. [1994] was adopted.

$$a(U_0 - U_t)^2 D^{0.6} = K \quad \text{Eq. 6-20}$$

The second parameter determining the solids profile according to Eq. 6-18 is the voidage above TDH (ε_∞). This value can be determined from the particle elutriation rate constant $K_{i\infty}$ for a mono-sized bed material [Colakyan et al., 1984]

$$1 - \varepsilon_\infty = \frac{K_{i\infty}}{\rho_p (U_0 - U_t)} \quad \text{Eq. 6-21}$$

In literature, a lot of different correlations can be found for $K_{i\infty}$ [Löffler et al., 2003]

$$K_{i\infty} = 0.011 \rho_p \left(1 - \frac{U_t}{U_0} \right)^2 \quad \text{Eq. 6-22}$$

Core-annulus structure

Fast fluidized or transport reactors exhibit strong radial gradients, with the content of particles near the column walls higher than in the core of the reactor. Simple core/annulus models for circulating fluidized beds assume upflow of gas and solids in a dilute central core and downflow of dense clusters in a relatively thin annular zone near the walls. The transport zone is modelled with a core – annulus flow structure, where core is a gas rich region and annulus is a solid rich region [Figure 6-9]. The voidage in the core at a given height is calculated from the mean porosity ε_z at that height [Namkung et al., 1998]

$$\varepsilon_c = 1 - 0.6(1 - \varepsilon_z) \quad \text{Eq. 6-23}$$

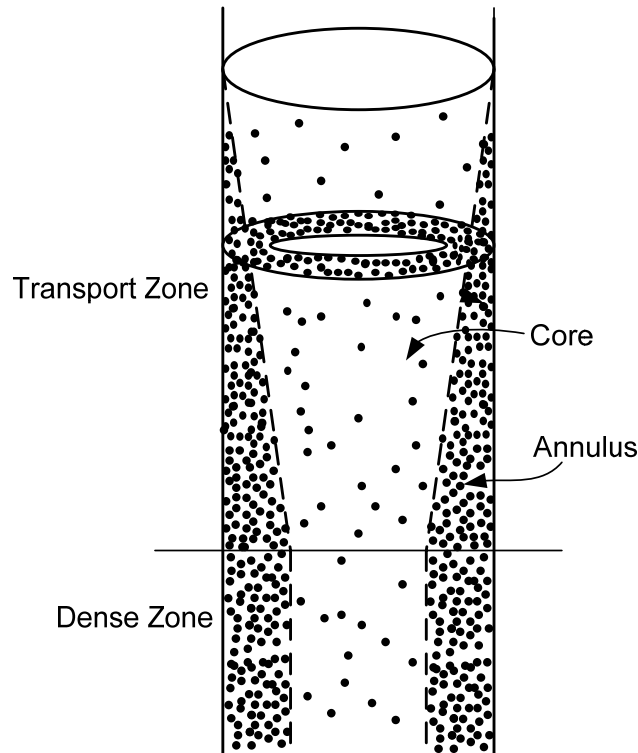


Figure 6-9: Core annulus structure for a fast fluidized bed.

The annulus is maintained at minimum fluidization condition. As seen in Figure 6-9 the diameter of core increases with the height of the riser and is calculated according to Eq. 6-24.

$$\varepsilon_a d_a^2 + \varepsilon_c d_c^2 = \bar{\varepsilon} D \quad \text{Eq. 6-24}$$

As shown in the transport zone [Figure 6-3], the up flowing gas stream splits into two streams in each cell. A part of the gas goes to the annulus [Eq. 6-25] and the remaining gas into the core.

$$Q_a = U_{mf} A_a \quad \text{Eq. 6-25}$$

It is assumed that the gas mixes instantaneously at the exit of cell. The combustion in the freeboard depends on the operating conditions, the design of the freeboard, char properties, size, and loading. The influences of these variables on freeboard combustion rates are not well known.

In order to get a good overview about the description of the fluid dynamics the prime equations are summarized in Table 6-4.

Table 6-4: List of primary equation used in hydrodynamic calculation of riser.

Name	Symbol	Expression	Reference
Gas flow in bubble	Q_B	$Q_B = Y(U_0 - U_{mf})$	
Correction Factor for Modified Two Phase Theory	Y	$Y = \frac{0.26 + 0.7 \exp(-0.0033 d_p)}{[0.15 + (U - U_{mf})]^{0.33}} \left(z + 4 \sqrt{\frac{A}{N_{or}}} \right)^{0.4}$	[Johnsson et al., 1991]
Bubble diameter	d_B	$d_B = 0.54 (U - U_{mf})^{0.4} \left(z + 4 \sqrt{\frac{A}{N_{or}}} \right)^{0.8} g^{-0.2}$	[Darton et al., 1977]
Initial bubble diameter	$d_{B,0}$	$d_{B,0} = 1.63 (U - U_{mf})^{0.4} \left(\frac{A}{N_{or}} \right)^{0.4} g^{-0.2}$	[Mori & Wen, 1975]
Maximum bubble diameter	$d_{B,max}$	$d_{B,max} = \frac{2U_t^2}{g}$	[Davidson & Harrison, 1963]
Velocity of single isolated bubble	$U_{B,\infty}$	$U_{B,\infty} = 0.71 \sqrt{g d_{B,eq}}$	[Clift et al., 1978]
Bubble velocity	U_B	$U_B = U_{B,\infty} + (U_0 - U_{mf})$	[Davidson & Harrison, 1963]
Bubble fraction	δ_B	$\delta_B = \frac{Y(U_0 - U_{mf})}{U_B}$	[Kunii & Levenspiel, 1990]
Average bed porosity	ε_z	$\varepsilon_z = 1 - (1 - \delta_B)(1 - \varepsilon_{mf})$	
Mass transfer coefficient	K_{BE}	$K_{BE} = \frac{U_{mf}}{4} + \sqrt{\frac{4\varepsilon_{mf} D U_B}{\pi d_B}}$	[Sit & Grace, 1978]
Minimum fluidization velocity	U_{mf}	$U_{mf} = \frac{\mu_g}{\rho_g d_p} \left(\sqrt{27.2^2 + 0.0408 Ar} - 27.2 \right)$	[Grace, 1982]
Porosity at minimum fluidization	ε_{mf}	$\varepsilon_{mf} = 0.478 Ar^{-0.018} \quad 177 < Ar < 4030$	[Doichev & Boichev, 1977]
Archimedes Number	Ar	$Ar = \frac{d_p^3 \rho_g (\rho_p - \rho_g) g}{\mu_g^2}$	

Porosity in transport zone	ε_z	$\frac{\varepsilon_z - \varepsilon_\infty}{\varepsilon_0 - \varepsilon_\infty} = \exp[-a(z - z_0)]$	[Zenz & Weil, 1958]
Decay constant	a	$a(U_0 - U_t)^2 D^{0.6} = K$	[Adanez et al., 1994]
Porosity above TDH	ε_∞	$1 - \varepsilon_\infty = \frac{K_{\infty}}{\rho_p(U_0 - U_t)}; K_{\infty} = 0.011\rho_p\left(1 - \frac{U_t}{U_0}\right)^2$	[Colakyan et al., 1984]
Porosity in core	ε_c	$\varepsilon_c = 1 - 0.6(1 - \bar{\varepsilon})$	[Namkung et al., 1998]
Diameter of core	d_c	$\varepsilon_a d_a^2 + \varepsilon_c d_c^2 = \bar{\varepsilon} D$	
Terminal velocity	U_t	$U_t = \sqrt{\frac{4}{3} \left(\frac{\rho_p - \rho_g}{\rho_g} \right) \frac{d_p g}{C_w}}$	
		$C_w = \begin{cases} \frac{24}{Re} & \text{for } Re_t < 1 \\ \frac{24}{Re} + \frac{4}{\sqrt{Re_t}} + 0.4 & \text{for } 1 < Re_t < 3000 ; Re_t = \frac{\rho_g U_t d_p}{\mu_g} \\ 0.43 & \text{for } Re_t > 3000 \end{cases}$	
Diffusivity	$D_{A,B}$	$D_{A,B} = \frac{1.43 T^{1.75} \times 10^{-7}}{\rho \sqrt{M_{A,B}} \left(\left(\sum_v \right)_A^{1/3} + \left(\sum_v \right)_B^{1/3} \right)^2}$	[Fuller et al., 1966]
Viscosity	μ_m	$\mu_m = \sum_{i=1}^n \frac{y_i \mu_i}{\sum_{j=1}^n y_j \phi_{ij}} ;$ $\phi_{ij} = \frac{\left[1 + \left(\frac{\mu_i}{\mu_j} \right)^{1/2} \left(\frac{M_j}{M_i} \right)^{1/4} \right]^2}{\left[8 \left(1 + \frac{M_i}{M_j} \right) \right]^{1/2}}$	[VDI-Wärmeatlas, 1997]

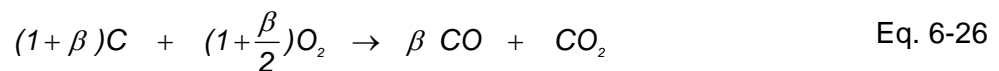
6.2 Reaction sub-model

In the DFB gasifier the fuel is fed into the gasification reactor. After feeding the fuel particle in the gasifier, it undergoes different processes, which are important to understand the fuel behaviour. The particles are firstly heated up, by means of conduction, convection and radiation. When the temperature reaches about 300-400°C, devolatilization/gasification of fuel particle begins. With further increase in temperature the gasification becomes fast and vigorous [Roider, 2002]. Due to the prolonged heating the volatiles escapes from the fuel and makes it porous. In literature lot of devolatilization model have been presented [Winter et al., 1995].

The remaining char is partly transported to the combustion reactor (riser) and combustion of char takes place there.

6.2.1 Char combustion

The porous fuel, post devolatilization is called char. It is rich in carbon and depleted in oxygen and hydrogen. Model assumes char to be a homogeneous matrix of carbon, oxygen and hydrogen. The composition of char is a model parameter. In general combustion of char begins after the evolution of volatiles. Sometimes there is also a overlapping of these processes. The char combustion reaction is much slower than the devolatilization process. Oxygen from bulk stream is transported to the char and reacts with the carbon of char particle heterogeneously to form CO and CO₂.



The reaction is strongly exothermic and is a very important heat source in combustion. The ratio of the molar production rate of carbon mono-oxide and carbon di-oxide depends on the surface temperature of the fuel particle and is given by the correlation from Arthur [1951] for natural graphite and coal char with oxygen partial pressure between 0.05 to 0.25 bar and a temperature range of 790 – 1690K.

$$\frac{CO}{CO_2} = 2500 \exp\left(\frac{51830}{RT_{p,s}}\right) \quad \text{Eq. 6-27}$$

Shrinking particle model

The char combustion is modelled as shrinking particle model (Figure 4.1) and it is assumed that the diameter of the char particle decreases while the density of the char remains

constant. Oxidation occurs in a thin layer close to the particle surface and no ash layer is formed. The combustion rate in term of mass transfer through the gas film can be described as

$$q = h_m (C_g - C_s) \quad \text{Eq. 6-28}$$

$$h_m = \frac{M_c \phi Sh D_g}{d_{char} RT_m} \quad \text{Eq. 6-29}$$

C_g is the partial pressure of oxygen in bulk gas. h_m is the mass transfer coefficient. ϕ is the mechanism factor and is 2 if the prime product is CO and 1 if the prime product is CO_2 . Sh is the Sherwood number describing the mass transfer. D_g is the molecular diffusivity of oxygen through the gas film. d_p is the instantaneous diameter of the char particle. T_m is the average gas film temperature. M_c is the molecular weight of carbon. The maximum combustion rate is obtained by setting the oxygen concentration on the carbon surface C_s to zero.

$$q = h_m (C_g) \quad \text{Eq. 6-30}$$

The chemical reaction rate of carbon with oxygen per unit time per unit external surface area of the particle may be written as

$$q = k_{char,s} C_s^n \quad \text{Eq. 6-31}$$

The temperature dependence of the rate constant is given by the following Arrhenius expression

$$k = k_o \exp\left(\frac{-E_{ap}}{RT_p}\right) \quad \text{Eq. 6-32}$$

The maximum combustion rate is obtained if the oxygen concentration at the surface is equal to the concentration in the bulk gas.

$$q = K_{char} C_g^n \quad \text{Eq. 6-33}$$

Since both diffusion limit and the chemical reaction limit are comparable to each other, therefore both rates have to be considered. The apparent order of reaction ' n ' for char combustion is obtained from the experiments and by the minimization of the root of mean square for the Arrhenius expression [Smith, 1982].

Table 6-5: Table for char combustion kinetics.

Reaction parameters	Char Combustion	Char steam gasification	Char dry Gasification
N	0.5	0.57	0.38
k_0	8.56E-02	2.62E+08	3.1E+06
E_a	18600	237000	215000
K (1073K)	1.06E-02	7.59E-04	1.05E-02
Reference	[Wartha, 1998]	[Barrio et al., 2000]	[Barrio & Hustad, 2000]

There is no sharp boundary between the various processes that the fuel particle experiences. The gasification of char in riser becomes pronounced when the oxygen present in the region is consumed. Therefore the gasification reactions are also implemented in the riser. The kinetics of the char reactions are present in Table 6-5.

Steam gasification



Dry gasification (with CO_2)



Gasification is also modelled by n^{th} order kinetics as

$$q_{st} = kC_{H_2O}^n \quad \text{Eq. 6-36}$$

$$q_{dry} = kC_{CO_2}^n \quad \text{Eq. 6-37}$$

At a given time char undergoes three reactions simultaneously i.e. one combustion and two gasification. The net carbon (char) combusted is

$$q_{net} = q + q_{st} + q_{dry} \quad \text{Eq. 6-38}$$

The hydrogen and oxygen present in the char is homogeneously released as hydrogen gas and oxygen gas (i.e. they are released in such a way that the weight fraction carbon, hydrogen and oxygen remains constant)

$$q_{H,net} = q_{net} \left(\frac{w_H}{w_C} \right) \quad \text{Eq. 6-39}$$

$$q_{O,net} = q_{net} \left(\frac{w_O}{w_C} \right) \quad \text{Eq. 6-40}$$

The hydrogen and oxygen gas released from char diffuses into the gas stream

$$\omega_{H_2} = \frac{q_{H,net}}{M_{H_2}} \quad \text{Eq. 6-41}$$

$$\omega_{O_2} = \frac{q_{O,net}}{M_{O_2}} \quad \text{Eq. 6-42}$$

The CO formed at the interface of char diffuses outward into the gas stream where it reacts with the oxygen to form CO_2 . The combustion of CO is catalysed by the presence of traces of water vapour [Howard et al., 1974], [Dryer et al., 1973]. Hydrogen released from the char reacts with oxygen to form water.



Air ratio

The apparent global air ratio lambda, λ is defined by neglecting the bypassing fraction of the char (i.e. only the actually converted char is considered).

$$\lambda = \frac{[\dot{n}y_{O_2}]_{in}}{[\dot{n}y_{O_2}]_{in} - \left[\dot{n} \left\{ y_{O_2} - 0.5y_{CO} - \sum_{C_xH_y} (x + 0.5y)y_{C_xH_y} \right\} \right]_{out}} \quad \text{Eq. 6-44}$$

6.2.2 Homogeneous reactions

In reaction engineering science, one objective is to investigate the homogeneous reaction system in a plug-flow reactor at defined temperatures and pressures. To get an insight of the process chemical kinetic modelling is a promising tool. The homogeneous reaction mechanisms are modelled as non-elementary (global) reactions where the rate expression

follows a power law expression in the concentrations (Eq. 6-45). The temperature dependence is modelled in Arrhenius form as shown in Eq. 6-48.

$$\frac{dC_i}{dt} = r_i = k[C_i]^n \quad \text{Eq. 6-45}$$

The solution depends on initial conditions as well as model parameter. For chemical kinetic modelling, these are the concentrations and the reaction rate constants.

Rate expression

If we consider a reaction system of N reversible or irreversible reactions involving M different chemical species, then the rate of change of concentration of species 'i' can be written as

$$\sum_{i=1}^M \frac{dC_i}{dt} = \sum_{j=1}^N \nu_{i,j} r_j \quad \text{Eq. 6-46}$$

The net rate for any reaction (j) is



$$r_C = k_{\text{for},j} [C_A]^{\nu_A} [C_B]^{\nu_B} - k_{\text{back},j} [C_C]^{\nu_C} [C_D]^{\nu_D} \quad \text{Eq. 6-47}$$

The kinetics data for the forward reaction rate are supplied to the model. Different kinetic data from different investigators are checked for the reaction modelling, but only those data were selected that resembles the process conditions. The forward rate constant $k_{\text{for},j}$ of the reaction j is generally described as function of temperature as Arrhenius/ modified Arrhenius equation.

$$k_{\text{for},j} = k_{0,j} T^{b_j} \exp\left(\frac{-E_j}{RT}\right) \quad \text{Eq. 6-48}$$

The pre-exponential factor $k_{0,j}$, the temperature exponent b_j , and the activation energy E_j of each reaction j has to be supplied as input to the model. For reversible reactions, the rate of the reverse reaction is calculated using thermodynamic data [Burcat, 1984]

The reverse rate constant $k_{\text{back},j}$ can be determined using the following relation through the equilibrium constant $K_{\text{eqm},j}$.

$$K_{\text{eqm},j} = \frac{k_{\text{for},j}}{k_{\text{back},j}} \quad \text{Eq. 6-49}$$

$$k_{\text{back},j} = \frac{k_{\text{for},j}}{K_{\text{eqm},j}} \quad \text{Eq. 6-50}$$

The equilibrium constant $K_{eqm,j}$ in concentration units can be calculated for the thermodynamic equilibrium constant.

$$K_{eqm} = K'_{eqm} \left(\frac{p}{RT} \right)^{\Delta \nu_j} \quad \text{Eq. 6-51}^\diamond$$

$$K'_{eqm,j} = \exp \left(\frac{-\Delta G^0}{RT} \right) \quad \text{Eq. 6-52}$$

$$\Delta G_j^0 = \Delta H_j^0 - T \Delta S_j^0 \quad \text{Eq. 6-53}$$

ΔH_j^0 and ΔS_j^0 are the standard enthalpy and entropy of the reaction. These can be calculated from the standard state enthalpy H_i^0 and the standard state entropy S_i^0 of the species i in reaction j .

$$\Delta H_j^0 = \sum_{i=1}^M \nu_{j,i} H_i^0 \quad \text{Eq. 6-54}$$

$$\Delta S_j^0 = \sum_{i=1}^M \nu_{j,i} S_i^0 \quad \text{Eq. 6-55}$$

To maintain the temperature of the riser, a part of the producer gas is recycled back to the riser. It contains, $CO, CO_2, CH_4, C_2H_4, C_3H_8, H_2, H_2O, O_2$ and N_2 . All higher hydrocarbons present in producer gas are lumped into the C_3H_8 content. Detailed composition of producer gas is mentioned in table 1-4. All gas phase reactions and rate kinetics are summarized in Table 6-6.

Figure 6-10 gives an overview of the solving method. To get a solution for the process, an iteration algorithm is used. The input of necessary data is done via the text files.

In the beginning of each zone the first estimation of the char flow rate, the temperature inside the zone and the char hold up is explicitly supplied to the model.

Once all the variables are initialized, the control flows into the 1st zone. Inside the zone the control goes to the 1st cell. In each cell the local thermochemical parameters (gas viscosity, density, enthalpy, entropy, free energy etc), fluid dynamic parameters (bed hold up, char hold up, bed porosity, gas flow rate etc) and reaction parameters (reaction rate, char conversion etc) and gas phase mass balance are performed. The information flows from once cell to next cell till the last cell of the zone is reached.

[♦] Pressure in this equation is in bar

When the end of zone is reached overall mass balance is performed. If the mass balance is not fulfilled then the char hold up in the zone is iterated. This loop is iterated till the overall mass balance is satisfied. When the overall mass balance is satisfied the energy balance is checked. If the energy balance is not satisfied then the temperature of the zone is iterated until the energy balance is fulfilled. The overall mass and energy balance across a zone gives the char hold up and the average temperature of the zone.

When the balances of the previous zone are satisfied, the control of the model goes to the next zone. In the beginning of next zone it checks whether an external gas (air, producer gas...) is added to the up flowing stream or not. If there is an addition of fluid then all gas stream are adiabatically and homogeneously mixed to a single stream. Inside the new zone all the local thermochemical, fluid dynamic and reaction parameters are calculated as done in previous zone.

The control of the model moves from one zone to another till the last zone. At the end of the last zone, the model checks the error between the calculated air ratio and the target air ratio. If the error is more than the tolerance limit then the char flow rate is iterated till the tolerance limit is satisfied.

Finally, when the target air ratio is reached, the output results generated are written in the text file.

Middle zone is a special case. In the beginning of each cell of middle zone there is an addition of spent scrubber liquid (water and tar loaded RME). The spent scrubber liquid once added to the cell changes its phase from liquid to gas and mix with the upflowing gas stream.

Table 6-6: Table for the reaction kinetics.

No.	Name of Reaction	Chemical Reaction	Reaction Rate [Mole / m ³ S]
(A)	Methane Combustion	$CH_4 + \frac{3}{2}O_2 \Leftrightarrow CO + H_2O$	$k_{CH_4} [CH_4]^{0.7} [O_2]^{0.8}$
(B)	Ethene Combustion	$C_2H_4 + 2O_2 \Leftrightarrow 2CO + 2H_2O$	$k_{C_2H_4} [C_2H_4] [O_2]$
(C)	Ethane Combustion	$C_2H_6 + \frac{5}{2}O_2 \Leftrightarrow 2CO + 3H_2O$	$k_{C_2H_6} [C_2H_6] [O_2]$
(D)	Propane Combustion	$C_3H_8 \Leftrightarrow CH_4 + C_2H_4$	$k_{C_3H_8} [C_3H_8]$
(E)	Hydrogen Combustion	$H_2 + \frac{1}{2}O_2 \Leftrightarrow H_2O$	$k_{H_2} [H_2]^{1.5} [O_2]$
(F)	Carbon monoxide combustion	$CO + \frac{1}{2}O_2 \Leftrightarrow CO_2$	$k_{CO} [CO] [O_2]^{0.5} [H_2O]^{0.5}$
(G)	CO - Shift reaction	$CO + H_2O \Leftrightarrow CO_2 + H_2$	$k_{shift} [CO] [H_2O]$

No.	Rate constant	Frequency factor (K_0)	b	Activation Energy (E_a)	Reference
(A)	$k_{CH_4} = k_0 T^b \exp\left(\frac{-E_a}{RT}\right)$	4.68E+18	0.5	167000	[Zimont & Trushin, 1969]
(B)	$k_{C_2H_4} = k_0 T^b \exp\left(\frac{-E_a}{RT}\right)$	1.00E+12	0	173300	[Van der Vaart, 1985]
(C)	$k_{C_2H_6} = k_0 T^b \exp\left(\frac{-E_a}{RT}\right)$	2.34E+18	0.5	167000	[Zimont & Trushin, 1969]
(D)	$k_{C_3H_8} = k_0 T^b \exp\left(\frac{-E_a}{RT}\right)$	1.00E+12	0	175800	[Van der Vaart, 1985]
(E)	$k_{H_2} = k_0 T^b \exp\left(\frac{-E_a}{RT}\right)$	5.18E+01	1.5	28400	[Vilienskii & Hezmalian, 1978]
(F)	$k_{CO} = k_0 T^b \exp\left(\frac{-E_a}{RT}\right)$	3.25E+7	0	125500	[Dryer & Glassman, 1973]
(G)	$k_{shift} = k_0 \varepsilon T^b \exp\left(\frac{-E_a}{RT}\right)$	3.00E-02	0	60270	[Weimer & Clough 1981]

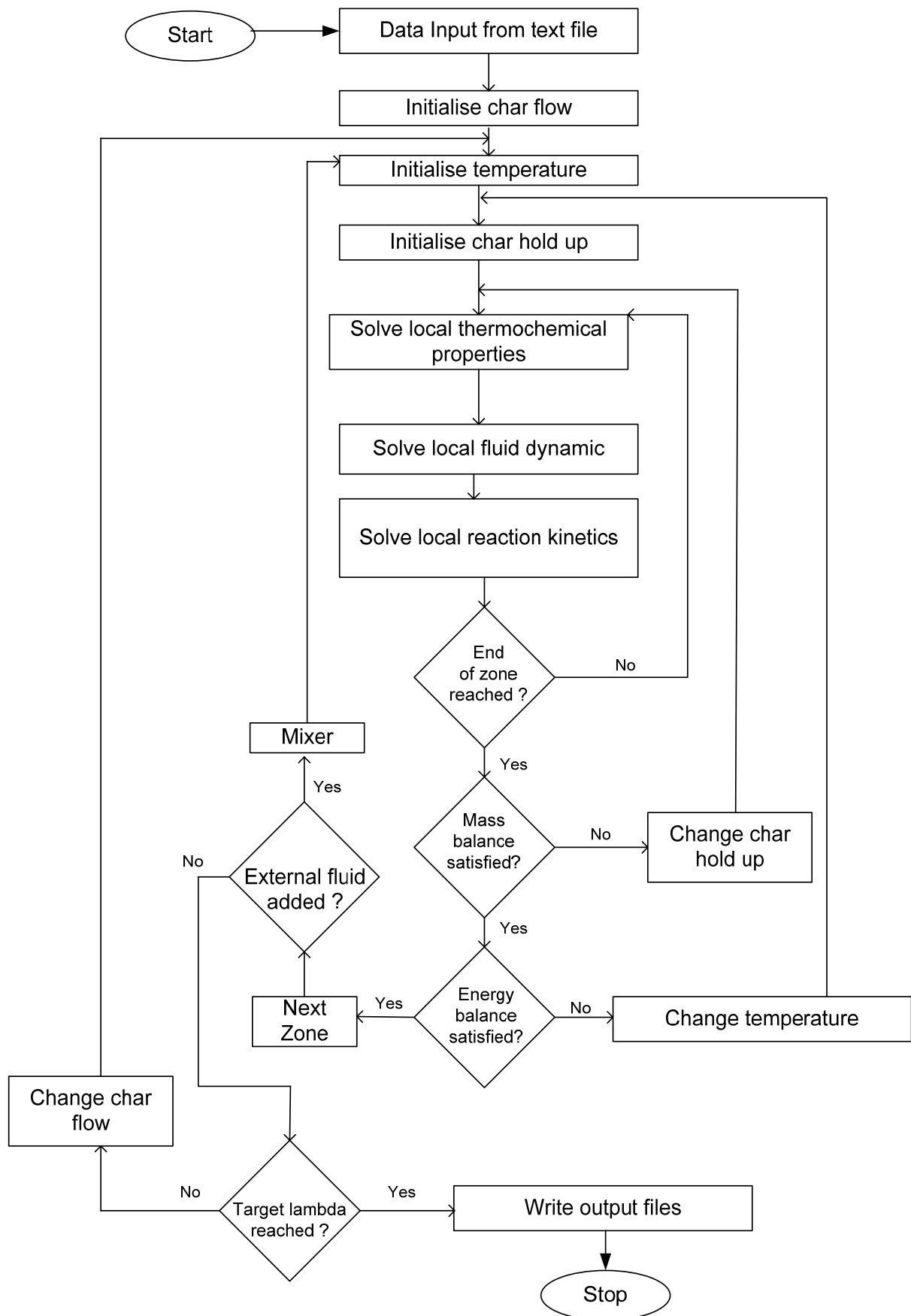


Figure 6-10: Overview of the solving scheme.

7 MASS AND ENERGY BALANCE

A model is a mathematical representation of a system or a process. The primary purpose of modelling is to better understand some existing systems or environments and their artefacts and to describe this understanding. Three primary physical laws underlying chemical engineering are conservation of mass, momentum and energy. The movement of mass and energy around a chemical process are evaluated using mass balance and energy balances. A mass balance (also called a material balance) is an accounting of material entering and leaving a system. Fundamental to the balance is the conservation of mass principle, i.e. that matter can not disappear or be created. This is a fundamental and quantitative way to understand complex systems/phenomena.

7.1 Mass balance

The mass that enters a system must either leave the system or accumulate within the system, i.e.

$$Mass_{in} = Mass_{out} \pm Mass_{accu} \quad \text{Eq. 7-1}$$

'in' 'out' and 'accu' denote what enters, exits and accumulates within the system boundary. For steady state,

$$Mass_{in} = Mass_{out} \quad \text{Eq. 7-2}$$

Dependent on the kind of the material transformation the mass balance can be formulated on one of the following kinds:

- Balance of the chemical elements (with chemical reactions).
- Balance of the chemical compounds (with purely physical procedures).
- Balance of the total mass stream.

The elemental balance applies to all processes except nuclear transformations. If no chemical reactions take place within the system investigated, the preservation of the chemical compounds can be formulated. In this case also the elemental balance is fulfilled automatically. When there is no change of the composition of the material across the system boundary then, it is sufficient, to formulate a balance of the total mass flowing in and out of the system.

7.1.1 Gas balance

The two different schemes of gas balance used in dense zone and in transport zone are discussed below.

Gas balance dense zone

The gas stream flowing in a system (cell) is made up of n different gaseous species (i), represented in mole fractions (y). Balances for the gaseous stream are performed for each species and in each cell.

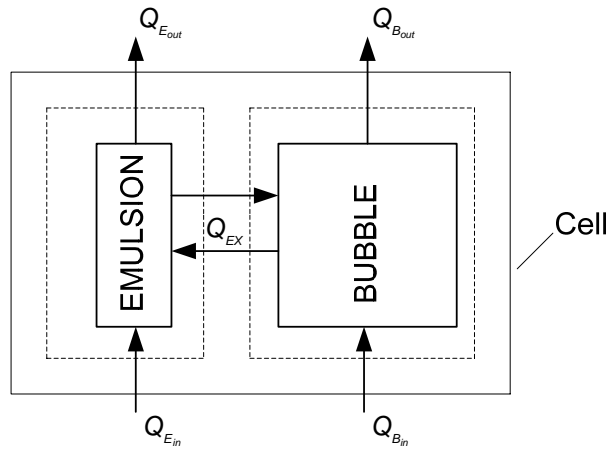


Figure 7.1: Gas balance in the dense zone.

$$Q_E \Big|_{in / out} = \sum_{i=1}^N \dot{n}_i y_i \Big|_{in / out} \quad \text{Eq. 7-3}$$

$$Q_B \Big|_{in / out} = \sum_{i=1}^N \dot{n}_i y_i \Big|_{in / out} \quad \text{Eq. 7-4}$$

$$\sum_{i=1}^n y_i = 1 \quad \text{Eq. 7-5}$$

Since the gas streams are in plug flow therefore the emulsion gas and bubble gas are balanced separately in each cell. For species 'i' the steady state balance is

$$\dot{n}_{i_{out}} = \dot{n}_{i_{in}} + \dot{n}_{i_{pro}} - \dot{n}_{i_{react}} \pm \dot{n}_{i_{Ex}} \quad (Emulsion) \quad \text{Eq. 7-6}$$

$$\dot{n}_{i_{out}} = \dot{n}_{i_{in}} + \dot{n}_{i_{pro}} - \dot{n}_{i_{react}} \mp \dot{n}_{i_{Ex}} \quad (Bubble) \quad \text{Eq. 7-7}$$

The production and reacted terms are defined as chemical reaction rates.

Gas balance transport zone

In transport zone gas balance is performed in similar way as it is done in dense zone, with emulsion and bubble gas stream of dense zone representing the annulus and core of transport zone respectively. Only difference is in the balances of the gaseous species. Figure 7.2 shows that there is no explicit formulation of the gas or solid exchange between the core and annulus. One of the major limitation of core-annulus model is, it gives relatively little conversion for gas-solid reaction kinetics. The reason being most of the gas slips through the core where as annulus that has high concentration of solid is deficient in gas. This limitation can be overcome very efficiently if the gas balance is implemented overall across a cell. Therefore in the transport zone the gas streams mass balance are not done separately (as in Eq. 7-6 and Eq. 7-7 of dense zone) for core and annulus gas but overall across a cell. For species 'i' in transport zone mass balance across a cell is

$$\dot{n}_{i_{out}} = \dot{n}_{i_{A_{in}}} + \dot{n}_{i_{C_{in}}} + \dot{n}_{i_{A_{pro}}} + \dot{n}_{i_{C_{pro}}} - \dot{n}_{i_{A_{react}}} - \dot{n}_{i_{C_{react}}} \quad \text{Eq. 7-8}$$

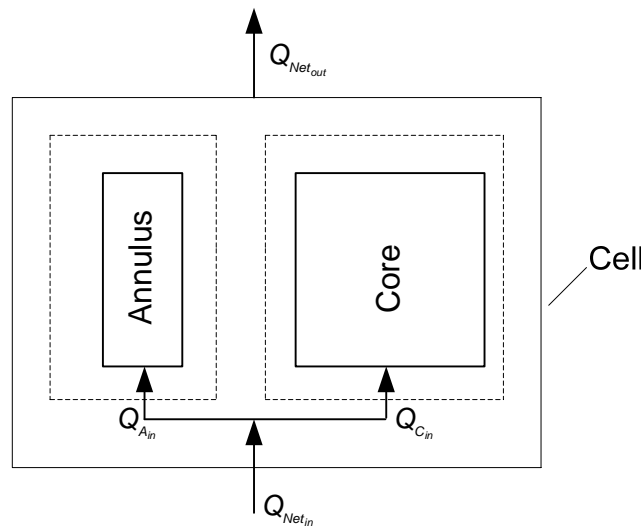


Figure 7.2: Gas balance in the transport zone/freeboard of riser.

7.1.2 Liquid balance

Liquid water and organic is added in the middle zone of the combustion reactor. It is added to the gas stream in between two consecutive cells. It is assumed that between two cells there is a mixer that mixes all in coming streams to a single stream as shown in Figure 7.3.

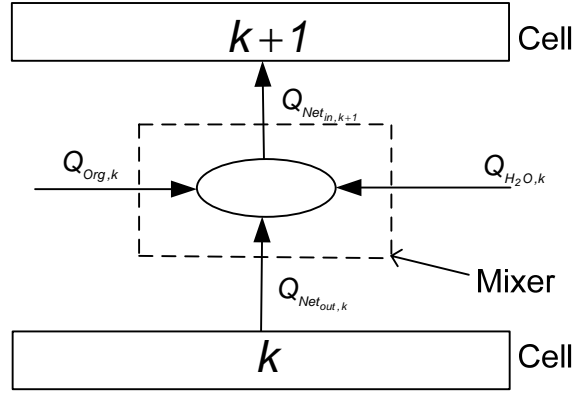


Figure 7.3: Liquid mixing in middle zone, a mixer between two consecutive cells.

The addition of water ($Q_{H_2O,k}$) and organic liquid ($Q_{Org,k}$) is modelled to follow a profile as shown in Figure 7.4. It can be either equally distributed or increase/decrease or parabolic (first increase than decrease) along height of middle zone. In this study the profile of liquid addition is assumed to be parabolic. The mass balance for Figure 7.3 is shown in Eq. 7-9.

$$Q_{Net,in,k+1} = Q_{Net,out,k} + Q_{H_2O,k} + Q_{Org,k} \quad \text{Eq. 7-9}$$

In terms of mole Eq. 7-9 can be written as

$$\dot{n}_{Net,in,k+1} = \dot{n}_{Net,out,k} + \dot{n}_{H_2O,k} + (\dot{n}_{CH_4} + \dot{n}_{H_2O} + \dot{n}_{CO} + \dot{n}_{H_2} + \dot{n}_{O_2})_{Org,k} \quad \text{Eq. 7-10}$$

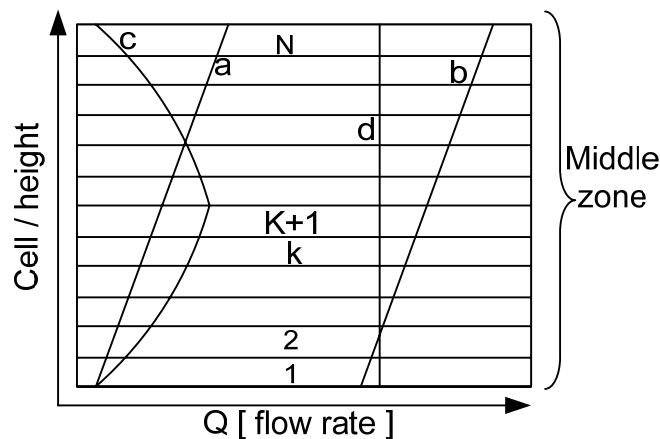


Figure 7.4: Profile of liquid addition (a: increasing, b: decreasing, c: parabolic, d: equal).

Water

At the system boundary (dotted line Figure 7.3), water is in the liquid state. But as water enters the system it evaporates to form steam (gas) and mixes with the gas stream.

Organic liquid

Merrick in his publication [Merrick, 1983] used the ultimate analysis of coal and the char (formed later) together with some statistical findings to define the volatile fraction in his model. The statistics says that

- 32.7 % of hydrogen becomes methane.
- 4.4 % of hydrogen becomes methane.
- 18.5 % of oxygen becomes carbon monoxide.
- 11 % of oxygen becomes carbon dioxide.

A model published by van den Bleek et al. (1990) also estimates the chemical composition (chemical species like CO , H_2O , SO_2 etc) of the volatile from the elemental composition.

Unlike gases and inorganic materials, organic liquid (tar loaded RME) is not chemically defined and is a complex material mixtures. It is defined only in terms of elemental composition i.e. (wt/wt) of C, H and O. As a rough assumption these elements were combined stoichiometrically to form chemically defined species as illustrated in Figure 7.5.

Depending upon whether C or H is limiting, C and H combines to form maximum possible number of CH_4 molecules. If H is limiting then the remaining C combines with O to form CO . If C is now limiting then O combines with another O to form O_2 , otherwise if O is limiting then C combines with the oxygen present in main gas stream to form CO , if yet C is not consumed than it react with H_2O of main gas stream to form CO and H_2 . Still if C is not consumed then it react with CO_2 of main gas stream to form CO . In extreme case when all O_2 , H_2O and CO_2 is consumes than the remaining C (from the RME) is loaded to the char.

If during the formation of CH_4 , C is limiting then the remaining H combines with O to form H_2O . If H is now limiting then O combines with another O to form O_2 otherwise remaining H combines to form H_2 . The dark colour line in Figure 7.5 shows a typical case.

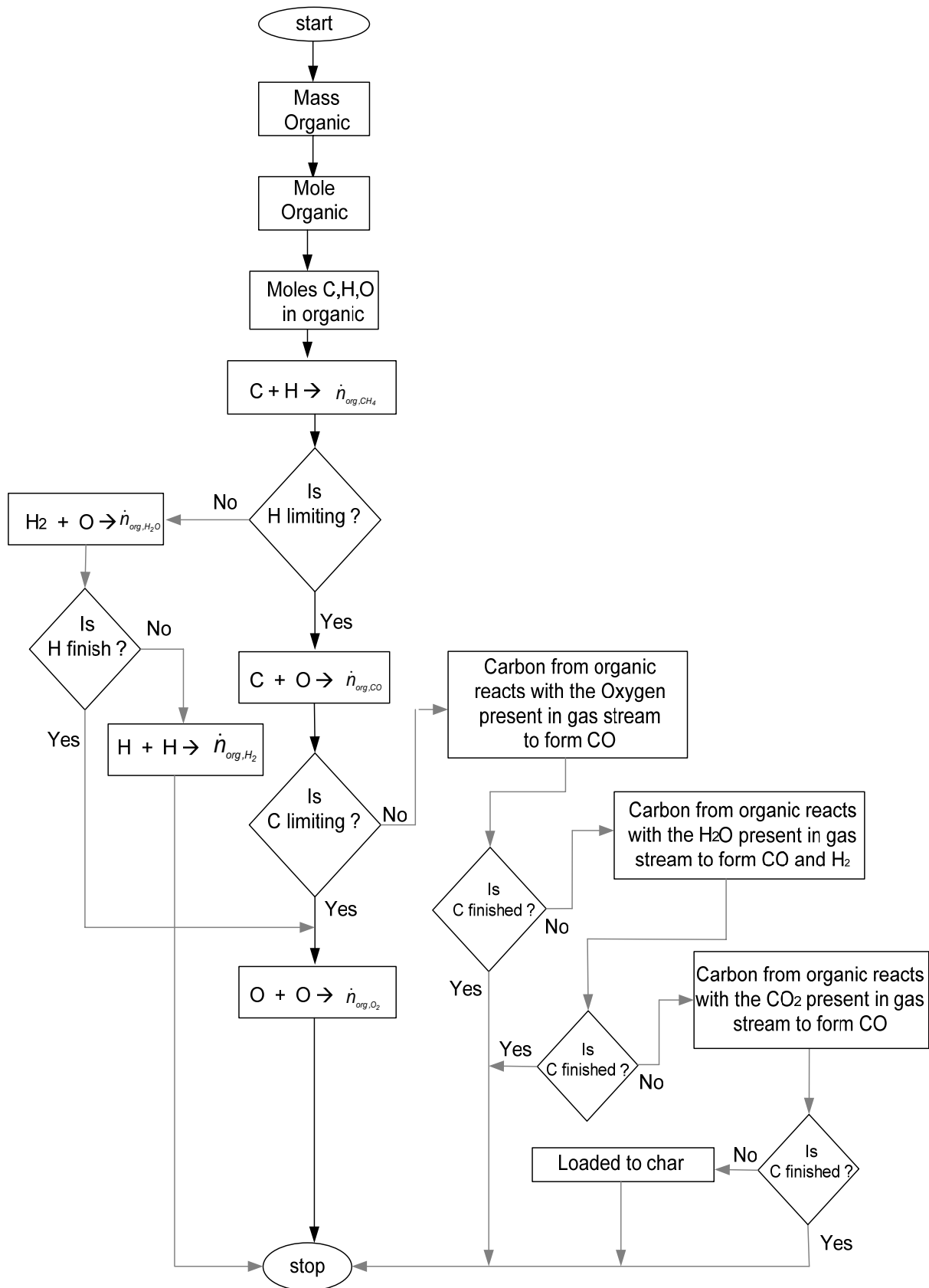


Figure 7.5: Algorithm for RME component definition from elemental balance.

7.1.3 Inert balance

The bed material circulating in the combustion reactor is inert and the mass balance for it is formulated over all across the whole height of combustion reactor.

$$\dot{m}_{inert,in} = \dot{m}_{inert,out} \quad \text{Eq. 7-11}$$

7.1.4 Char balance

Char is a chemically active material that undergoes combustion and is the main source of heat for the gasification reaction. Char balance is performed over all for the entire zone i.e. dense, middle and transport zone. Char flowing in the system boundary is an input parameter, where as char hold up is calculated from the balances.

Char exiting the system boundary is

$$\dot{m}_{char,out} = m_{char} \frac{\dot{m}_{bed,in}}{m_{bed}} \quad \text{Eq. 7-12}$$

The total char combusted in a zone is sum of the char combusted in the cells present in the zone

$$\dot{m}_{char,react} = \sum_{k=1}^N \dot{m}_{char,react,k} \quad \text{Eq. 7-13}$$

In each cell char combusted is proportional to the char hold up in that cell

$$\dot{m}_{cha,react,k} \propto m_{char,k} \quad \text{Eq. 7-14}$$

$$\dot{m}_{cha,react,k} = K m_{char,k} \quad \text{Eq. 7-15}$$

where K is kinetic constant. Carbon hold up in a cell is

$$m_{char,k} = \frac{m_{char}}{N} \quad \text{(dense zone)} \quad \text{Eq. 7-16}$$

$$m_{char,k} = \alpha m_{bed,k} \quad \text{(transport zone)} \quad \text{Eq. 7-17}$$

$$\alpha = \frac{m_{char}}{m_{bed}} \quad \text{Eq. 7-18}$$

α in Eq. 7-17 above ensures that as we move higher in the bed, like the bed hold up carbon hold up also decreases.

Overall char balance in a zone is

$$\dot{m}_{char,in} = \dot{m}_{char,out} + \dot{m}_{char,react} \quad \text{Eq. 7-19}$$

From Eq. 7-19 the char input ($\dot{m}_{char,in,cal}$) to the zone is calculated. This char input is compared with the proposed char flow rate ($\dot{m}_{char,in,tar}$) as shown in Eq. 7-20.

$$|\dot{m}_{char,in,tar} - \dot{m}_{char,in,cal}| < \sigma \quad \text{Eq. 7-20}$$

A Newton–Rapson method with analytical formulation of the derivative is applied to iterate the char input rate ($\dot{m}_{char,in}$) so that the LHS of Eq. 7-20 can be minimized.

7.2 Energy balance

Energy conservation law states that the total amount of energy in a closed system remains constant. In other words, energy can be converted from one form to another, but it cannot be created or destroyed. Energy balance is applied whenever the temperature within the system changes. The overall enthalpy balance across a zone, delivers the average zone temperatures.

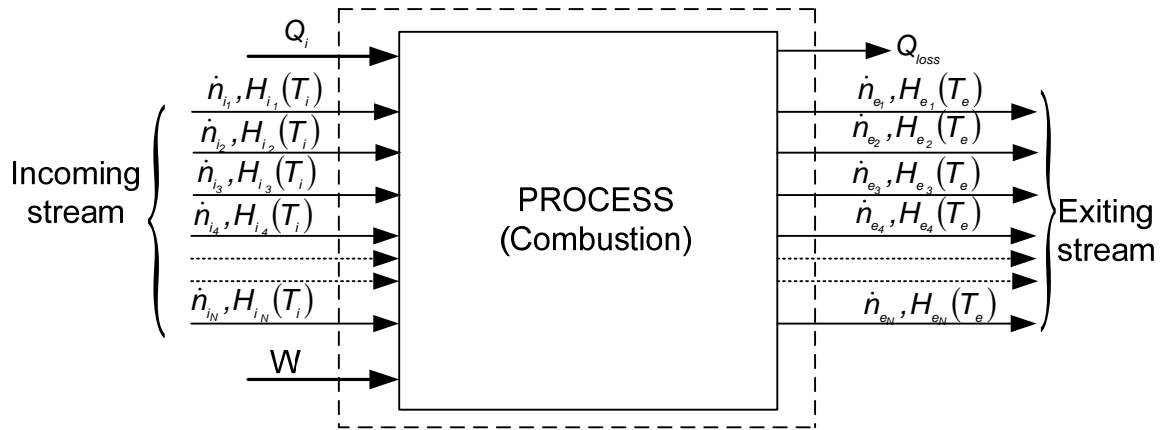


Figure 7.6: Overall energy balance in a zone.

Energy balance at steady state condition is

$$Input = output + loss \quad \text{Eq. 7-21}$$

Net energy input (Eq. 7-22) and output (Eq. 7-23) as shown in Figure 7.6 is

$$Q_i + W + \sum_{j=1}^N \dot{n}_{ij} H_{ij}(T_i) \quad \text{Eq. 7-22}$$

$$\sum_{j=1}^N \dot{n}_{oj} H_{oj}(T_o) \quad \text{Eq. 7-23}$$

Eq. 7-21, Eq. 7-22 and Eq. 7-23 when combined gives the general energy balance Eq. 7-24.

$$Q_i + W + \sum_{j=1}^N \dot{n}_{ij} H_{ij}(T_i) = \sum_{j=1}^N \dot{n}_{oj} H_{oj}(T_o) + Q_{\text{loss}} \quad \text{Eq. 7-24}$$

where Q_i , Q_{loss} and W is the heat added, heat lost and mechanical work done on the system respectively. In the present model it is assumed that there is no addition or loss of energy and there is no mechanical work done on the system i.e.

$$Q_i = W = Q_{\text{loss}} = 0 \quad \text{Eq. 7-25}$$

Hence the simplified energy balance equation for model is

$$\sum_{j=1}^N \dot{n}_{ij} H_{ij}(T_i) = \sum_{j=1}^N \dot{n}_{oj} H_{oj}(T_o) \quad \text{Eq. 7-26}$$

The enthalpy of a substance is the heat content in the substance. Conventionally enthalpy is defined by the following equation as

$$H(T) = \Delta H_{f,298}^0 + \Delta H_{T_o}^T \quad \text{Eq. 7-27}$$

where $\Delta H_{f,298}^0$ represents the enthalpy of formation at standard state (i.e. $T = 298K$; $P = 1 \text{ bar}$). $\Delta H_{T_o}^T$ is the change in enthalpy due to change in temperature from T_o to T . By convention it is assumed that the heat of formation of pure element at standard state is zero. From Eq. 7-24 it is clear that kinetic and potential energies of the flowing fluids are not considered in the energy balance. This simplification is justified and often used in process engineering because it has almost no effects on the total energy flowing.

8 RESULTS AND DISCUSSIONS

The following discussion focuses on the result of modelling and simulation of the riser that is defined in the previous chapters. The result for standard operating conditions are shown in the following section (8.1)

Subsequently, based on this standard case, the sensitivity of various parameters is investigated and the results are presented in section 8.2.

For parameters that were either found sensitive or are important for the process-optimization, parameter variation are carried out further over a larger range of values in section 8.3

8.1 Standard condition

For the demonstration plant, the model is executed first for the typical operating condition based on actual plant data. The standard conditions defined in Table 9-1 are explicitly known parameters except bed circulation rate, char properties (diameter, density and composition). Bed circulation and char properties are the input parameters from the gasifier. Since the gasifier and combustion reactor are a coupled and a closed system at high temperature it is almost impossible to take a sample from the connecting leg (Figure 6-1). The values of the unknown parameters are supplied either from the overall plant balance [Proell, 2004] or from experiments done at pilot plant scale. The effects of these indeterminate parameters are investigated further in this chapter.

Fluidized bed combustion covers a wide range of conditions. Starting from bubbling fluidized bed combustion to circulating fluidized bed combustion. In each fluidized regime the bed behaviour (hold up, temperature, gas velocity, gas concentration etc) varies significantly. The dense zone i.e. the bottom of the riser is in bubbling regime while the transport zone is in fast fluidized regime. In the first part of this chapter, the fluidized bed behaviour in different regimes is investigated.

The dense zone is the part of riser up to the height of 2 m. The middle zone is the region between 2 to 4 m, above that is the upper zone. Middle zone and upper zone together makes the transport zone (Figure 6-3).

Table 8-1: Input parameter to the riser model (standard operating condition).

Input Parameter	Value	Unit
Diameter of column	0.61	[m]
Diameter of bed at upper section	0.66	[m]
Total height of riser	12	[m]
Height of dense zone	2	[m]
Diameter of particle	500E-6	[m]
Diameter of char	0.008	[m]
Density of particle	2960	[kg / m ³]
Density of coke	200	[kg / m ³]
Volume flow of bottom air	720	[Nm ³ / hr]
Volume flow of primary air	2880	[Nm ³ / hr]
Volume flow of secondary air	860	[Nm ³ / hr]
Volume flow of producer gas	466	[Nm ³ / hr]
Volume flow of water in	0.058	[m ³ / hr]
Volume flow of RME	0.0687	[m ³ / hr]
Temperature of bottom air at inlet	60	[° C]
Temperature of primary air at inlet	400	[° C]
Temperature of producer gas	78.8	[° C]
Temperature of secondary air	460	[° C]
Temperature of water	80	[° C]
Temperature of RME	80	[° C]
Temperature bed material	850	[° C]
Bed circulation rate	37.00	[kg / s]
Air ratio for net fuel converted (λ)	1.02	[-]
Char Composition	C	0.8286
	H	0.0314
	O	0.14
RME Composition	C	0.8940
	H	0.1016
	O	0.0044

The profile of the different velocities U_o , U_t and U_{mf} are shown in Figure 8-1. It can be seen that the terminal velocity (U_t) is almost constant at a value of 4.5 m/s. The superficial velocity (U_o) increases significantly at the boundary of the zones. This increase is due to the

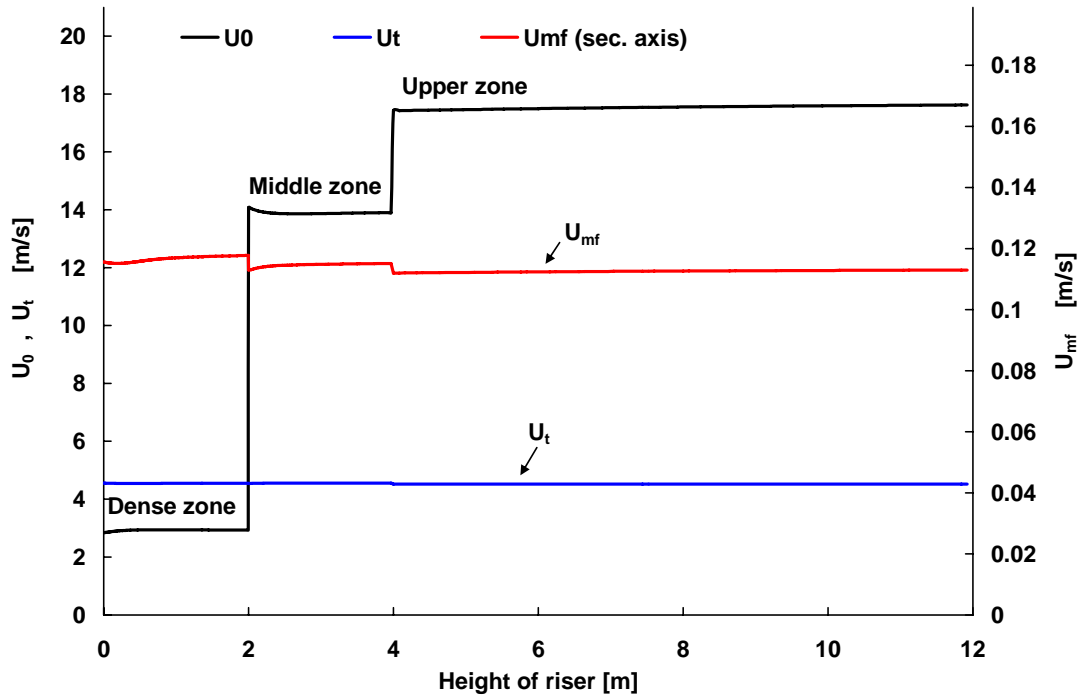


Figure 8-1: U_o , U_t and U_{mf} along the height of riser.

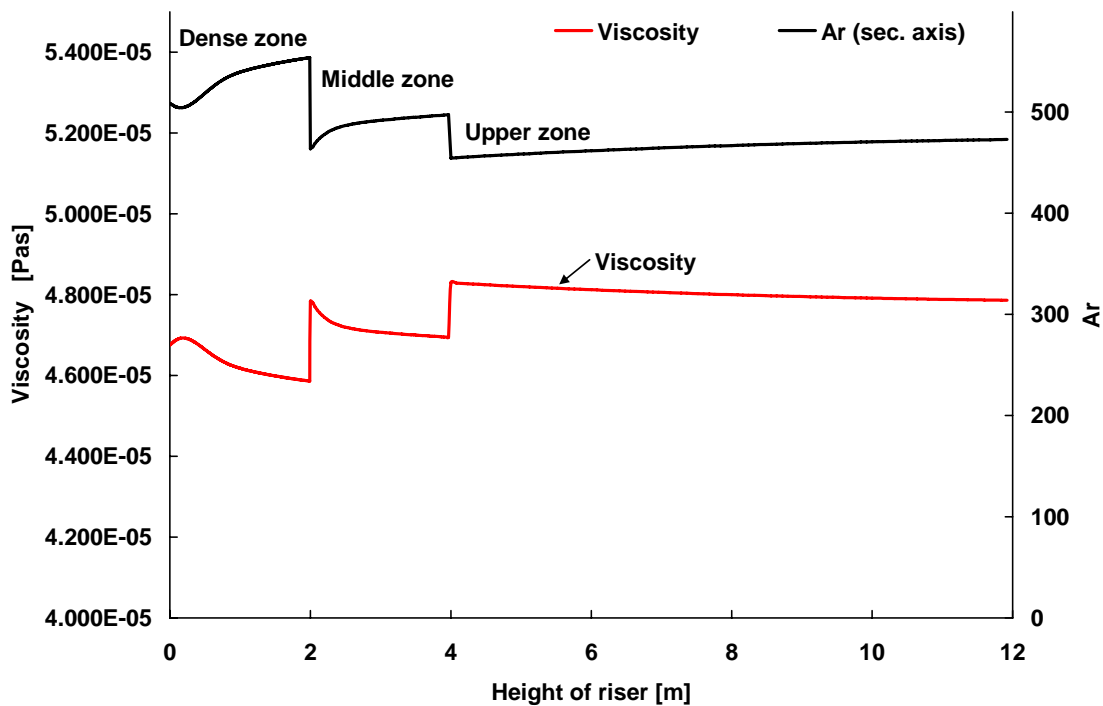


Figure 8-2: Archimedes number and viscosity along the height of riser.

addition of external fuel, primary and secondary air. Within a zone the superficial velocity is almost constant. Small deviation is due to gas release (from char) or gas phase reaction kinetics. It can be seen in Figure 8-1 that within a zone the minimum fluidization velocity increases over height. This is due to the change in gas properties (composition, density and viscosity). U_{mf} is about 0.115 m/s. The average superficial velocity (U_o), in the dense zone is about 2.87 m/s (25 times the U_{mf}) where as in the upper zone i.e. at the top of the riser U_o is 17.5 m/s (150 times U_{mf}).

The bottom of the riser (dense zone) is in bubbling regime and is modelled with the modified two phase theory. The bubble properties in the dense zone are shown in Figure 8-3. The bubble rise velocity, U_b gradually increases from 0.92 m/s to 3.7 m/s. The diameter of the bubble, d_b increases from 0.032 m to 0.36 m (~60% the diameter of column). The bubble reaches its maximum size at the height of 0.6 m. The bubble fraction that was almost constant at 0.54 up to a height of 0.6 m increases almost linearly after the bubble reaches its maximum size. The bubble properties indicate that from the height above 0.6 m the bed is in the transition from bubbling bed to slugging bed.

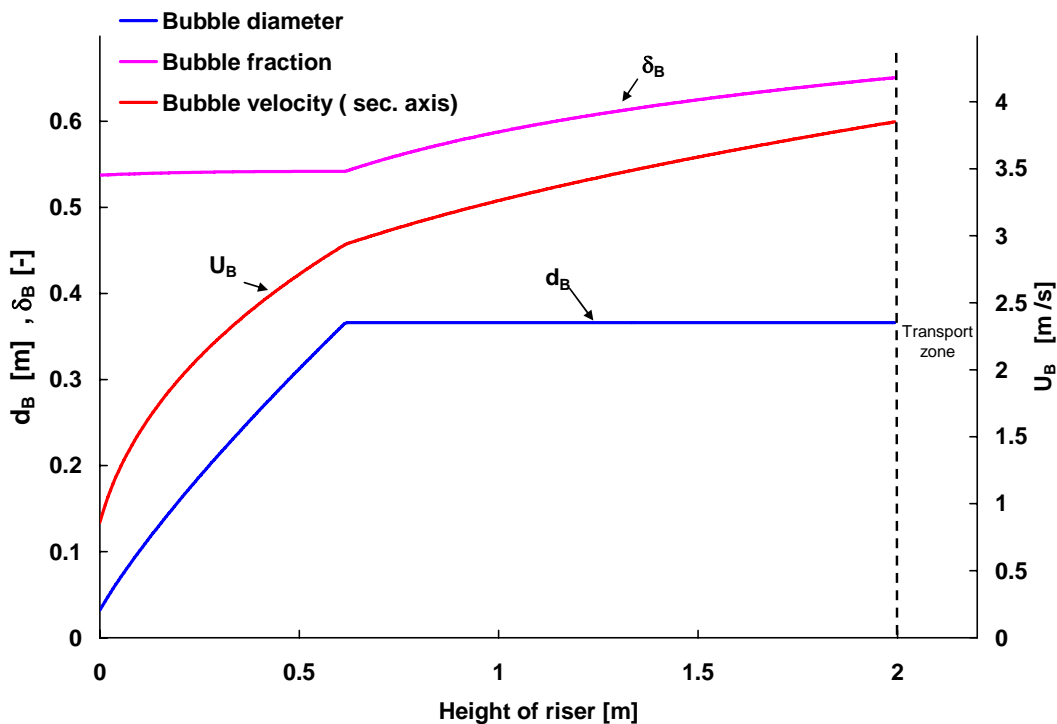
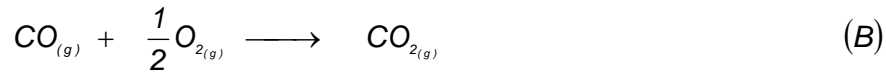
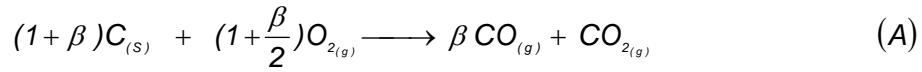


Figure 8-3: Bubble properties in riser.

The bottom of the riser (dense zone) is modelled with modified two phase theory, where as the transport zone is modelled as core annulus structure. In both these cases there are two

phases a solid rich phase and a solid lean phase (or gas rich phase). The net volumetric gas flow, Q_g is the sum of volumetric flow in solid rich phase, Q_2 (emulsion, annulus) and gas rich phase, Q_1 (bubble, core). The fraction of gas flowing in these two phases is shown in Figure 8-4. It can be seen in this figure that in the transport zone most of the gas is flowing in the core where as in dense zone the gas in the bubble phase increases gradually over the height. The increased bubble flow, G_B (Figure 8-5) is partly due to the increased bubble velocity and partly due to an increase in the value of Y . As seen in Figure 8-6, the value of Y changes with height, due to change in the gas and bed properties and gradually increases from 0.17 to 0.88. The net gas flow (Q_g) initially increases (Figure 8-5), this is due to the addition of CO (gas) and CO_2 (gas) formed from char (solid) combustion.



Reaction 'A' shows that $(1 + \beta)$ moles of solid char reacts with $\left(\frac{2 + \beta}{2}\right)$ moles of oxygen to form $(1 + \beta)$ moles of gas. $\frac{\beta}{2}$ moles of gas is produced from this heterogeneous reaction. Initially water is absent, so there is no further combustion of CO . In CO combustion (reaction 'B') 1 mole of CO reacts with half mole of oxygen to form 1 mole of CO_2 . When reactions 'A' and 'B' take place in comparable order of magnitude than $\Delta m_g \sim 0$.

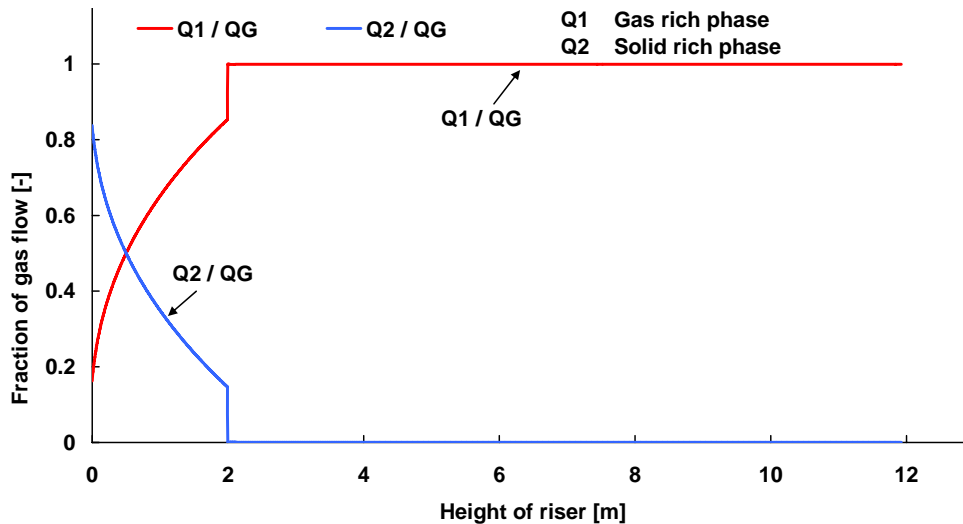


Figure 8-4: Volume fractions of gas in two phases inside the riser.

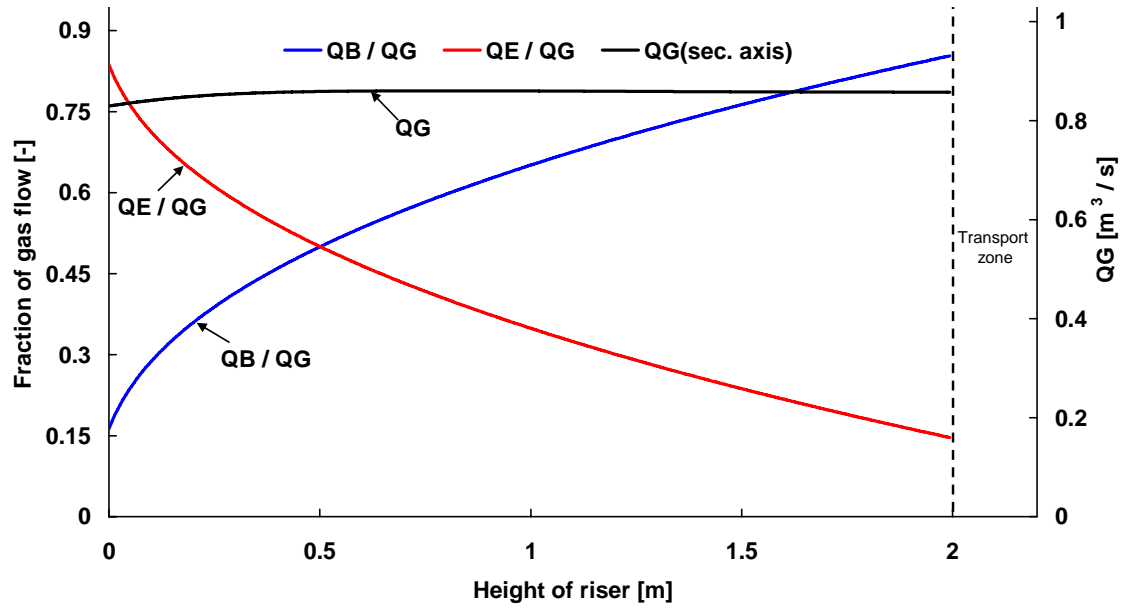


Figure 8-5: Fraction of gas distributing between bubbles and emulsion in riser.

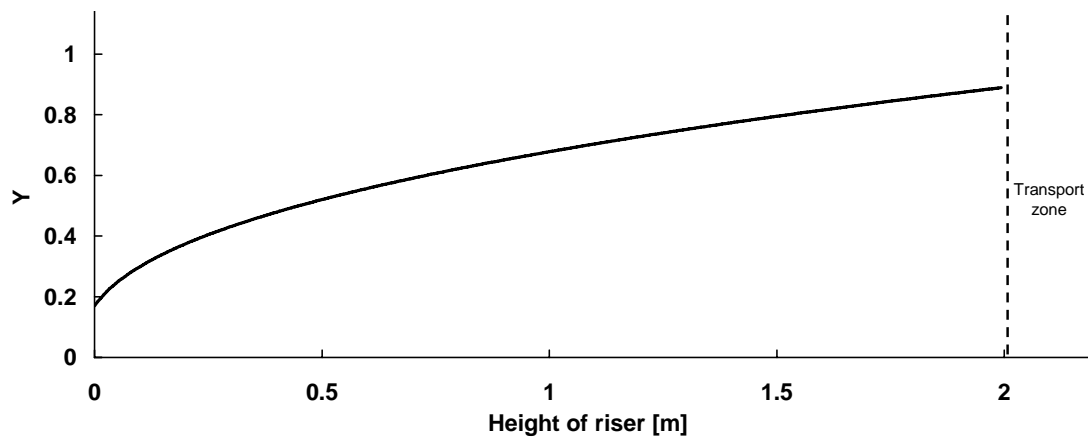


Figure 8-6: Correction factor Y (modified two phase theory) in bottom dense zone.

In Figure 8-7, the solid concentration i.e. bed concentration [kg_{bed}/m^3] and the char concentration [kg_{bed}/m^3] is shown along the height of the riser. In the dense zone when the bed is in typical bubbling regime (up to a height of 0.5 m) the bed concentration is constant at $785 kg/m^3$. When the bed is in transition phase the bed concentration decreases from $785 kg/m^3$ to $600 kg/m^3$. This decrease is due to the increase in bubble fraction (Figure 8-3). At the height of 2 m the concentration drops immediately from $600 kg/m^3$ to $480 kg/m^3$. This is because of the addition of primary air the superficial velocity of gas increases and the bed shifts from bubbling fluidization regime to the fast fluidization regime. This shift in regime is due to primary air addition. In the middle zone the bed concentration gradually decreases from $480 kg/m^3$ to $375 kg/m^3$. The slope of the bed concentration

curve changes at height of 4 m, due to secondary air addition and the bed concentration decreases further from 375 kg/m^3 to 225 kg/m^3 . The char concentration also follows a similar profile over the height of the riser (Figure 8-7). In the dense zone the char concentration is uniform at about 5 kg/m^3 . This is because the model assumes equal distribution of char in each cell of the dense zone. Therefore there is no change in char concentration to be observed in dense zone.

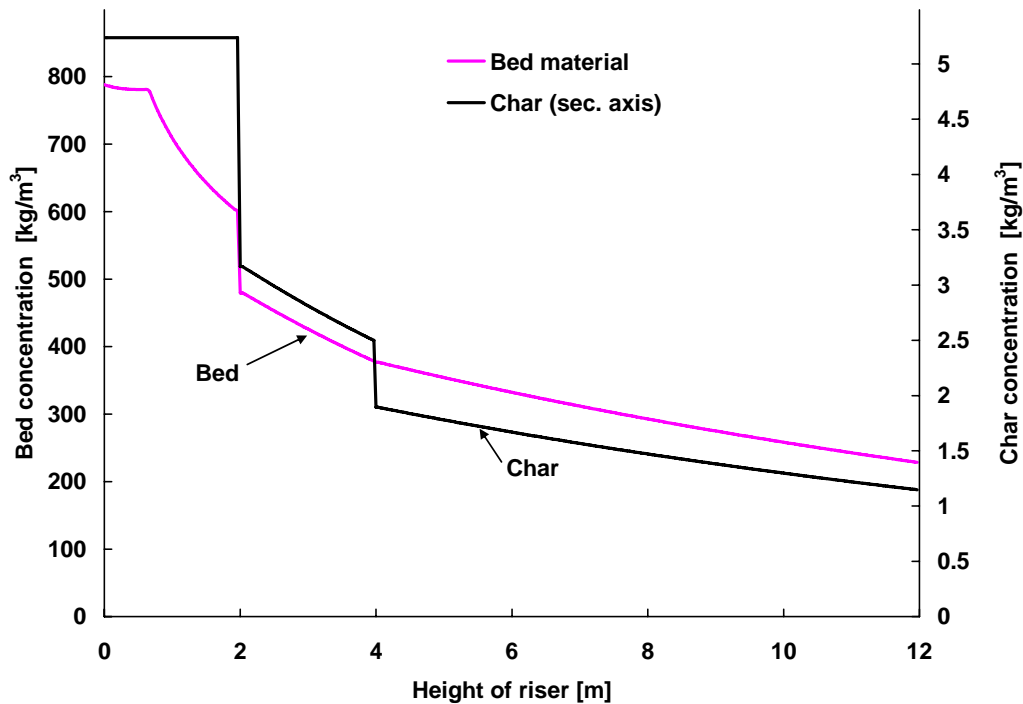


Figure 8-7: Bed and char hold up along the height of riser.

Figure 8-8 shows the fraction of volume occupied by the bed material in annulus $[Vol_{bed \text{ in annulus}} / Vol_{annulus}]$ and fraction of volume occupied by the bed material in core $[Vol_{bed \text{ in core}} / Vol_{core}]$ in the transport zone. As can be seen 57% of the annulus volume is occupied by the bed material and is constant over the entire height of riser. The maximum percentage of the core volume occupied by the bed material is 12 % and it gradually decreased over height to a value of 5%.

In terms of overall volume fraction i.e. (Vol_{bed} / Vol_{cell}) in the dense zone around 26 % of the volume is occupied by bed material. This volume fraction decreases from 26 % to 20 % when the bed is in transition (0.5 m to 2 m height of riser). At the height of 2 m the volume fraction of bed material immediately drops down to 16% and then it gradually decreases over height to 8 % at the exit of the riser.

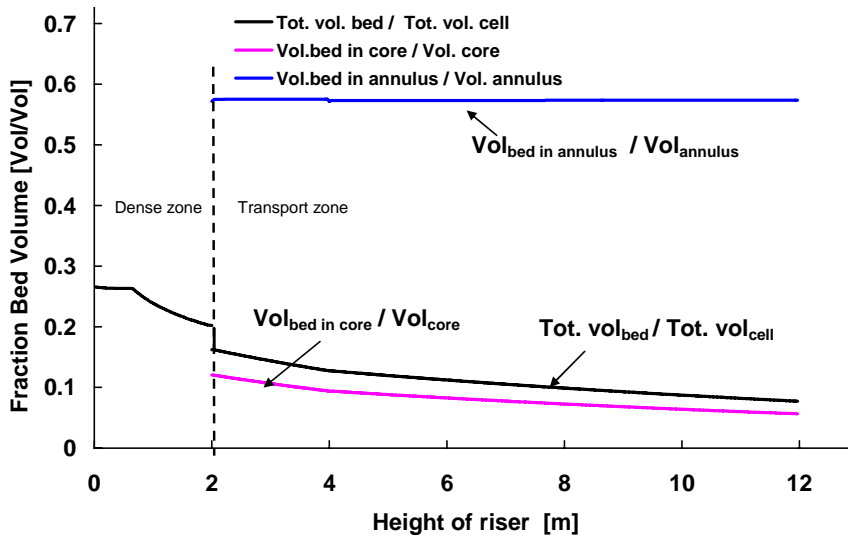


Figure 8-8 : Volume fractions of bed material along the height of riser.

Figure 8-9 shows the concentration of the bed material and char in core and annulus of the transport zone. The bed concentration in the annulus is at approximately 1702 kg/m^3 before the secondary air addition and after the addition it drops to 1697 kg/m^3 . The char concentration in annulus is at approximately 11.5 kg/m^3 before the secondary air addition and after the addition it drops to 8.2 kg/m^3 . For core, the bed concentration gradually drops from 356 kg/m^3 to 167 kg/m^3 . The char concentration in core slowly drops from 2.3 kg/m^3 to 1.8 kg/m^3 before the secondary air addition and after the addition it drops from 1.4 kg/m^3 to 0.84 kg/m^3 .

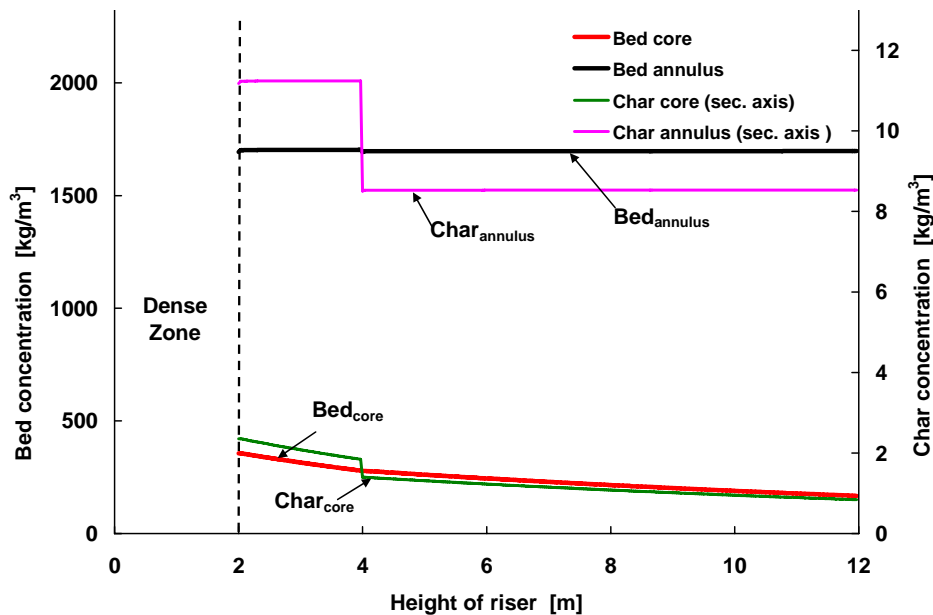


Figure 8-9: Char and bed concentration in riser.

Figure 8-10 shows the average porosity of the bed along the height of the riser. In the dense zone the bed porosity is initially constant at a value of 0.73. Then it increases from 0.73 to 0.8 due to increased bubble fraction (Figure 8-3). In the transport zone the bed porosity increases from 0.8 to 0.9. The slope of the mean porosity and the core porosities are relatively steep in the middle zone between 2 and 4 m of height, this is due to the evaporation of water taking place in middle zone. Due to the secondary air addition the slope of the curve changes at height of 4 meter. In Figure 8-10 in addition to the average porosity, the porosity above transport disengaging height (TDH), the annulus porosity and the core porosity are also shown for the transport zone. The porosity of the annulus is modelled to be at minimum fluidization condition and is almost constant at a value of ε_{mf} (0.427). The porosity above TDH is very close to unity (0.999). The mean porosity and the core porosity both increases with height of riser.

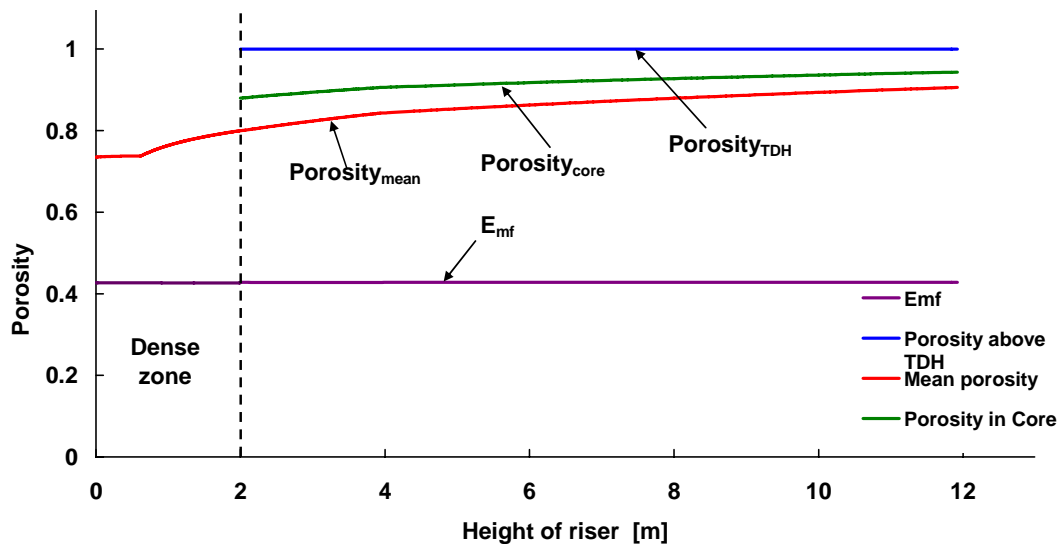


Figure 8-10: Porosity along the height of riser.

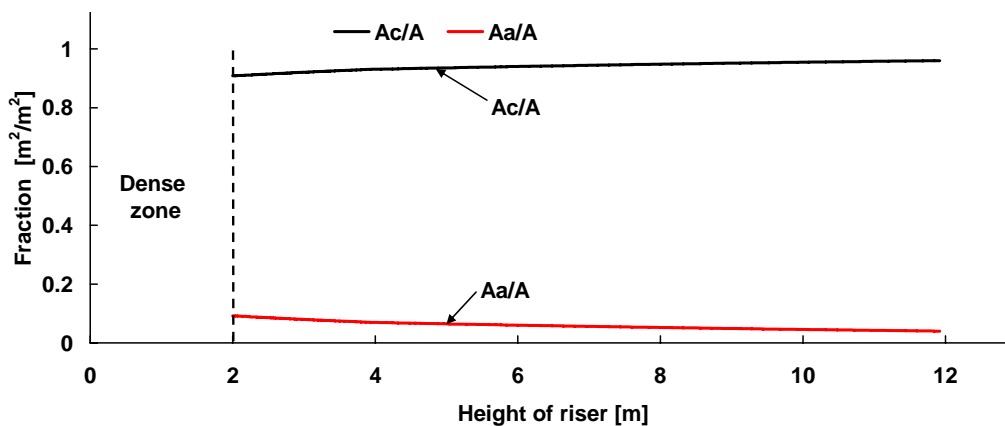


Figure 8-11: Fraction of cross sectional area between core and annulus along the height.

In Figure 8-11 the fraction of the net cross sectional area occupied by core and annulus are shown. The annulus is the region in the vicinity of the wall while the core is the central part of the riser. It can be seen in figure as the height in the transport zone increases the annulus shrinks from 10 % to 4 % while the core expands from 90% to 96% of the cross-sectional area.

The exiting composition of the flue gas predicted from the simulation run is summarized in Table 8-2. The predicted gas composition is subject of uncertainty, because of the lack of gas analysis either inside or immediately at the exit of the riser. Nevertheless the gas phase profile along the height of the riser is shown in Figure 8-12. The concentration is represented in mole fractions on the y axis. As seen in Figure 8-12 the concentration of CO_2 and H_2O increases while that of CO and O_2 decreases along the height of the riser. At a height of 2 and 4 meter the local concentration of CO_2 , H_2O goes down while that of O_2 is increased, this is due to the primary and secondary air addition at that heights. The concentration of CO is relatively high in the middle zone (2-4 m) because of the combustion of the producer gas added there.

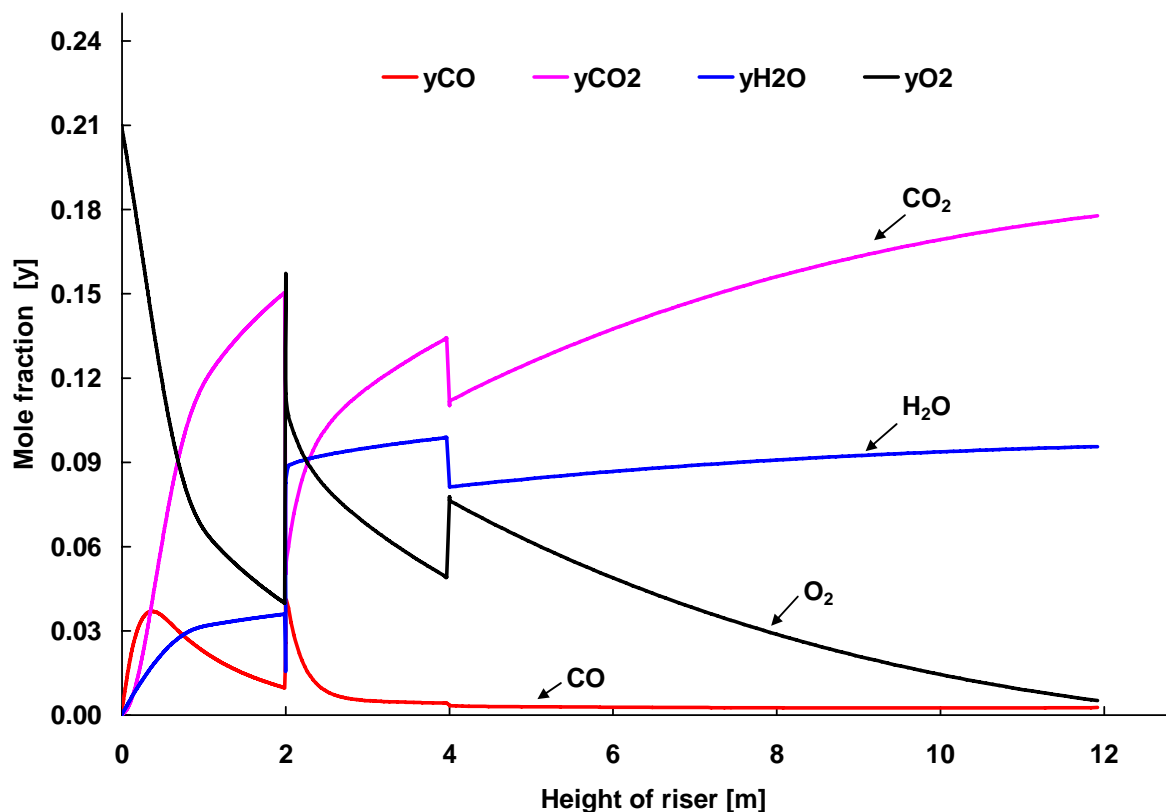


Figure 8-12: The mean gas phase profile along the height of riser.

Figure 8-13 shows a magnified view of dense zone. The oxygen in emulsion phase goes down swiftly. When O_2 is consumed in the emulsion phase gasification reactions dominates there. When O_2 is consumed in emulsion phase the hydrogen concentration in emulsion starts to built up (Figure 8-14). In the bubble phase H_2 and CO concentration is negligible because both H_2 and CO exchanged (mass transfer) are quickly converted to water and CO_2 due to excess of O_2 in the bubble phase.

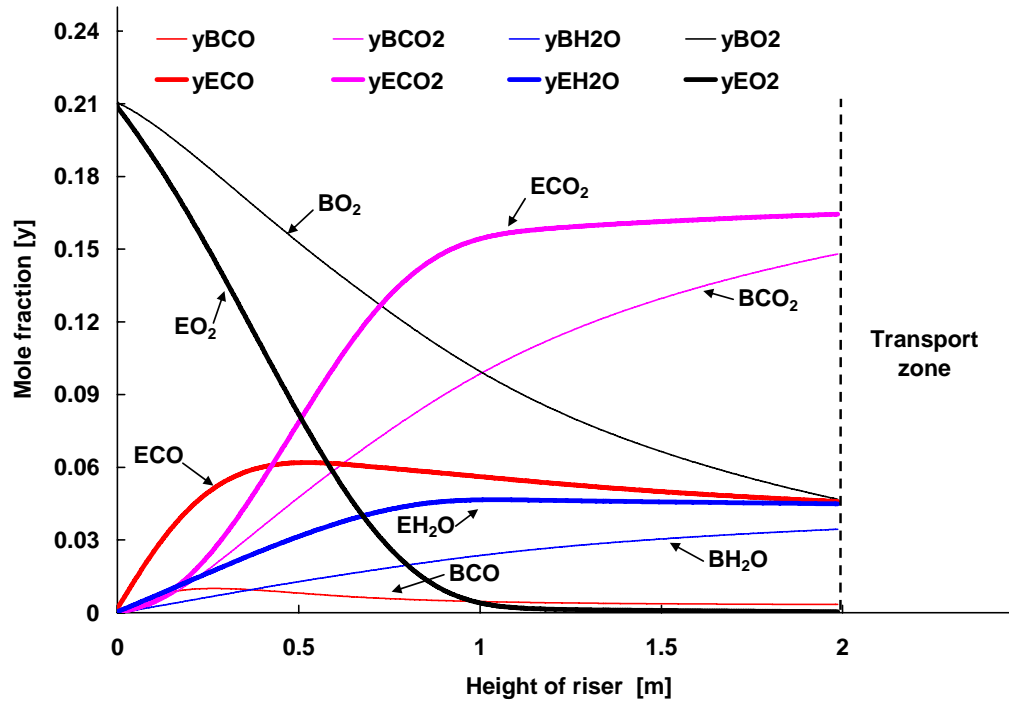


Figure 8-13: Gas composition in bubble and emulsion of riser.

Table 8-2: Flue gas composition at the exit of the riser.

Gas Composition	y (Mole Fraction)
CO	0.002700
CO_2	0.177753
CH_4	0.000000
C_2H_4	0.000000
C_2H_6	0.000000
C_3H_8	0.000000
H_2	0.000212
H_2O	0.095641
O_2	0.005191
N_2	0.718503

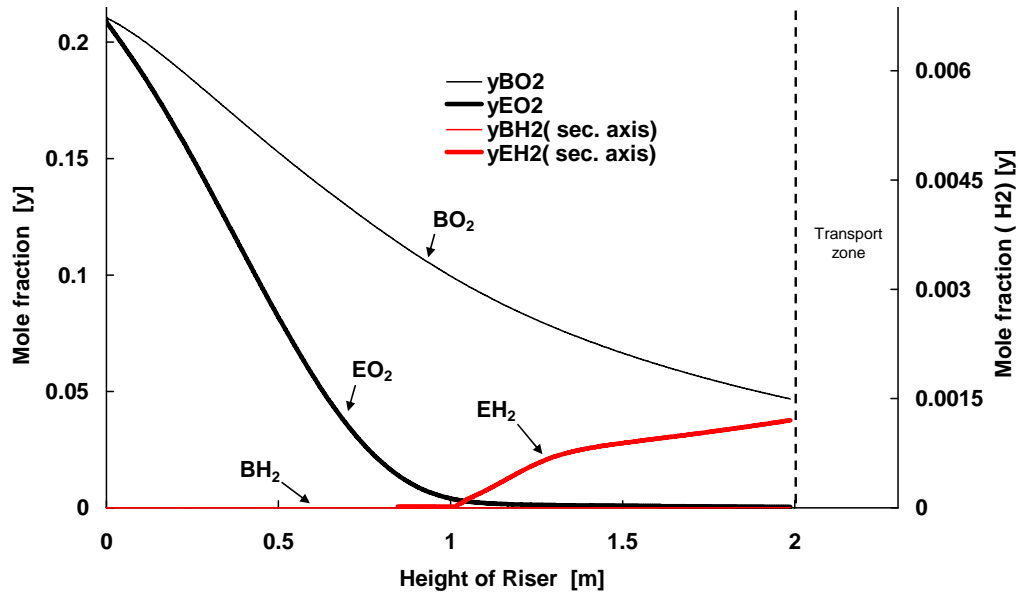


Figure 8-14: Hydrogen and oxygen profile in dense zone.

Figure 8-15 shows the amount of char combusted [$\text{kg} / \text{m}^3 \text{s}$], char gasified [$\text{kg} / \text{m}^3 \text{s}$] along the height of riser. It can be seen in the figure that most of the char reacted can be attributed to the combustion reaction. In the dense zone initially all the char conversion is due to char combustion reaction, but after 1 m of height char combustion is only 63% of total char reacted (remaining char is gasified). In middle zone approximately 87% of total char reacted is combusted remaining 23 % are gasified. At the exit of the riser oxygen is depleted while the fraction of steam has increased. This indicates that combustion reaction will be slowed down while that of gasification reaction will dominate. It can be observed in the upper zone where the percentage of char combustion gradually drops from 87% to 56 % and char gasification increasing from 13% to 44 %.

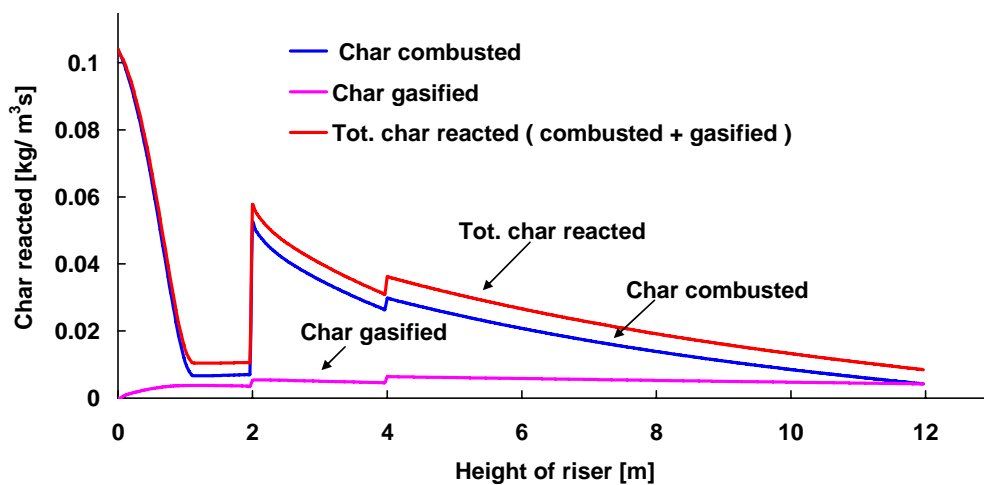


Figure 8-15: Profile of char reacted along the height of riser.

In Figure 8-16 char hold up (kg/cell) (primary y axis) and fraction of char reacted (char reacted / char hold up)(kg/s / kg) are shown. As the height increases in transport zone, the char hold up decreases from 0.036 kg/cell to 0.14 kg/cell. The change in char hold up is very sharp at heights of 2 and 4 m. This is due to change in bed characteristic due to primary and secondary air addition at these heights respectively.

Though char hold up decreases along the height of the riser, the fraction of char reacted (along the height of riser) increases. The curve of fraction of char reacted shifts up at the point of injection of primary and secondary air, hence giving more conversion. In the dense zone the amount of char reacted falls down steeply and after the height of 1 m. The curve becomes parallel to the x axis, showing that only a limited amount of char is reacted. It can be seen in Figure 8-14, that O_2 goes down very swiftly in emulsion phase and is completely consumed at height of 1 m. In the same line char combustion also goes down very swiftly till 1 m. After 1 m the amount of oxygen that is exchanged from bubble and the gasification reactions are responsible for further char conversion.

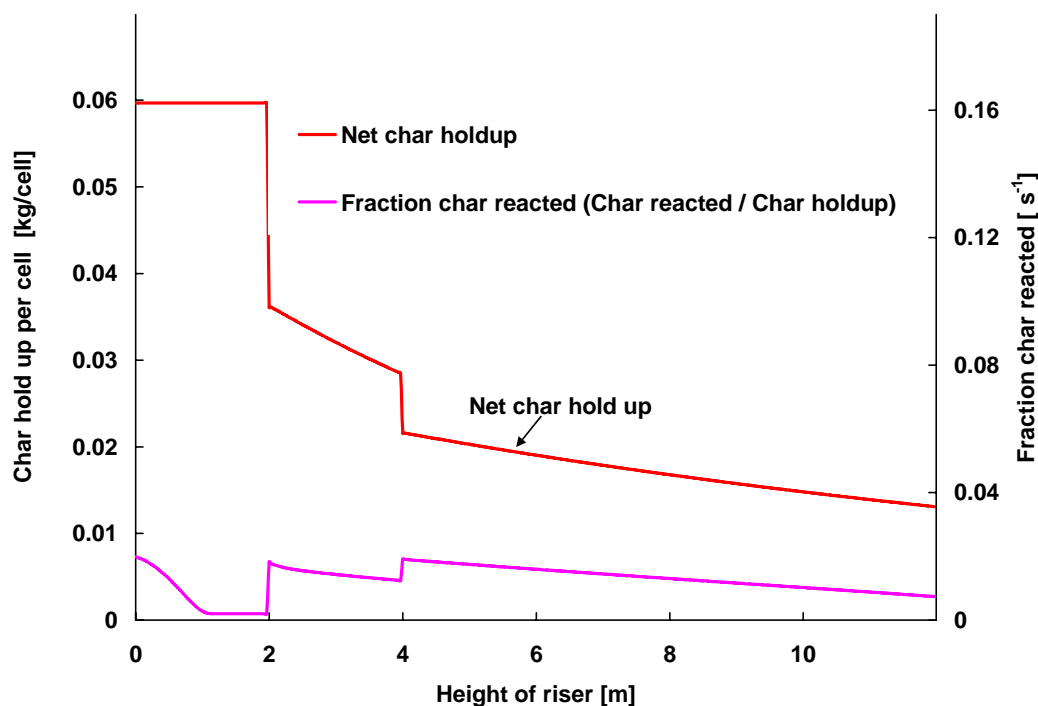


Figure 8-16: Profile of char hold up and fraction of char reacted along the height of riser.

Figure 8-17 shows the average temperature profile in the three zones of the riser. The temperature predicted by the model is in good agreement with the measured value. The error in predicted temperature is less than 1% of the measured value at the Guessing power plant. The model slightly overpredicts the temperatures reached, what can be attributed to either

the neglect of heat losses and also to possible inaccuracies in the prescribed operating parameters (solid circulation rate, air feed rate, air ratio with respect to exhaust gas). In order to focus on the effects of single parameters on the model results, a sensitivity study is carried out in the following section.

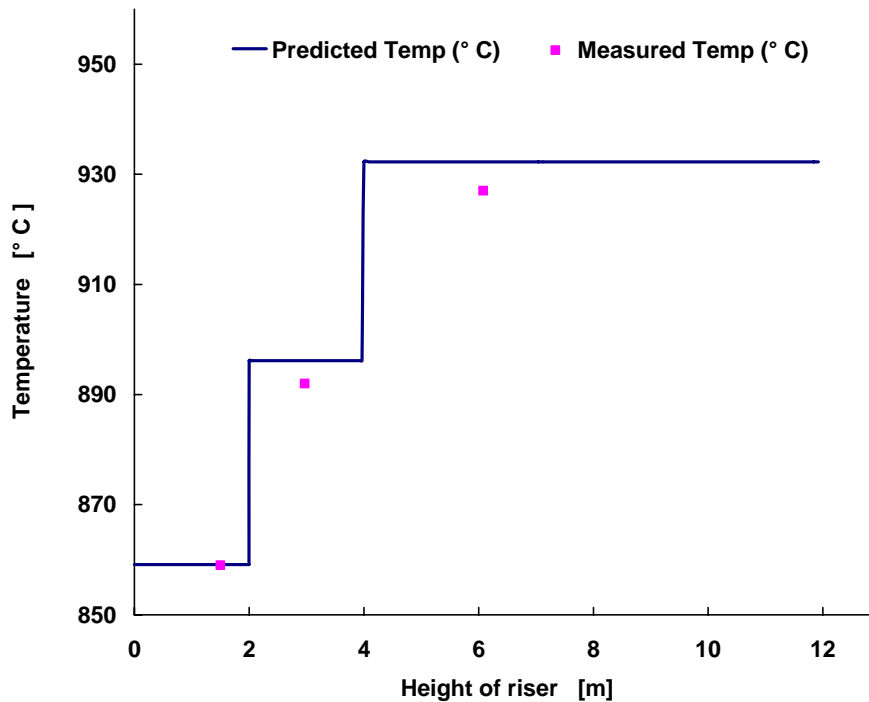


Figure 8-17: Average temperature profile in the dense, middle and upper zone of riser.

8.2 Sensitivity analysis

A mathematical model is defined by a series of equations, inputs, parameters, and variables. Input is subject to many sources of uncertainties like errors of measurement, lack of information and poor or only partial understanding of the system. A good modeling practice requires an evaluation of the model parameter, possibly assessing the uncertainties associated with the modeling process and with the outcome of the model itself. This can be done by sensitivity analysis. A sensitivity analysis is the process of varying model input parameters over a reasonable range (range of uncertainty in values of model parameters) and observing the relative change in model response. Sensitivity analyses are also beneficial in determining the direction of future data collection activities. Data for which the model is relatively sensitive would require more attention, as opposed to data for which the model is relatively insensitive.

A general representation of the system is

$$f = (x_1, x_2, x_3, \dots, x_n; \xi_1, \xi_2, \xi_3, \dots, \xi_n) = 0 \quad \text{Eq. 8-1}$$

Where x is the variable like concentration, height, porosity etc that changes during the modelling session, where as ξ is a model parameter (eg. reactor geometry, particle size...) that remains constant during the simulation run. The linear sensitivity coefficient χ_i . For the system 'f' with regard to the parameter ξ_j is defined as

$$\chi_i = \frac{\partial f}{\partial \xi_i} \quad \text{Eq. 8-2}$$

The linear sensitivity coefficient rejects the influence of only small deviations of the parameters. This is because the modelling system in general is a non linear system Therefore relative or logarithmic sensitivity coefficients χ_i^{rel} are defined as in Eq. 8-3.

$$\chi_i^{rel} = \frac{\xi_i}{f} \frac{\partial f}{\partial \xi_i} = \frac{\partial \ln f}{\partial \ln \xi_i} \quad \text{Eq. 8-3}$$

Discrete formulation of Eq. 8-3 is

$$\chi_i^{rel} = \frac{\xi_i}{f} \frac{\Delta f}{\Delta \xi_i} = \frac{\xi_i}{f} \frac{f(x_j, \xi_i) - f(x_j, k \xi_i)}{\xi_i - k \xi_i} = \frac{1 - \frac{f_k}{f}}{1 - \frac{k \xi_i}{\xi_i}} = \frac{1 - \frac{f_k}{f}}{1 - k} \quad \text{Eq. 8-4}$$

Eq. 8-4 is used in the model for evaluation of the relative sensitivity $f_k = f(x_j, k \xi_i)$. The parameter k is 0.9 for -10% variation and 1.1 for the + 10% variation. The result of the variation are evaluated with respect to the standard value. Therefore, the relative system response σ_i^{rel} is defined as

$$\sigma_i^{rel} = \frac{f_k(x_j, k \xi_i)}{f(x_j, \xi_i)} \quad \text{Eq. 8-5}$$

With this definition, the system reactions of the different variations are already comparable if $|1 - k|$ is the same. When dealing with σ_i^{rel} , it has to be kept in mind, that a remarkable sensitivity is present if $|1 - \sigma_i^{rel}| \geq 0.1$. This corresponds to a discrete relative sensitivity coefficient of $|\chi_i^{rel}| \geq 1$. A summary of the relative discrete sensitivity coefficients χ_i^{rel} , for the parameters for which a sensitivity analysis is performed is presented in Table 8-3. The sensitivity analysis is performed for a constant air ratio (λ) of 1.02.

It can be seen in the table that the air (bottom, primary and secondary) flow rates and initial air temperatures are relatively insensitive toward the average temperature of the zones. Char flow rate, char hold up and exit CO concentration are moderately sensitive to the air flow rates and temperature. Char hold up and exit CO concentration are relatively sensitive to primary air flow rate.

Char flow rate, hold up and CO concentration are uniformly sensitive toward producer gas flow rate. The average temperature of the middle zone is sensitive to the producer gas flow rate. The system is relatively insensitive toward the temperature of the producer gas.

Sensitivity analysis shows that the system is very sensitive to the bed material's flow rate (kg/s) as well as the initial bed temperature ($^{\circ}C$). It affects the char flow rate, char hold up, average temperature of all (3) zones and the CO concentration in the flue gas.

Char flow rate, hold up and CO concentration are moderately sensitive toward char density and char size. Char input rate is more sensitive to size while the char hold up is relatively more sensitive to char density. The Exit CO concentration is equally sensitive to char size and density. The variables (char flow rate, hold up and CO concentration) are moderately sensitive to the char composition too. The average temperatures of the zones are relatively insensitive to the char properties (density, size and composition).

Among all heterogeneous reactions the system is more sensitive to char combustion reaction followed by steam gasification, and almost insensitive toward the dry gasification reaction.

In the above section the effect of the parameter on variables were highlighted. If the variables were considered individually, it can be seen (Table 8-3) that the char input rate is most sensitive to the initial temperature of bed material, followed by bed material circulation. Char hold up is again very sensitive to initial temperature of bed material.

The CO concentration is very sensitive to the initial temperature of bed material and primary air flow rate.

The average temperatures of the zones are relatively insensitive to most of the model parameter except the initial temperature of bed material.

Parameter	Variable												
		Rate char input [kg/s]		Exit CO concentrati on [ppm]		Char hold up [kg]		Temperature [°C] (dense zone)		Temperature [°C] (middle zone)		Temperature [°C] (Upper zone)	
		(+)	(-)	(+)	(-)	(+)	(-)	(+)	(-)	(+)	(-)	(+)	(-)
Bottom air	Q	0.02719	-0.02719	0.01554	-0.01503	-0.00344	0.00420	0.00063	-0.00062	0.00049	-0.00046	0.00106	-0.00102
	T	0.00302	0.00302	0.01243	0.01191	0.00347	0.00351	0.00005	-0.00004	0.00011	0.00013	0.00011	0.00009
Primary air	Q	0.02115	-0.02115	0.13589	-0.13499	0.04302	-0.03991	0.00009	-0.00008	0.00031	-0.00030	0.00546	-0.00547
	T	-0.00302	0.00302	0.00481	-0.00477	-0.00371	0.00370	-0.00001	0.00001	0.00109	-0.00108	0.00111	-0.00109
Secondary air	Q	0.01511	-0.01511	0.03400	-0.03437	0.01791	-0.01803	0.00006	-0.00006	0.00034	-0.00035	0.00157	-0.00158
	T	-0.00302	0.00302	-0.00719	0.00721	-0.00361	0.00361	-0.00001	0.00001	-0.00007	0.00007	0.00029	-0.00028
Producer gas	Q	-0.04532	0.04532	-0.04373	0.04299	-0.04182	0.04178	-0.00019	0.00018	0.00181	-0.00181	-0.00008	0.00006
	T	0.00302	0.00302	0.01245	0.01199	0.00349	0.00350	0.00001	0.00001	0.00011	0.00013	0.00012	0.00009
Bed	m	0.11178	-0.11178	0.03091	-0.03069	0.04526	-0.04678	-0.00091	0.00111	-0.00499	0.00537	-0.00765	0.00732
	T	-0.38973	0.38973	-0.22697	0.22681	-0.46512	0.45986	0.09744	-0.09743	0.09039	-0.08991	0.08697	-0.08726
Water	Q	7.71E-07	7.71E-07	2.222E-06	2.222E-06	7.719E-07	-7.718E-07	0.0E+00	0.0E+00	-1.5E-07	1.5E-07	-9.4E-08	9.4E-08
	T	0.0003	0.0003	0.01187	0.01187	0.00350	0.00350	0.00001	0.00001	0.00007	0.00007	0.00012	0.00012
RME	Q	5.71E-07	5.71E-07	5.8E-05	-5.8E-05	3.4E-06	-3.4E-06	0.0E+00	0.0E+00	1.4E-06	-1.4E-06	7.2E-07	-7.2E-07
	T	0.0003	0.0003	0.01187	0.01187	0.00350	0.00350	0.00001	0.00001	0.00007	0.00007	0.00012	0.00012

Table 8-3: Relative sensitivity coefficient for model parameter. The coefficient are reported for constant air ratio($\lambda = 1.02$).

Table 8-3 continued.

Parameter	Variable												
Char		Rate char input [kg/s]		Exit CO concentration [ppm]		Char hold up [kg]		Temperature [°C] (dense zone)		Temperature [°C] (middle zone)		Temperature [°C] (Upper zone)	
		(+)	(-)	(+)	(-)	(+)	(-)	(+)	(-)	(+)	(-)	(+)	(-)
	ρ	0.05287	-0.05289	0.03039	-0.03041	0.07423	-0.07528	-0.00015	0.00016	-0.00058	0.00060	-0.00011	0.00010
	d_c	0.06240	-0.06173	0.03087	-0.03070	0.06733	-0.06634	-0.00016	0.00017	-0.00059	0.00062	-0.00011	0.00009
	w_c	-0.06070	0.06069	0.06439	-0.06485	0.03441	-0.03431	0.00018	-0.00018	0.00046	-0.00047	-0.00007	0.00008
Reaction	C	-0.05740	0.05780	-0.03981	0.03933	-0.06451	0.06695	0.00013	-0.00013	0.00059	-0.00055	0.00021	-0.00022
	st	-0.00911	0.00904	0.00357	-0.00376	-0.01161	0.01097	-0.00006	0.00005	-0.00021	0.00019	-0.00005	0.00006
	dry	-0.00302	0.00302	0.00197	-0.00201	-0.00411	0.00411	0.000001	0.000001	-0.00002	0.00002	0.00001	-0.00001

8.3 Parameter variation

In this section the parameter variations of those parameters are carried out that were found to be sensitive in the previous section. The parameter are varied over a larger range of data, unlike in the sensitivity analysis where the parameter have been varied by just $\pm 10\%$ of the standard value (Table 8-1) The graphs are drawn for different values of one operating parameter on the x axis while keeping all other operating parameters constant at the values of standard condition (Table 8-1).

8.3.1 Temperature of bed material

The temperature of the bed material has a very prominent effect on the performance of the riser. For a constant air ratio ($\lambda = 1.02$) when the feed temperature of the bed material increases the char circulation decreases, while the average bed temperature in the three zones increases as seen in Figure 8-18. It is quite obvious because high temperature in the reactor increases the reaction rates and hence more char is combusted. When the feed temperature of the bed material is increased by a factor of 1.024 then the char feed rate is decreased by a factor of 1.044 (for constant λ). When more char is combusted, more energy is released and the average temperature of the dense, middle and upper zone increases. There is an acute effect of bed temperature on the CO composition of flue gas. It can be seen in Figure 8-19 that the CO concentration decreases with the increase in the temperature of the bed material. This is because higher temperatures accelerate CO combustion.

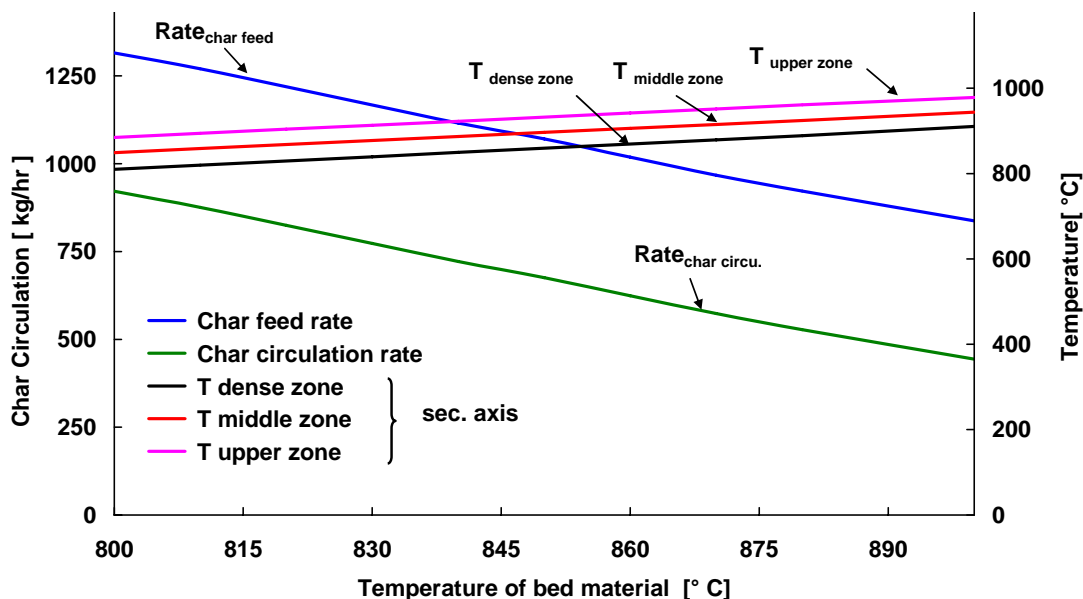


Figure 8-18: Effect of variation of the temperature of bed material on the char circulation rate and on the average temperature of the dense, middle and upper zone of riser.

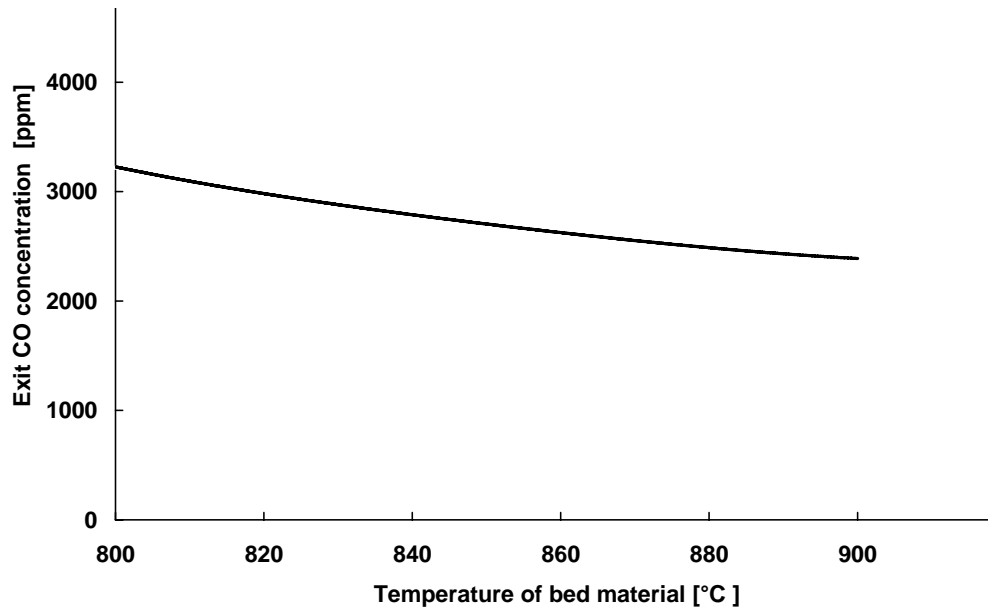


Figure 8-19: Effect of variation of the initial temperature of bed material [°C] on the CO concentration [ppm] of the flue gas.

8.3.2 Char composition

Wood chips are introduced in the gasifier. Inside the gasifier the wood chips undergo a complex processes of gasification. The residence time of the wood chips in the gasifier is adjusted in a way that once the volatiles are released the residual char is sent to the combustion reactor (riser). Char is the main feed/fuel to the combustor. However, the exact composition of this char is not known. Therefore it becomes extremely important to study the effect of the variation in composition of char. The carbon concentration (weight carbon / weight char) is varied from 50% carbon to 100 % carbon. It was found that for a constant air ratio ($\lambda = 1.02$), as the concentration of carbon in the char increases, the amount of char circulating back to the gasifier decreases (Figure 8-20). There is no prominent effect of char composition on the average temperature of the three zones. It can be seen that when the composition of char is 100% carbon then the average temperature of dense zone goes down, while that of the middle zone increases. This is because when char is 100 % carbon there is no hydrogen (to form steam) or oxygen release from the char. Hence, once the oxygen in emulsion is consumed (Figure 8-14) heterogeneous char reaction stops and the dense zone starts to cool. The CO produced from char combustion is not further combusted to CO₂ due to the absence of steam. Remaining char is then transported to the middle zone. In the middle zone there is addition of oxygen (primary air) and steam. Oxygen helps in char combustion where as steam help is CO combustion. Therefore the mean temperature of the middle zone increases (Figure 8-20).

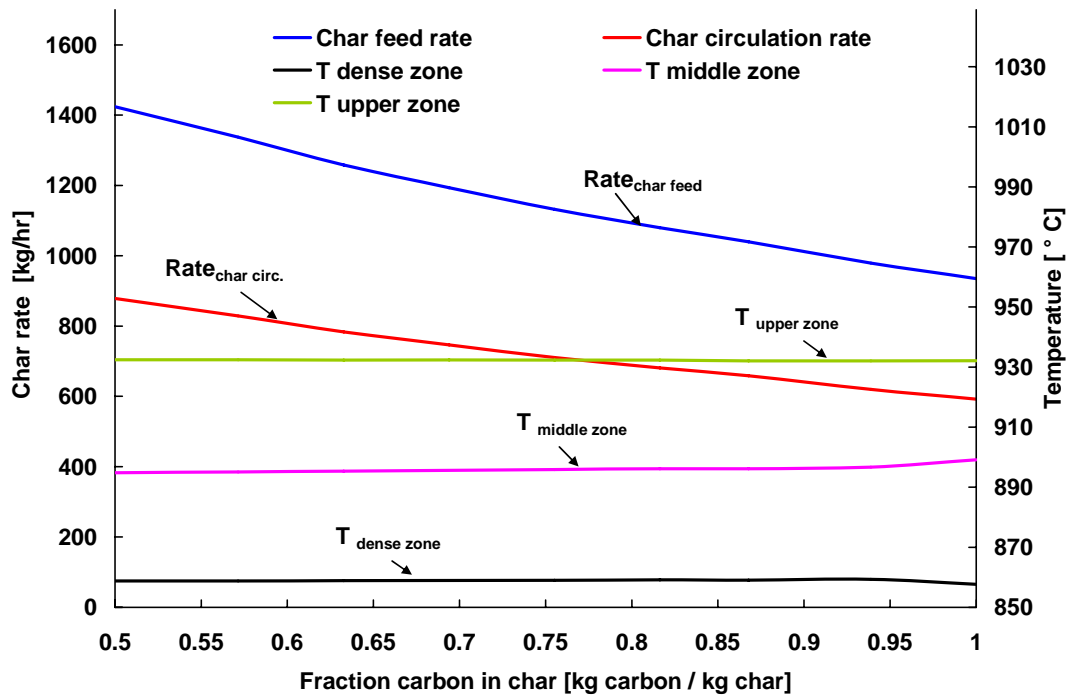


Figure 8-20: Effect of char composition on char circulation rate [kg/hr] and on the average temperature [°C] of the dense, middle and upper zone of the riser.

The CO concentration in the exit flue gas increases linearly with increasing carbon concentration in the char(Figure 8-21)

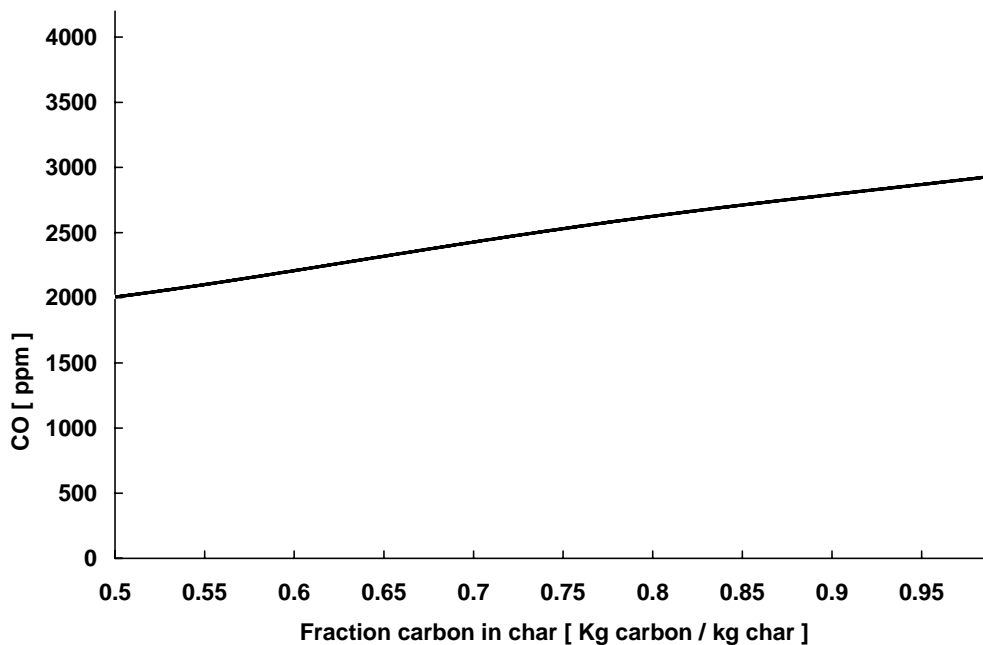


Figure 8-21: Effect of char composition on CO concentration [ppm] of flue gas.

8.3.3 Char size

Among all the char properties the most effective and sensitive parameter is the mean char size. The size of the char is studied for a size range of 0.5 mm to 30 mm. Assuming constant carbon conversion (constant λ), the feed rate of char increases with increasing diameter of char (Figure 8-22) and except for very small diameter there is always a back circulation of char into the gasifier. The back circulation of char into the gasifier is due to the incomplete combustion of char in the riser. The incomplete combustion of char in the combustion reactor is due to the low residence time of solids in the combustion reactor. Some pieces of solid char were actually found in the leg of the cyclone at the Guessing plant. As seen in Figure 8-22 for char sizes below 0.5 mm, the incoming char is completely combusted inside the riser and there is no char circulating back to the gasifier. Due to the increased heat capacity of the solid inventory (due to increased char hold up) the average temperature of the zones decreases when the size of the char increases.

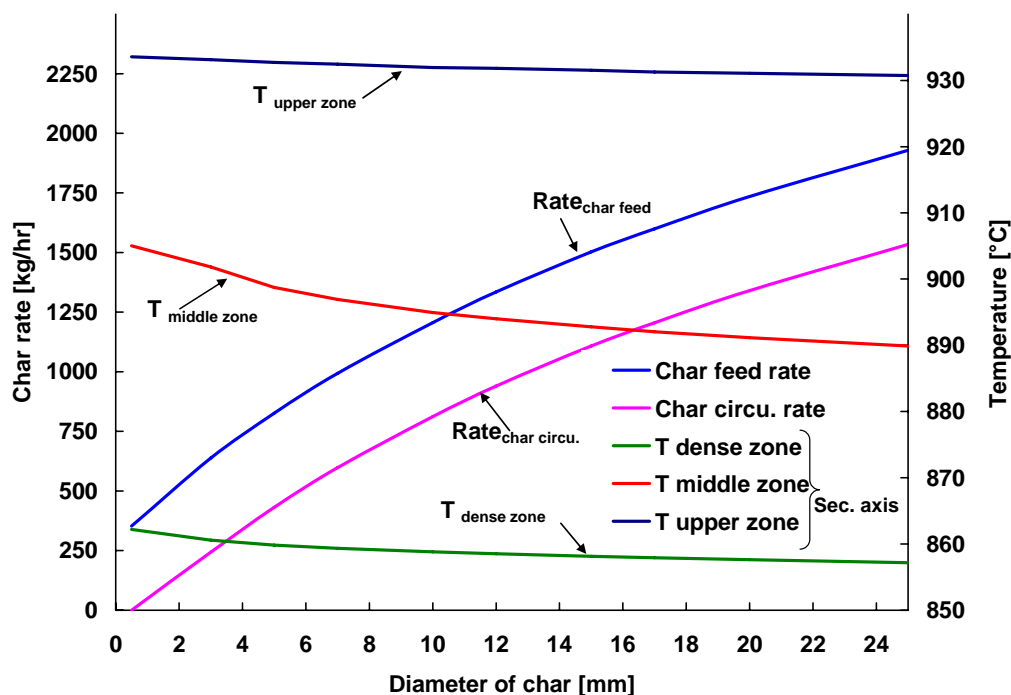


Figure 8-22: Effect of char size on char circulation [kg/hr] and average temperature in dense, middle and upper zone or riser.

The CO concentration in the exit flue gas drops down very swiftly in the small char size range (Figure 8-23). This is due to the complete combustion of char in riser. It can be generalized that the CO concentration decreases with decreasing char size.

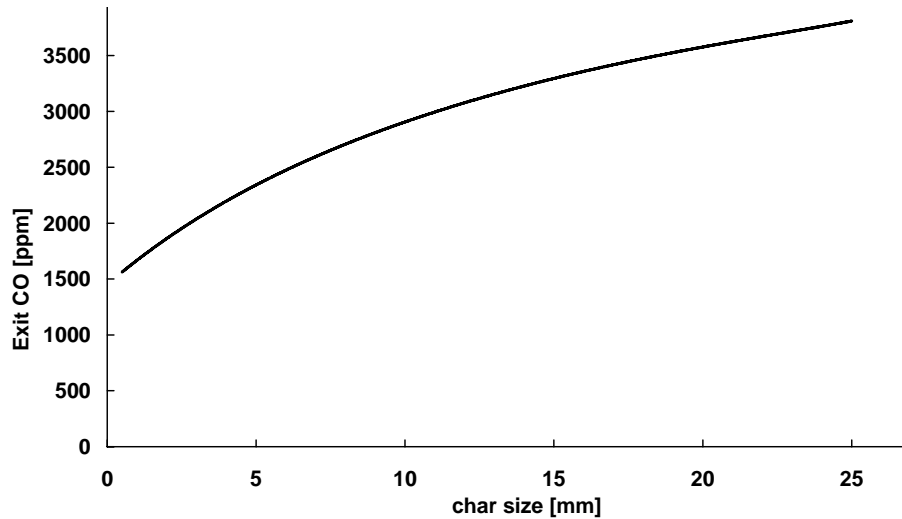


Figure 8-23: Effect of char size on CO concentration [ppm] of flue gas.

8.3.4 Char density

The effect of change in density is similar to the effect of char size. The only difference is that change in density is relatively less sensitive than the char size. From Figure 8-24 it can be concluded that if the char is made more porous for a constant char size then the performance of the riser is improved. The CO concentration in the flue gas also increases with increasing char density (Figure 8-25).

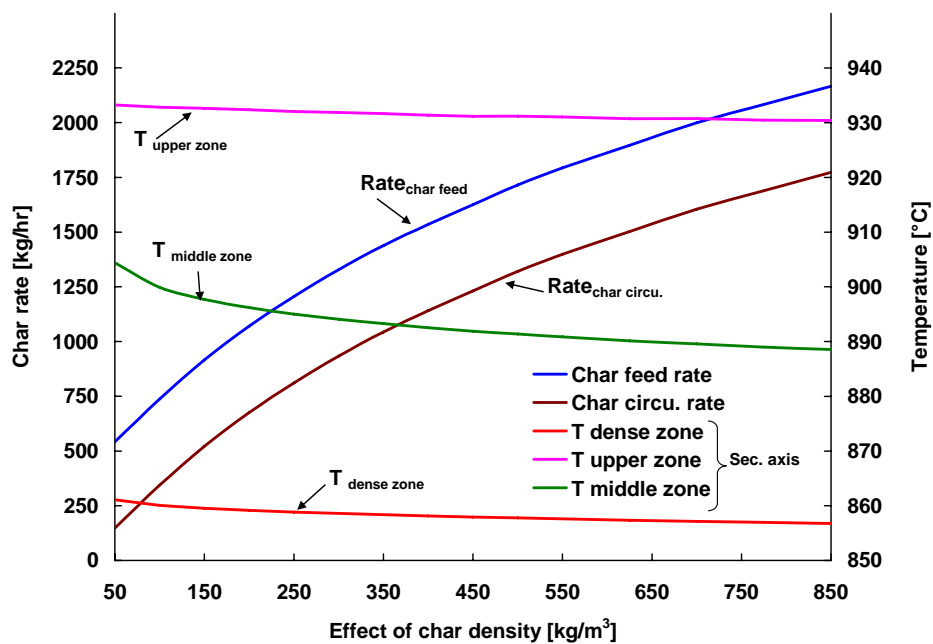


Figure 8-24: Effect of char density on char circulation [kg/hr] and average temperature in dense, middle and upper zone or riser.

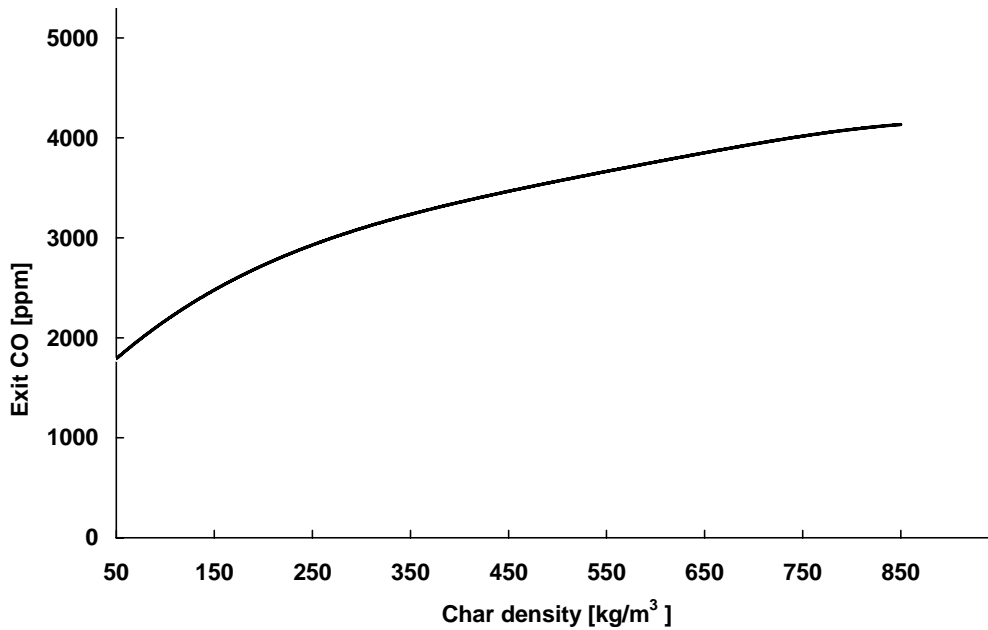


Figure 8-25: Effect of char density on CO concentration [ppm] of the flue gas.

From the simulation results of the char properties it can be generalised that small size char particle with low density and high carbon content increases the efficiency of the riser. Among all char physical properties size is most critical and sensitive. In complete combustion of char always results in CO concentration in the flue gas.

8.3.5 Producer gas flow rate

The effect of the producer gas feed rate on the char circulation is shown in Figure 8-26, it shows that that for a constant air ratio (λ) (i.e. constant char conversion) the amount of char circulation decreases as the producer gas feed rate increases. The temperature of the middle zone is also increased due to the increased feed rate of producer gas. This is because producer gas has a higher heating value and is a mixture of highly and easily combustible gases. Higher temperature accelerates the reaction rate and more char is combusted. This means that for a limited amount of char to be combusted less char must be fed to the combustion reactor if the feed rate of producer gas is increased (Figure 8-26). The relation between char circulation and producer gas feed rate is almost linear. If the producer gas flow rate is halved then the char flow rate is increased by a factor of 1.2 (for constant air ratio). Figure 8-26 shows that if producer gas supply has to be closed than to meet same conversion nearly 1580 kg /hr of char has to be supplied in the riser.

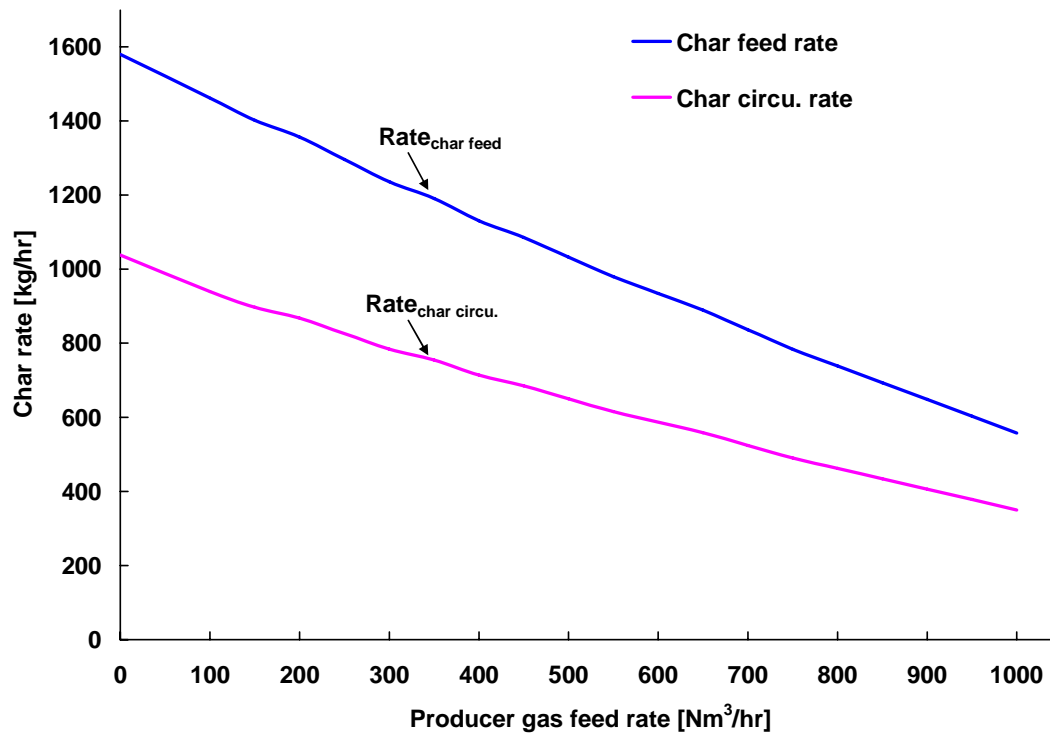


Figure 8-26: Effect of producer gas flow rate on char feed and circulation rate.

Figure 8-27 shows the CO concentration (ppm) in the flue gas as the function of producer gas flow rate. It shows that as the producer gas flow rate increases, the CO concentration decreases. This is because, with the increased producer gas flow the enthalpy of the system increases and hence the temperature of the riser increases, consequently accelerating the CO combustion and decreasing the CO concentration in the flue gas.

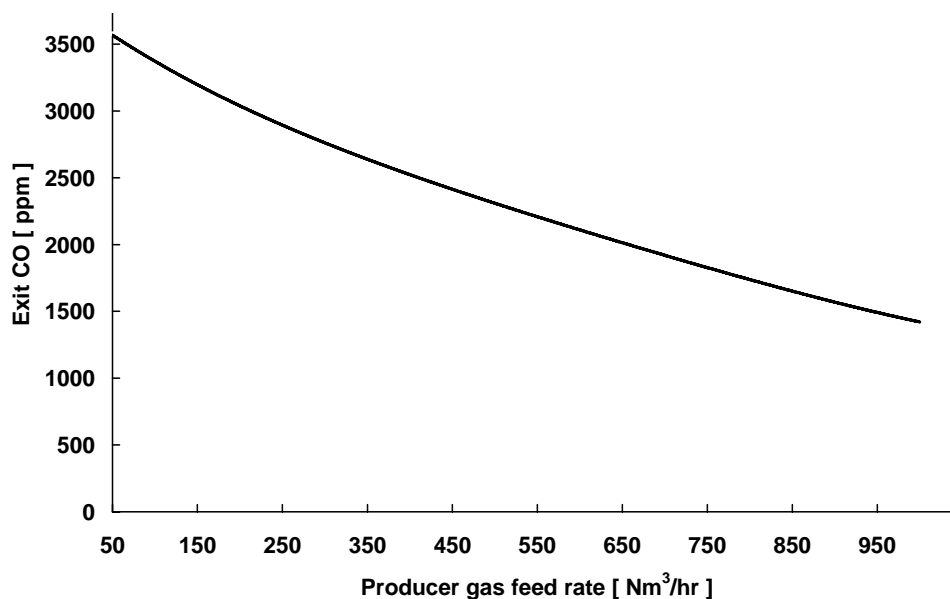


Figure 8-27: Effect of producer gas flow rate on the CO composition (in the flue gas).

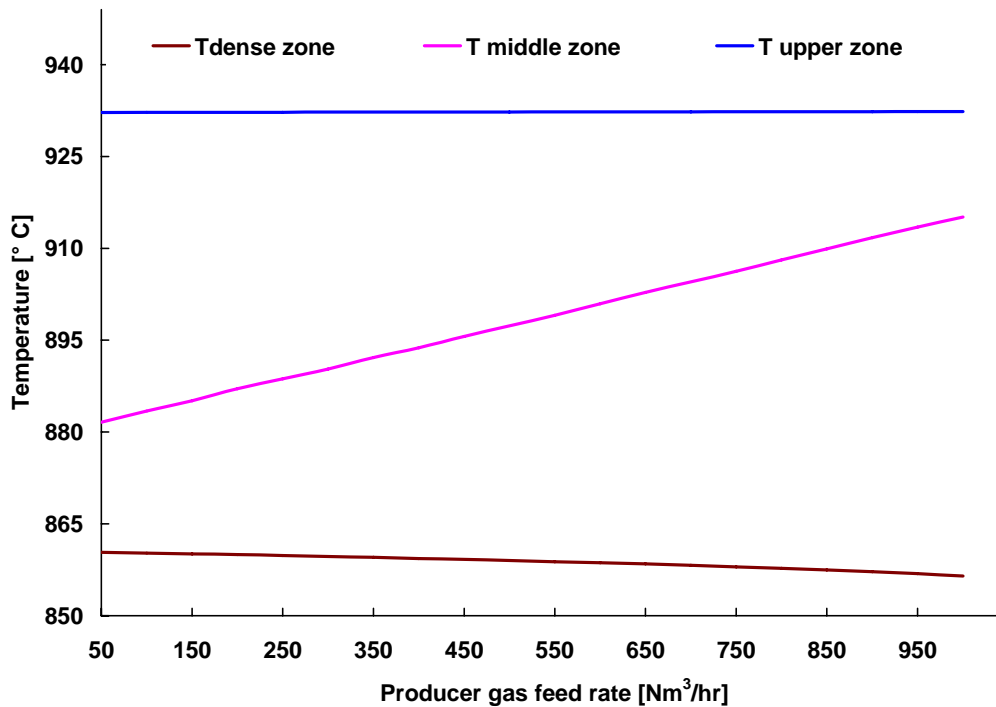


Figure 8-28: Effect of producer gas flow rate on average temperature of zones.

Higher producer gas feed rate has a small effect on the temperatures of the dense and upper zones. For a constant air ratio (of 1.02) the model reduces the char feed rate for increased value of producer gas flow rate. Hence when the char feed decreases, the average temperature of the zone also decreases. The effect is more visible in the temperature of middle zone (where producer gas is added). The heat released due to the combustion of the producer gas increases the average temperature of the middle zone. In the upper zone there is very little increase in temperature because the heat capacity of the bed material is so high that the change in temperature is not visible.

Producer gas at different bed temperatures

Figure 8-26 is re-plotted with different feed temperatures of the bed material (Figure 8-29) and it is found that as the initial temperature of the bed material circulation increases the curve shifts down, i.e. for constant producer gas flow rate and constant air ratio ($\lambda = 1.02$), if the feed temperature of bed material is increased char circulation rate is decreased. It can be seen in Figure 8-29 that for a constant producer gas flow of 470 Nm³/hr char circulation rates for bed temperatures of 800 °C, 850 °C, and 900 °C are 1350 kg/hr, 1025 kg/hr, and 825 kg/hr respectively. The figure emphasizes how the need for producer gas recirculation is influenced by the rate of char feed to the riser. If measures are found to increase the char feed, the producer gas recycle can be significantly reduced. Higher temperature of the bed temperature of the bed material by 12 % the producer gas needed is decreased by 52 %.

Higher temperature of the bed material also lowers the CO concentration in the exit flue gas (Figure 8-30) because higher temperature accelerates the CO combustion.

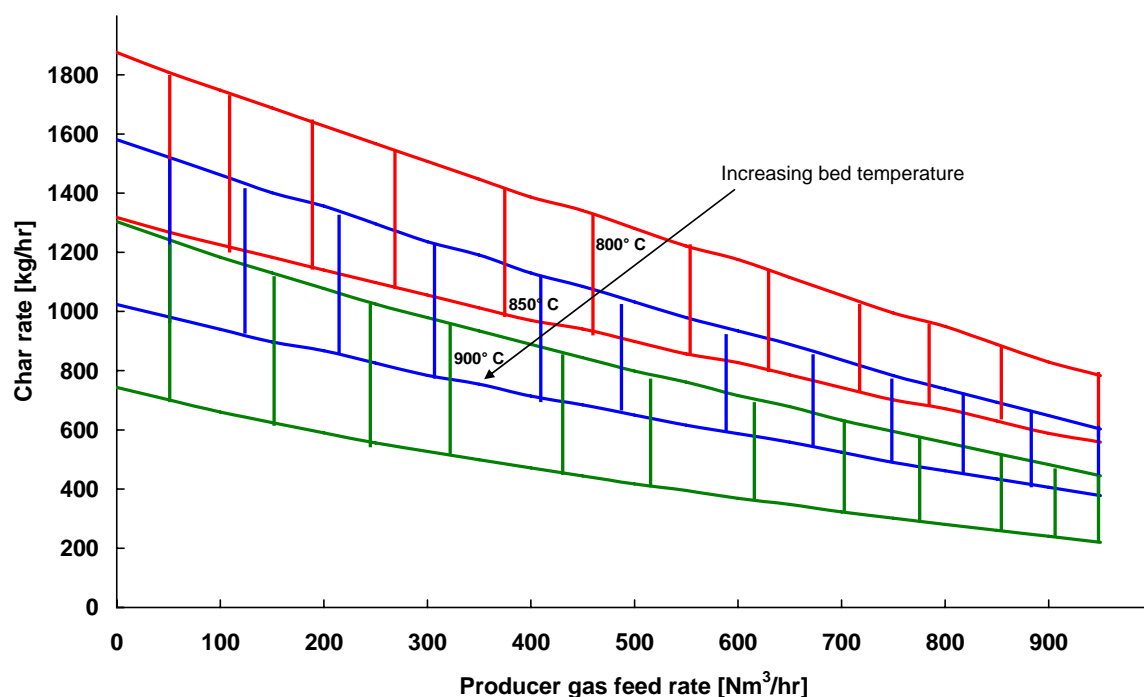


Figure 8-29: Comparison of char rates and producer gas feed rates at different bed temperatures.

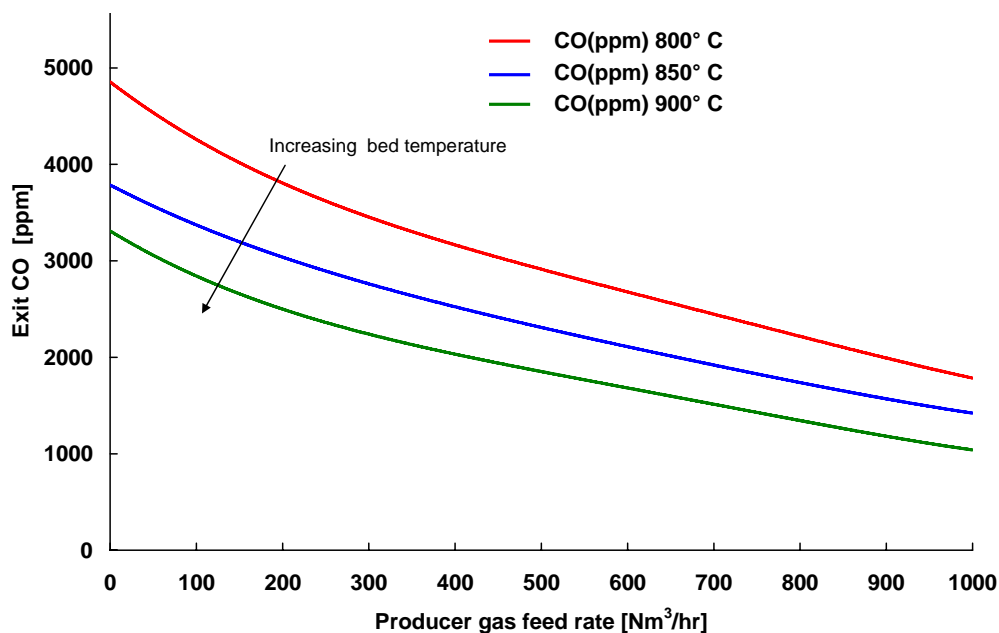


Figure 8-30: Comparison of CO concentration and producer gas feed rate at different bed temperatures.

8.3.6 Bed circulation rate

Bed circulation rate is the amount of bed material that is circulating between the gasifier and the combustion reactor. Char from the gasifier is transported to the combustor together with the bed material. The heat released in the combustion reactor is transported back to the gasifier along with the circulating bed material. It can be seen in Figure 8-31, with increase in bed circulation rate the average temperature of each zone decreases. This is because higher bed material circulation means a higher heat capacity of the solids in the steady state heat balance of the riser. The difference between the bed material feed temperature (850 °C) and the exit temperature of the upper zone represents the temperature difference between gasifier and combustion reactor of the dual fluidized bed system.

Figure 8-32 shows the effect of bed circulation rate on the char circulation. It can be seen that for a constant air ratio ($\lambda = 1.02$) as the bed circulation rate increases the char circulation rate also increases, because as the solid flow rate increases, the solid velocity increases and hence the residence time decrease. To meet the target air ratio ($\lambda = 1.02$) with reduced residence time more char has to be supplied. The relation between bed circulation rate and char circulation rate is linear. When bed circulation rate is doubled the char circulation rate is also doubled.

The graph also shows the CO concentration in the exit flue gas as a function of bed circulation. As the bed circulation increases the CO concentration in the flue gas also increases, this is due to the incomplete combustion of solid char and CO.

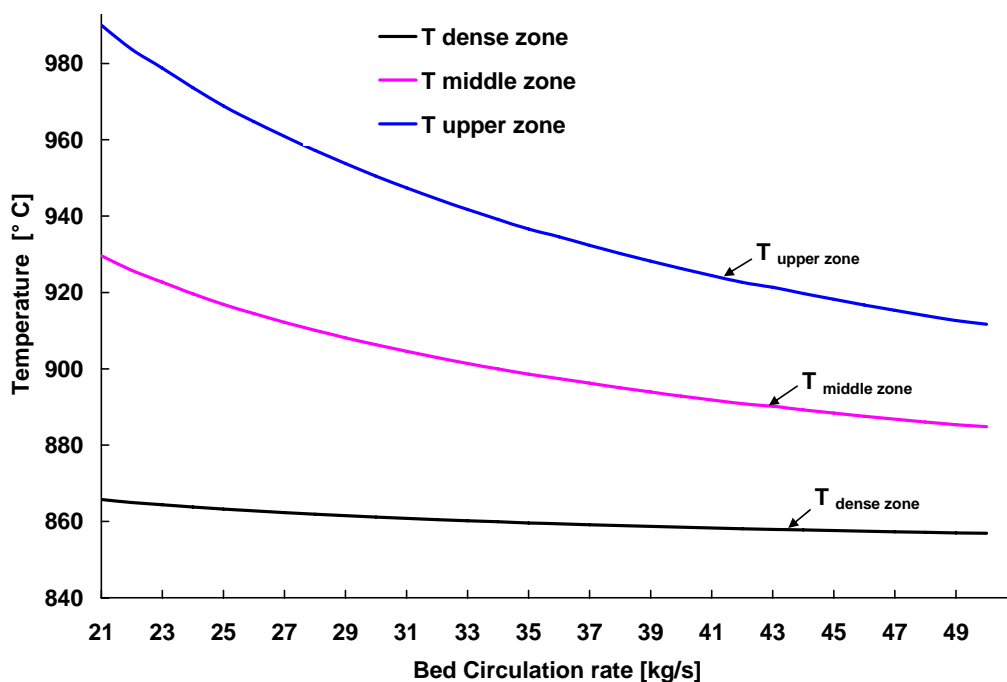


Figure 8-31: Effect of bed circulation on the average temperature of the zones.

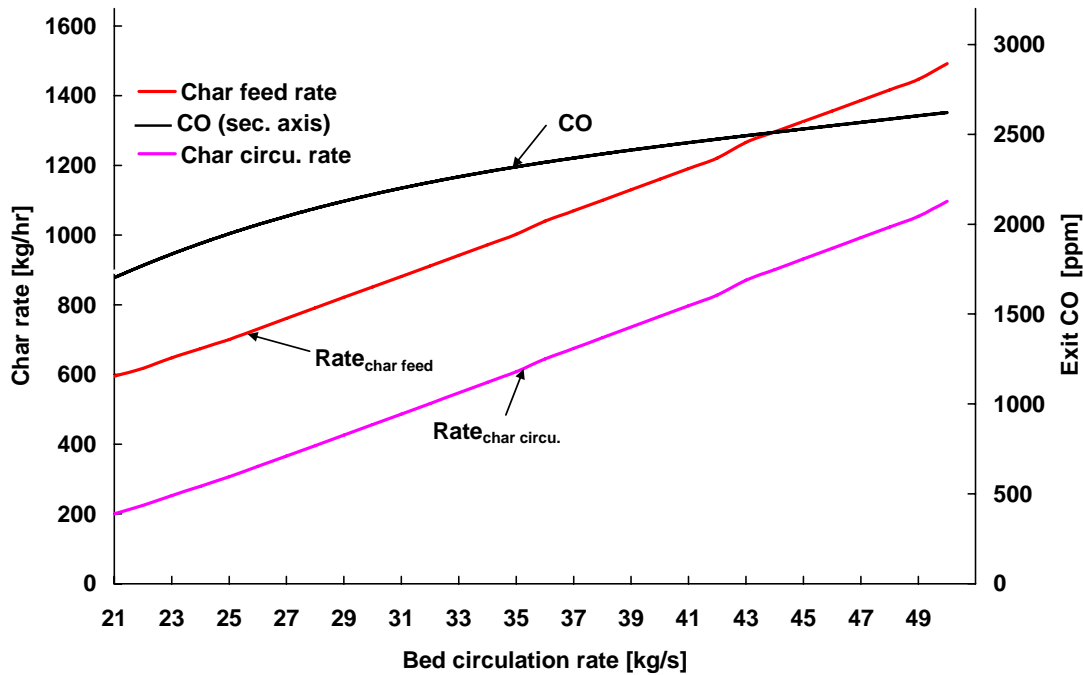


Figure 8-32: Char circulation and CO concentration in flue gas at different bed circulation rate.

8.3.7 Air distribution

Figure 8-33 shows the effect of air distribution between primary and secondary air. This graph is drawn for constant bottom air flow rate as mentioned in Table 8-1. Total air as mentioned in figure (Figure 8-33) is the sum of primary air and secondary air as mentioned in Table 8-1. In Figure 8-33, x axis is the percentage of the 'total air' as primary air. The remaining air is secondary air (e.g. the value 30 on x-axis means that 30% of the 'total air' is supplied as primary air and the remaining 70 % as secondary air). The simulation results show that as more and more air is supplied as primary air less char has to be circulated for a constant air ratio ($\lambda = 1.02$). It can be seen that after 55%, the system reaches its saturation limit and further increase in amount of air as primary air has only little effect on char circulation. However, for the initial lower primary air percentage the slope of graph is very steep. The concentration of CO in the exit flue gas is insensitive towards the air distribution and remains uniform at a value of about 2300 ppm

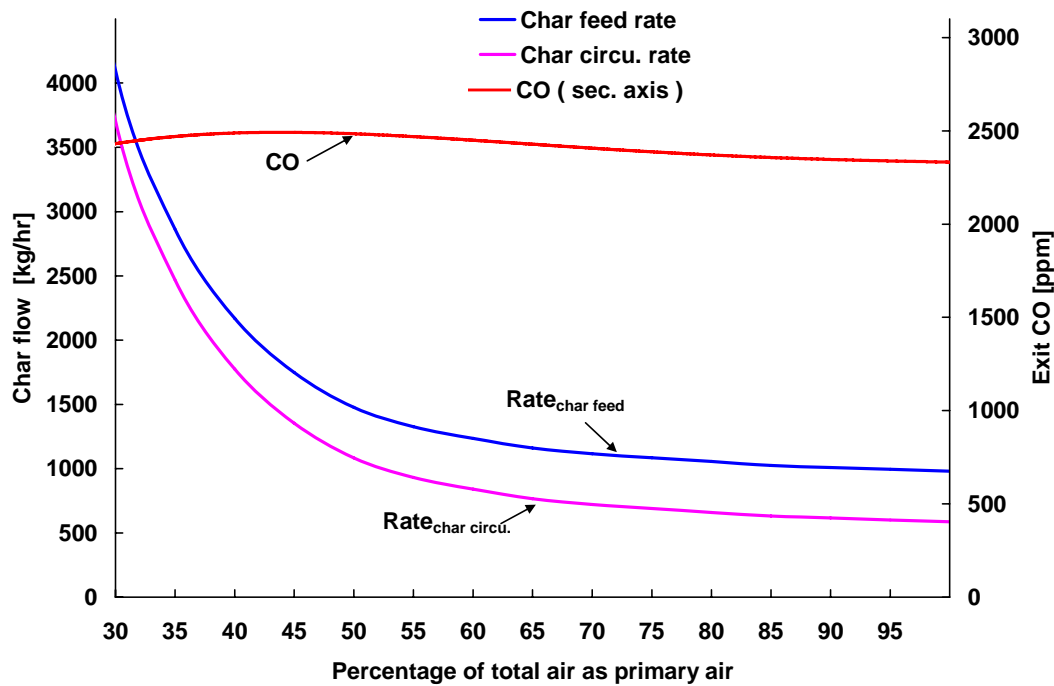


Figure 8-33 : Char circulation and CO concentration as a function of air distribution.

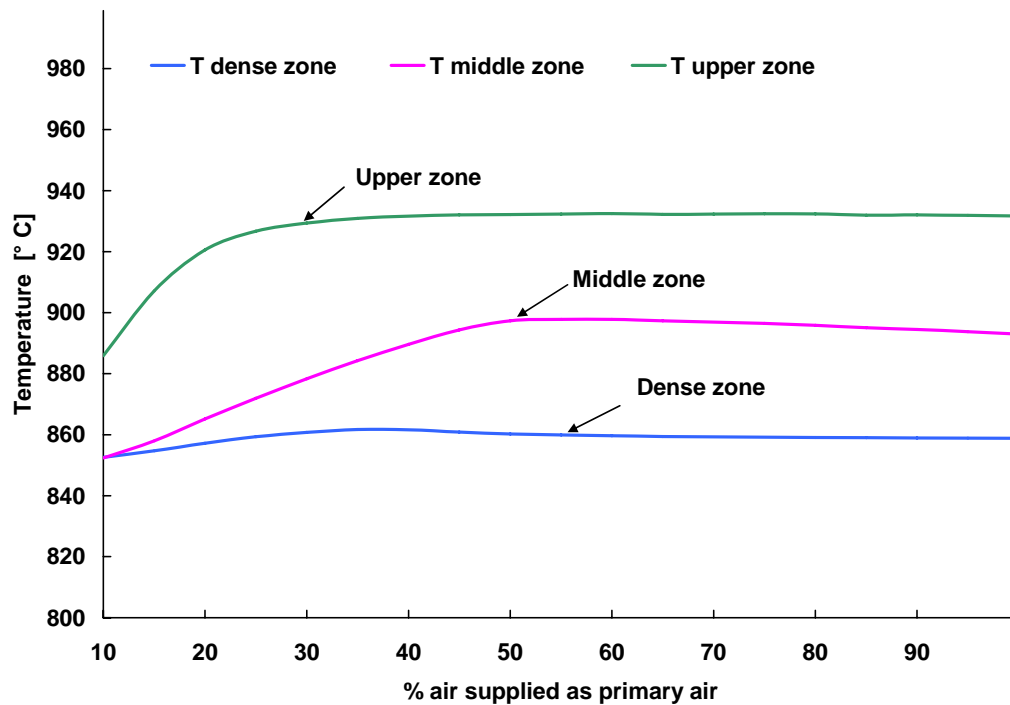


Figure 8-34: Effect of air distribution on the average temperature of the zones.

Figure 8-34 shows the temperature profile for the air distribution between primary and secondary air. The temperature of the dense zone is increased from 1125K to 1130K as the

primary air flow rate is increased to 40% and then it attains the equilibrium value. Similarly the temperature of upper zone also increases from 1185K to 1204K and then it reaches at equilibrium value at 30%. The temperature of the middle zone is also increases from 1125K to 1170K before reaching at equilibrium value at 50%.

8.3.8 Mixing pattern of spent scrubber liquid

The RME water emulsion coming from the scrubber is recycled back to the riser (combustion reactor). In the model this organic stream is added in the middle zone. This stream changes its phase from liquid to gas once it enters the cell of middle zone. The mixing pattern is not precisely known. So the change of phase and gas mixing pattern were simulated. The term increasing, decreasing and parabolic means that the RME emulsion (organic stream) added in the cells of the middle zone (Figure 8-3) increases, decreases or first increases than decreases (parabolic) with height of the middle zone. As shown in Figure 8-35, the water profile is only affected in the middle zone of the riser. At the boundary of the middle zone the gas composition is similar in all cases. Table 8-4 shows that the mixing and evaporation profile has practically no effect on the overall performance of the riser.

Table 8-4: Comparision of the mixing pattern of the spent scrubber solution in the riser.

zones	parameters	profiles of water addition		
		Increasing	parabolic	decreasing
Dense zone	Char HoldUp[kg]	2.535	2.535	2.535
	Temperature[°C]	859.146	859.146	859.146
	Char in [kg/hr]	1070.555	1070.555	1070.555
Middle zone	Char HoldUp[kg]	1.615	1.615	1.6151
	Temperature[°C]	896.221	896.222	896.221
Upper zone	Char HoldUp[kg]	3.4167	3.4167	3.4167
	Temperature[°C]	932.352	932.352	932.352
	Char out [kg/hr]	675.524	675.525	675.526
	yCO	0.00241	0.00241	0.00241
	yCO ₂	0.178	0.178	0.178
	yO ₂	0.005	0.005	0.005
	yH ₂ O	0.0958	0.0958	0.0958

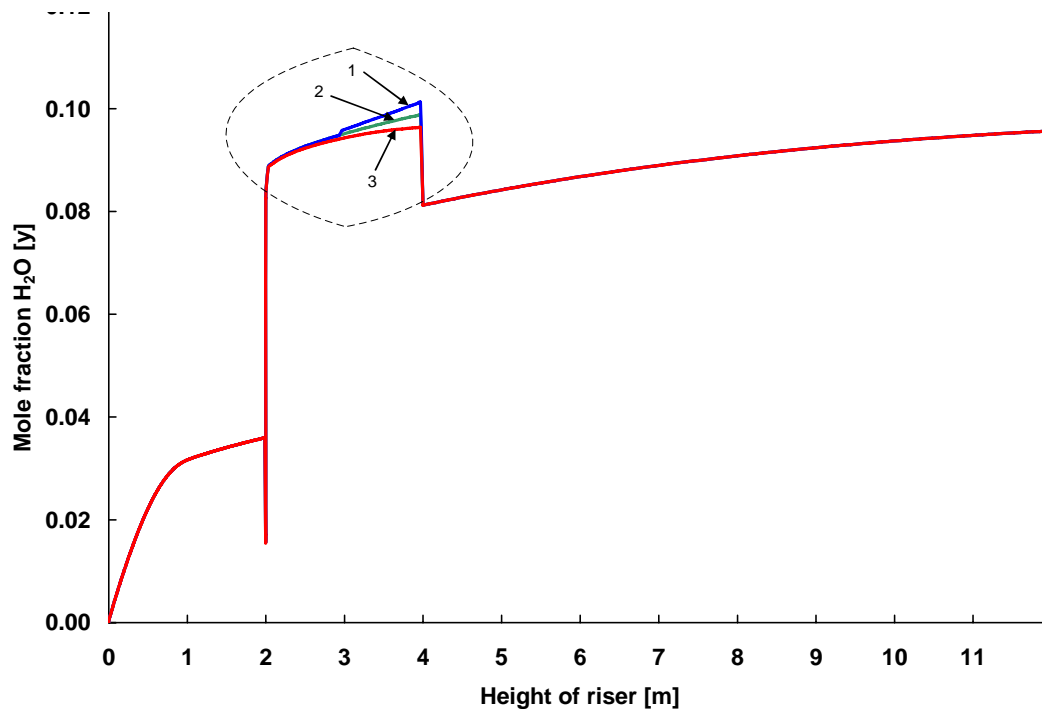


Figure 8-35: Effect of different profiles of water addition in middle zone (1: increasing, 2: parabolic, 3: decreasing)

SUMMARY AND CONCLUSIONS

For better understanding of the Dual Fluidized Bed (DFB) gasification process, modelling and simulation was performed. The gasifier of the DFB was modelled in previous work. In this current research work the modelling and simulation study of the combustion reactor (riser) has been done. The objective of the current work has been to make a mathematical model to predict the temperature and composition (gas phase) along the height of the riser.

It is a one dimensional steady state model of a fast fluidized bed. Model assumes gases to be ideal and in plug flow. The solids are assumed to be Geldart type B, attrition free and perfectly mixed. The fluid dynamic parameters are evaluated with the material properties of the inert bed. The residual wood post gasification is called char. The char is assumed to be spherical and a homogeneous matrix of carbon, hydrogen and oxygen. Char physical and chemical properties (diameter, density, composition) and bed material circulation rate are input parameter to model. The model assumes no heat loss.

From the hydrodynamic point of view the model divides the combustion reactor into three zones namely dense, middle and upper zone. Dense zone is assumed to be in bubbling regime and is modelled assuming to follow the modified two phase theory. Middle zone and upper zone together makes the transport zone and the transport zone is modelled with a core-annulus flow structure.

Middle zone is a special case. Apart from residual char combustion, the middle zone is also modelled to serve as a sink for the small amounts of rich tar solvent and tar contaminated water occurring in the plant.

Char particle follows the shrinking particle model i.e. constant particle density and decreasing particle size. It is also assumed that heterogeneous char combustion is controlled by the combined effect of mass transfer (to particle surface) and reaction at the char surface. nth order reaction kinetics are employed for the homogeneous as well as heterogeneous reactions inside the combustion reactor.

The model developed is capable to deal with changes in riser geometry (height, diameter, angle etc) and any fuel type (solid, liquid and gases). The model developed is in good agreement with any fluidization regime ranging from bubbling to fast fluidization. The model fails when superficial velocity of gas is less than minimum fluidization i.e. when the bed is operated as fixed bed.

The average temperature profile of the riser predicted by the model is in good agreement with measured data. Due to lack of gas analysis inside the fluidized bed, the predicted gas composition profile was not verified. Nevertheless, the exit and composition of the flue gas is in the range of the model prediction.

Sensitivity analysis of the model showed that the initial temperature of bed material and bed material circulating between the two fluidized bed (gasifier and combustion reactor) is the most critical parameter, because this solid acts as the heat carrier between the two reactors. Other sensitive parameters are char size and char density. Further, the effects of variations in typical and sensitive operating parameters were investigated over a large range of data points.

Parameter variations at the simulation model show that the residual char from the gasifier is only partly converted in the riser (combustion reactor). Un-combusted char is transported back into the gasifier and leads to an increase of char present in the whole system finally stabilizing the char hold up at an equilibrium value. However, the extent of char conversion and also the calculated char hold up are dependent on the properties of char particles and on the residence time of the solid and gas in the system.

Future work is to couple the two separate mathematical models of gasifier and combustion reactor to a single modelling unit. The coupled model (as a single unit) will be closer to the real process. It is also planned to do gas analysis inside the gasification plant at Guessing for validation of the mathematical model.

REFERENCES

- [1] Abdel-Hafez, A.H.(1988): Simplified overall rate expression for shrinking core bituminous char combustion, *Chem. Eng. Sc.*, Vol. 43, pp. 839-845.
- [2] Abed, R.(1985): *Ind. Eng. Chem. Fundamentals*, Vol. 24, p.78.
- [3] Adanez, J., Gayan, P., Garcia-Labiano F. and de Diego L.F.(1994): Axial voidage profiles in fast fluidized beds, *Powder Technology*, Vol. 81, pp. 259–268.
- [4] Adanez, J., Gayan, P., de Diego, L. F., Garcia-Labiano, F. and Abad, A.(2003): Combustion of Wood Chips in a CFBC. Modelling and Validation, *Industrial and Engineering Chemistry Research*, Vol. 42(5), pp. 987-999.
- [5] Andersson, B.-A. and Leckner, B.(1989): Particle Mass Flux in the Freeboard of a Fluidized Bed Boiler, *Powder Technol.*, Vol. 58, pp. 25-37.
- [6] Andrei, M.A., Sarofim, A.F. and Beer, J.M.(1983): Nat. Meeting AIChE, Houston, Texas, Paper no.F, session 7.
- [7] Annamalai, K., Sweeten, J.M. and Ramalingam, S.C.(1987): Estimation of gross heating values of biomass fuels, *Transactions of ASAE*, Vol. 30, pp. 1205–1208.
- [8] Antal, J. M.(1981): Biomass as a Non Fossil Fuel Source; KLASS.
- [9] Arena et al.(1988): *Circulating Fluidized Bed Technology II*, P. Basu, ed., p. 16, Compiegne.
- [10] Arena, U., Chirone, R., Matteo, D., Miccio, M. and Salatino, P.(1995): Some issues in modelling bubbling and circulating fluidized-bed coal combustors, *Pow. Tech.*, Vol. 82(3), pp. 301-316
- [11] Arthur, J.A.(1951): Reaction between carbon and oxygen, *Trans. Faraday Soc.*, Vol 47, pp. 164-178.
- [12] Avedesian, M.M. and Davidson, J.F.(1973): Combustion of Carbon Particles in a Fluidised Bed, *Trans. Inst. Chem. Eng.*, Vol. 51, pp. 121-131.
- [13] Babu, S.P., Shah, B. and Talwalkar, A.(1978): Fluidization Correlations for Coal Gasification Materials – Minimum Fluidization Velocity and Bed Expansion Ratio, *AIChE Symp. Ser.*, Vol. 74(176), pp. 176-186.
- [14] Basu, P. and Fraser, S.A.(1991): *Circulating Fluidized Bed Boilers*, Butterworth-Heinemann, Boston, p. 95.
- [15] Basu, P.(1999): Combustion of coal in circulating fluidized-bed boilers: A review, *Chem. Eng. Sci.*, Vol. 54, pp. 5547.
- [16] Bader, R., Findlay, J. and Knowlton, T. M.(1988): Gas/solid flow patterns in a 30:5 cm diameter circulating fluidized bed. In P. Basu, J. F. Large (Eds.), *Circulating fluidized bed technology II* (pp. 123–128). Oxford, England: Pergamon Press.
- [17] Baehr, H.D.(2000): *Thermodynamik – Grundlagen und technische Anwendungen*, 10. Auflage, Springer-Verlag, Berlin, Heidelberg, New York.
- [18] Barin, I.(1993): *Thermochemical data of pure substances*, Edition, Band 1 and 2, VCH Weinheim.
- [19] Baeyens, J.(1981): *Gas Fluidization, Short Course*, Institute of Chemical Engineering, University of Bradford.
- [20] Bai, D., Issangya, A. S., Zhu, J.-X. and Grace, J. R.(1997): Analysis of the Overall Pressure Balance around a High-Density Circulating Fluidised Bed, *Industrial and Engineering Chemistry Research*, Vol. 36, p.3898.
- [21] Bain, R.L., Overend, R.P. and Craig, K.R.(1998): Biomass-fired power generation. *Fuel Process. Technol.* Vol. 54, pp. 1–16.
- [22] Baker, E. G.; Mudge, L. K. and Brown, M. B.(1987): *Ind. Eng. Chem. Res.* Vol. 26, p1335.
- [23] Barrio, M., Gobel, B., Risnes, H., Henriksen, U., Hustad, J.E. and Sorensen, L.H.(2000): Steam gasification of wood char and the effects of hydrogen inhibition on chemical kinetics, *Progress in thermochemical biomass conversion*, Tirol, Austria.
- [24] Barrio M. and Hustad J. E. (2000): CO₂ gasification of birch and the effect of CO inhibition on the calculation of chemical kinetics", *Progress in Therochemical Biomass Conversion*, Tirol, Austria.

- [25] Belgiorno,V., Feo,G. De , Rocca C. Della and Napoli R. M. A.(2003): Energy from gasification of solid wastes, Waste Management, Vol. 23(1), pp. 1-15.
- [26] Benson, S.A., Jones, M.L. and Harb, J.N.(1993): Chapter 4 - Ash Formation and Deposition, in Fundamentals of Coal Combustion for Clean and Efficient Use, Ed L.D. Smoot, Elsevier Science, New York.
- [27] Berruti, F. and Kalogerakis, N.(1989): Modelling the internal flow structure of circulating fluidized beds. Canadian Journal of Chemical Engineering, Vol. 67, 1010–1014.
- [28] Bi H., Fan L.S.(1992): Existence of Turbulent Regime in Gas-Solid Fluidization, AIChE J., Vol. 38(2), pp. 297-301.
- [29] Boie, W.(1957): Vom Brennstoff zum Rauchgas – Feuerungstechnisches Rechnen mit Brennstoffkenngrößen und seine Vereinfachung mit Mitteln der Statistik, Teubner, Leipzig.
- [30] Botterill, J.S.M.(1989): Fluidized Bed Behavior at High Temperature and Pressures, in Transport in Fluidized Particle Systems,L.K. Doraiswamy and A.S. Mujumdar (Ed.), Elsevier, Amsterdam, Netherlands, pp. 33-70.
- [31] Bourgeois, P. and Grenier, P.(1968): Ratio of Terminal Velocity to Minimum Fluidizing Velocity for Spherical Particles, Can. J.Chem. Eng., Vol. 46, pp. 325-328.
- [32] Braun, A.(1997): Mathematische Modellierung der Schadstoffemission bei der Kohleverbrennung in Wirbelschichtfeuerungen, Ph.D.-thesis, RWTH Aachen, Germany.
- [33] Breault, R. W., Mathur, V. K.(1989): High Velocity Fluidized Bed Hydrodynamic Modeling. I. Fundamental Studies of Pressure Drop, Industrial and Engineering Chemistry Research, Vol. 28, p.684.
- [34] Brereton, C. and Stromberg, L.(1986): Circulating Fluidized Bed Technology, P. Basu, ed., p. 133, Pergamon, New York.
- [35] Bridgewater, A.V.(1995): The technical and economic feasibility of biomass gasification for power generation. Fuel Vol. 74(5), pp. 631–653.
- [36] Bridgewater, A. V.(2001): Blackwell Science: London, pp. 977-997.
- [37] Burcat, A., McBride, B.(1997): Ideal gas thermodynamic data for combustion and air pollution use, Technion Israel Institute of Technology, Aerospace Engineering Report, TAE 804. (garfield.chem.elte.hu/Burcat/burcat.html).
- [38] Campbell, E.K. and Davidson, J.F.(1975): The Combustion of Coal in Fluidised Beds, Inst. Fuel Symp. Ser., Vol. 1, pp. A 2.1- A2.9.
- [39] Canada, G.S., McLaughlin, M.H. and Staub F.W.(1976): AIChE Symp. Ser., Vol. 74(176), p27.
- [40] Caram, H.S. and Amundson, N.R.(1979): Ind. Eng. Chem. Process Des. Dev., Vol. 18, pp. 80–96.
- [41] Catipovic, N.M., Jovanovic, G.N. and Fitzgerald, T.J.(1978): AIChE , Vol. 24, pp. 543.
- [42] Chatterjee, P.K., Datta, A.B. and Kundu. K.M.(1995): Can. J. Chem. Eng. 73, pp. 204–210.
- [43] Chase, M.W.Jr., Davies, C.A., Davies, J.R.Jr., Fulrip, D.J., McDonald, R.A., Syverud, A.N.(1985): JANAF thermochemical tables, 3rd edition, Journal of Physical and Chemical Reference Data, 14, Supplement 1.
- [44] Chavarie (1973): Ph.D. thesis, McGill University.
- [45] Chen, T.P., Saxena, S.C.(1978): A Mechanistic Model Applicable to Coal Combustion in Fluidized Beds, AIChE Symp. Ser.,Vol.74, pp. 149-161
- [46] Chen, T.P. and Saxena, S.C.(1977): Mathematical Modeling of Coal Combustion in Fluidized Beds with Sulphur Emission Control by Limestone or Dolomite, Fuel, Vol. 56, pp. 401-413.
- [47] Chitester, D.C., Kornosky, R.M., Fan, L.S. and Danko, J.P.(1984): Characteristics of Fluidization at High Pressure, Chem. Eng.Sci., Vol. 39, pp. 253-261.
- [48] Chaouki, J., Godfroy, L., Pugsley, T.S. and Patience, G.S.(1995): Hydrodynamics of Circulating Fluidized Bed Risers: A Review, Canadian J. Chem. Eng., Vol. 73, pp. 579.

- [49] Clift, R., Grace, J.R. and Weber, M.E.(1978): Bubbles, Drops and Particles, Academic Press, New York.
- [50] Clift, R. and Grace, J.R.(1985): Continuous Bubbling and Slugging, in Fluidization, Second Edition, J.F. Davidson, R. Clift, D.Harrison (Eds.), Academic Press, London, pp. 73-132.
- [51] Colakyan, M. and Levenspiel, O (1984): Elutriation of Fluidized Beds, Powder Technol., Vol. 38, pp. 223-232.
- [52] Corella, J., Aznar, P. M., Herguido, J., González-Saíz, J., Delegado, J., Iglesias, I. J., Alday, J. F., Rodríguez-Trujillo, L. J.(1988): Proceedings of the Euroforum-New Energies Congress, Germany.
- [53] Crescitelli, S., et al.,(1978): Chisa Conf., p.1, Prague.
- [54] Darton R.C., La Nauze R.D., Davidson J.F. and Harrison D.(1977): Bubble growth due to coalescence in fluidized beds ,Trans. Inst. Chem. Eng., Vol. 55 , pp. 274–280.
- [55] Darton, R.C.(1979): A Bubble Growth Theory of Fluidized Bed Reactors, Trans. Inst. Chem. Eng., Vol. 57, pp. 134-138.
- [56] Davidson, J.F. and Harrison, D.(1963): Fluidised Particles, Cambridge University Press, Cambridge, UK.
- [57] Davidson, J.F. and Harrison, D.(1966): Behavior of a Continuously Bubbling Fluidized Bed, Chem. Eng. Sci., Vol. 21, pp. 731-738.
- [58] Davidson, J.F. and Harrison, D.(1971): Fluidization, Academic Press inc London Ltd, UK.
- [59] Davidson, J.F., Harrison, D and Guedes, de Carvalho, J.R.F.(1977): Ann. Rev. Fluid Mech., Vol. 9, pp. 55-86.
- [60] Davidson, J.F. and Schüller, B.O.G.(1960): Bubble-Formation at an Orifice in an Inviscid Liquid, Trans. Instn. Chem. Eng., Vol. 38, pp. 335-342.
- [61] Davies, R.M. and Taylor, G.I.(1950): Proc. Roy. Soc. Ser., Ser A 200, pp. 375-390.
- [62] Deemter, J.J. van,(1980): Fluidization III, J.R. Grace and J.M. Matsen, eds., p. 69, Plenum, New York.
- [63] Doichev, K., Boichev, G.(1977): Investigation of the Aggregative Fluidized Bed Voidage, Powder Technol., Vol. 17, pp. 91-94.
- [64] Drift, A. Van de., Doorn J. Van and Vermeulen, J.W.(2001): Ten residual biomass fuels for circulating fluidised-bed gasification. Biomass and Bioenergy, Vol. 20, pp. 45–56.
- [65] Dryer, F. L. and Glassman, I.(1973): High temperature oxidation of CO and CH₄ , In 'Fourteenth Symposium(International) on Combustion', The Combustion Institute, Pittsburgh, pp. 987-1003.
- [66] Ducarne, E. D., Dolignier J. C., Marty, Eric., Martin, G. and Delfosse, L.(1998): Modelling of gaseous pollutants emissions in circulating fluidized bed combustion of municipal refuse, Fuel, Vol. 77(13) , pp. 1399-1410.
- [67] Durao, D.F.G, Ferrao, P. and Heitor, M.V.(1989): On modelling the burning of a high ash coal in a fluidized bed ,Combust. Sci. and Tech., Vol. 64, pp. 81-95.
- [68] Durao, D.F.G, Ferrao, P., Gulyurtlu, I. and Heitor, M.V.(1990): Combustion kinetics of a high ash coal in fluidized beds, Comb. and Flame , Vol. 79, pp. 162 - 174.
- [69] Dutta, C., Wen, Y. and Belt, R. J.(1987): Ind. Eng. Chem. Proc. Des. Dev., Vol. 19, pp. 345-351.
- [70] Fane, A.G and Wen, C.Y.(1982): Fluidized-Bed Reactors, in Handbook of multiphase Systems, Hetsroni, G. (Ed.), Hemisphere, Washington, pp. 8.105-8.151.
- [71] Farris, M., Paisley, M A, Irving, J, and Overend, R. P.(1998): The biomass gasification process by Battelle/Ferco: Design, Engineering, Construction and start up, http://www.gasification.org/Docs/1998_Papers/gtc9823.pdf
- [72] Field, M.A., Gill, D.W., Morgan, B.B. and Hawksley, P.G.W.(1967): Combustion of pulverized coal ,BCURA, Leatherhead, England.
- [73] Fitzgerald, T., Bushnell, D.B., Crane, S. and Shieh, Y.C.(1983): Testing of Cold Scaled Bed Modeling for Fluidized Bed Combustors, Proc. 7th International Conference on Fluidized Bed Combustion, Vo1.2, p.766.

- [74] Franco, C., Pinto, F., Gulyurtlu I. and Cabrita I.(2003): The study of reactions influencing the biomass steam gasification process, *Fuel*, Vol. 82(7), pp. 835-842.
- [75] Fuller, E.N., Schettler, P.D. and Giddings, C.(1966): A new method for predicting of binary gas-phase diffusion coefficient, *Ind. Engg. Chem.*, Vol. 58(5), pp. 19-28.
- [76] Fusey, I., Lim, C.J. and Grace, J.R.(1986): *Circulating Fluidized Bed Technology*, P. Basu, ed., p. 409, Pergamon, New York.
- [77] Geldart, D.(1967): *Proc. Int. Symp. Fluid.*, p. 171.
- [78] Geldart, D.(1972): Effect of Particle Size and Size Distribution on the Behaviour of Gas-Fluidised Beds, *Powder Tech.*, Vol. 6, pp. 201-215.
- [79] Geldart, D.(1973): Types of Gas Fluidization, *Powder Technol.*, Vol. 7, pp. 285-292.
- [80] Geldart, D. and Abrahamsen, A.R.(1978): Homogeneous Fluidisation of Fine Powders Using Various Gases and Pressures, *Powder Technology*, Vol. 19, p. 133.
- [81] Geldart, D.(1985): Elutriation, in *Fluidization*, Second Edition, J.F. Davidson, R. Clift and D. Harrison (Eds.), Academic Press, London, UK, pp. 383-412.
- [82] Geldart, D.(1986): Single Particles, Fixed and Quiescent Beds, in *Gas Fluidization Technology*, D. Geldart (Ed.), Wiley, Chichester, UK, pp. 11-32.
- [83] Gibbs, B.M.; Beer, J.M. and Pereira, F.J.(1980): A Simplified Model for NO Formation from Fuel-Nitrogen in Fluidised Bed Combustion, *Fluidized Combustion: Systems and Applications*, Symp. Ser., No. 4, pp. V4.1-V4.12.
- [84] Gil, J., Aznar, M.P., Caballero, M.A., Francés, E. and Corella, J. (1997): Biomass gasification in fluidized bed at pilot scale with steam-oxygen mixtures. Product distribution for very different operating conditions, *Energy and Fuels*, Vol. 11, pp.1109-1118.
- [85] Glicksman, L.R.(1984): Scaling Relationships for Fluidized Beds, *Chemical Engineering Science*, Vol 39(9) , pp. 1373-1379.
- [86] Godard, K. and Richardson, J.F.(1968): Distribution of Gas Flow in a Fluidised Bed, *Chem. Eng. Sci.*, Vol. 23, p. 660.
- [87] Goel, S.K., Beer, J.M. and Sarofim, A.F.(1995): Significance of Destruction Reactions in Determining Net Emission of Nitrogen Oxides, 13th Int. Conf. Fluid. Bed Combust., ASME, pp. 887-898.
- [88] Gogolek, P.E.G. and Grace, J.R.(1995): Fundamental Hydrodynamics Related to Pressurized Fluidized Bed Combustion, *Prog. Energy Combust. Sci.*, Vol. 21, pp. 419-455.
- [89] Goodrum, John W. and Eiteman, Mark A.(1996): Physical properties of low molecular weight triglycerides for the development of bio-diesel fuel models, *Bioresource Technology*, Vol. 56(1), pp. 55-60.
- [90] Gordon, S. and McBride, B.(1971): Computer program for calculation of complex chemical equilibrium composition, rocket performance, incident and reflected shocks and Chapman-Jouguet detonations, NASA Report SP-273.
- [91] Grace, J.R. and Harrison, D.(1969): The Behaviour of Freely Bubbling Bed, *Chem. Eng. Sci.*, Vol. 24, pp. 497-508.
- [92] Grace, J.R.(1971): An Evolution of Models for Fluidized Bed Reactors, *AIChE Symp. Ser.*, Vol. 67(116), pp. 159-167.
- [93] Grace, J.R. and Clift, R.(1974): On the two phase theory of fluidization, *Chem. Eng. Sci.*, Vol. 29, pp. 327-334.
- [94] Grace, J.R.(1982): Fluidized Bed Hydrodynamics, in *Handbook of Multiphase Systems*, G. Hetsroni (Ed.), Washington Hemisphere Publishing, Washington.
- [95] Grace, J.R.(1984): Generalized Models for Isothermal Fluidized Bed Reactors, in 'Recent Advances in the Engineering Analysis of Chemically Reacting Systems', Doraiswamy, L.K. (Ed.), Wiley, New Delhi.
- [96] Grace, J.R.(1986a): Modeling and Simulation of Two-Phase Fluidized Bed Reactors, in *Chemical Reactor Design and Technology*, de Lasa H.D. (Ed.), Martinus Nijhoff , pp. 245-289.
- [97] Grace, J.R.(1986b): Fluidized Beds as Chemical Reactors, in *Gas Fluidization Technology*, Geldart, D. (Ed.), John Wiley and Sons, Chichester, New York, Brisbane, Toronto, Singapore.

- [98] Grace, J. R., Avidan, A. A. and Knowlton, T. M.(1997): Circulating Fluidized Beds, Chapman and Hall, New York.
- [99] Gupta, S. K. and Berruti, F.(1000): Evaluation of the gas–solid suspension density in CFB risers with exit effects. Powder Technology, Vol. 108, pp. 21–31.
- [100] Gururajan, V.S., Agarwal, P.K. and Agnew, J.B.(1992): Trans IChemE, Vol. 70, pp. 211–237.
- [101] Haider, M.(1993): Ein stationäres Simulationsmodell für Dampferzeuger mit Zirkulierender Wirbelschichtfeuerung, Ph.D. thesis, Vienna University of Technology, Vienna, Austria.
- [102] Halder, P.K. and Basu, P.(1987): The kinetic rate of combustion of electrode carbon in the temperature range of 1000-1200K, Canadian J.of Chem. Eng., Vol. 71, pp. 3-9.
- [103] Hannes,J., Renz, U. and van der Bleek, C.M.(1995): The IEA model for circulating fluidized bed combustion , 13th Int. Conf. Fluid. Bed Combust., ASME, pp. 287-296.
- [104] Hannes, J. P.(1996): Mathematical modelling of circulating fluidized bed combustion. Ph.D. thesis, Technical University of Delft, Delft, Denmark.
- [105] Harris, B. J. and Davidson, J. F.(1994): Modeling options for circulating fluidized beds: A core/annulus deposition model. In A. A. Avidan(Ed.), Circulating fluidized bed technology IV (pp. 32–39). NewYork: AIChE.
- [106] Hartge, E.U.(1986): Flow Structure in Fast Fluidized Beds, Fluidization V (Ostergaard, Sorensen, eds.) Engineering Foundation, New York, pp. 345-352.
- [107] Hartge, E.U., Li, Y. and Werther, J.(1986): Circulating Fluidized Bed Technology, P. Basu, ed., p. 153, Pergamon, New York.
- [108] Hartleben, B.(1983): Mathematische Modellierung von Blasenbildenden Kohlewirbelschicht-Feuerungsanlagen, Ph.D.-thesis, Siegen University, Germany.
- [109] Hastaoglu, M.A., Berruti, F. and Hassam, M. S.(1988): A generalised Gas/solid reaction model for circulating fluidized beds- an application to wood pyrolysis, In P. Basu, J. F. Large (Eds.), Circulating fluidized bed technology II (pp. 123–128). Oxford, England: Pergamon Press.
- [110] Hiller, R. (1995): Mathematische Modellierung der Kohleverbrennung in einer Circofluid-Wirbelschichtfeuerung, Ph.D.-thesis, Dortmund University, Germany, Verlag Shaker.
- [111] Hilligardt, K. and Werther, J.(1986): Local Bubble Gas Hold-up and Expansion of Gas/Solid Fluidized Beds, Ger. Chem. Eng., Vol. 9, pp. 215-221.
- [112] Hofbauer, H., Stoiber, H., Veronik, G.(1995): Gasification of organic material in a novel fluidization bed system. In: Proceedings of the first SCEJ Symposium on fluidization, Tokyo, pp. 291–299
- [113] Hofbauer, H., Veronik, G., Fleck, T. and Rauch, R.(1997): The FICFB gasification process, In: In: Bridgwater, A.V., Boocock, D., (Hrsg.): Developments in thermochemical biomass conversion, Blackie Academic and Professional, Glasgow, U.K., Vol. 2, pp. 1016-1025.
- [114] Hofbauer, H., (2005): Plenary Lecture,14th European Biomass Conference and Exhibition Biomass for Energy, Industry and Climate Protection, Paris, France, 17-21 October.
- [115] Horio, M., Rengarajan, P., Krishnan, R. and Wen, C.Y.(1977): Fluidized Bed Combustion Modelling, Report prepared for National Aeronautics and Space Administration under contract No. NAS3-19725.
- [116] Horio, M. and Wen, C.Y.(1978): Simulation of Fluidized Bed Combustors: Part I. Combustion Efficiency and Temperature Profile, AIChE Symp. Ser., Vol. 74(176), pp. 101-111.
- [117] Horio, M. et al., (1986): in Circulating Fluidized Bed Technology, P. Basu, ed., p. 255, Pergamon, New York.
- [118] Horio, M., Nonaka, A., Sawa, Y. and Muchi, I.(1986): A new Similarity Rule for Fluidized Bed Scale-up, AIChE Journal, Vo1.32(9), pp. 1466- 1482.
- [119] Horio et al.(1988): in Circulating Fluidized Bed Technology II, P. Basu, ed., p.13, Compiegne.

- [120] Howard, J.B., Williams, G.C. and Fine, D.H.(1974): Kinetics of Carbon monoxide oxidation in post flame gases, 14 Symp.(Int.) on Combust., The combustion Institute, pp. 975-986.
- [121] Huttenhuis, P.J.G, Kuipers, J.A.M. and van Swaaij, W.P.M.(1996): The Effect of Gas-phase Density on Bubble Formation at a Single Orifice in a Two-dimensional Gas-fluidized Bed, Chem. Eng. Sci., Vol. 51(24), pp. 5273-5288.
- [122] Jennen, T., Hiller, R., Koneke, D. and Weinspach, P.M.(1999): Modelling of gasification of wood in a circulating fluidized bed, Proceedings of Circulating Fluidized Bed Technology VI, pp. 431–36.
- [123] Jimenez, L. and Gonzales, F.(1991): Study of the physical and chemical properties of ligno cellulosic residues with a view to the production of fuels, Fuel, Vol. 70, pp. 947–950.
- [124] Johnsson, F., Andersson, S. and Leckner, B.(1991): Expansion of a Freely Bubbling Fluidized Bed, Powder Technol., Vol. 68, pp. 117-123.
- [125] Kaiser, S., Weigl, K., Schuster, G., Tremmel, H., Friedl, A., Hofbauer, H.(1000): 1st World Conference and Exhibition on Biomass for Energy and Industry, Sevilla.
- [126] Kehlenbeck, R., Yates, J., Di Felice, R., Hofbauer, H., Rauch, R. (2001): Novel Scaling Parameter for Circulating Fluidized Beds, AIChE Journal, Vol. 47, pp. 582–589.
- [127] Kehoe, P.W.K. and Davidson, J.F.(1971): Inst. Chem.Eng. Symp. Ser., Vol. 33, p.97.
- [128] Kirschbaum, Miko U. F.(2003): To sink or burn - A discussion of the potential contributions of forests to greenhouse gas balances through storing carbon or providing bio fuels, Biomass and Bioenergy, Vol. 24 (4-5), pp. 297-310.
- [129] Kulasekaran, S., Linjewile, T.M. and Agarwal, P.K.(1999): Mathematical Modelling of Fluidized Bed Combustion 3.Simultaneous Combustion of Char and Combustible Gases, Fuel, Vol. 78(4), pp. 403-417.
- [130] Kunii, D. and Levenspiel, O.(1990): Entrainment of Solids from Fluidized Beds I. Hold-Up of Solids in the Freeboard, II.Operation of Fast Fluidized Beds, Powder Technol., Vol. 61, pp. 193-206.
- [131] Kunii, D. and Levenspiel, O.(1991): Fluidization Engineering, Second Edition, Butterworth-Heinemann, Boston.
- [132] Kunii, D. and Levenspiel, O.(1999): Fluidization Engineering, Wiley, New York, USA.
- [133] Kwauk et al.(1988): Circulating Fluidized Bed Technology, P. Basu, ed. p. 9, Compiegne.
- [134] Large, J.F., Martinie, Y. and Bergougnou, M.A.(1976): Interpretative Model for Entrainment in a Large Gas-Fluidized Bed, J. Powd. Bulk Solids Tech., Vol. 1, pp. 15-21.
- [135] Lei, H. and Horio, M.(1998): A comprehensive pressure balance model of circulating fluidized beds. Journal of Chemical Engineering Japan, Vol. 31(1), pp. 83–94.
- [136] Lewis, W.K., Gilliland, E.R. and Glass, W.(1959): Solid Catalysed Reaction in a Fluidized Bed, AIChE J., Vol. 5, pp. 419-426.
- [137] Lim, K.S., Zhu, J.X., and Grace, J.R.(1995): Hydrodynamics of gas–solid fluidization. International Journal of Multiphase Flow, Vol. 21, pp. 141–193.
- [138] Löffler, G.(2001): A Modelling Study on Fuel-nitrogen Conversion to NO and N₂O Related to Fluidized Bed Combustion., PhD thesis, TU Wien.
- [139] Löffler, G., Kaiser S., Bosch K. and Hofbauer H.(2003): Hydrodynamics of a dual fluidized-bed gasifier—Part I: simulation of a riser with gas injection and diffuser, Chem. Eng. Sci, Vol. 58(18), pp. 4197-4213.
- [140] Louis, J.F., Tung, S.E. and Park, D.(1982): Modelling of Fluidized Bed Combustion of Coal, Vol. 1-7, Massachusetts Institute of Technology. Energy Laboratory, Cambridge, USA.
- [141] Massirilla, L.(1973): AIChE Symp. Ser., Vol. 69(128), p11.
- [142] Mathis, J.F. and Watson, C.C.(1956): Effect of Fluidization on Catalytic Cumene Dealkylation, AIChE J., Vol. 2, pp. 518-524.
- [143] May, W.G.(1959): Fluidized-Bed Reactor Studies, Chem. Eng. Prog., Vol. 55(12), pp. 49-56.

- [144] Merrick, D.(1983): Mathematical models of the thermal decomposition of coal, part 1-6, *Fuel*, Vol. 62(5), pp. 534-570.
- [145] McKendry, P.(2002): Energy production from biomass (part 1): overview of biomass, *Bioresource Technology*, Vol. 83(1), pp. 37-46.
- [146] Monceaux et al.(1986): *Fluidization V*, K. Ostergaard and A. Sorensen, eds., p.337, Engineering Foundation, New York.
- [147] Mori, S and Wen, C.Y.(1975): Estimation of bubble diameter in gaseous fluidized beds, *AIChE J*, Vol. 21, pp. 109–115.
- [148] Namkung, W. and Kim, S. D.(1998): Gas back mixing in a circulating fluidized bed. *Powder Technology*, Vol. 99, pp. 70–78.
- [149] Orcutt, J.C., Davidson, J.F. and Pigford, R.L.(1962): Reaction Time Distribution in Fluidized Catalytic Reactors, *Chem. Eng. Prog. Symp. Ser.*, Vol. 58,(38), pp. 1-15.
- [150] Ouyang, S., Lin, J. and Potter, O. E.(1993): Ozone decomposition in a 0.254 m diameter circulating fluidized bed reactor, *Pow. Tech.*, Vol. 74 (1), pp.73-78.
- [151] Paisley, M. A. , Farris, M. C., Black, J. W., Irving, J. M. and Overend R. P.(2000): Preliminary operating results from the Battelle/FERCO gasification demonstration plant in Burlington, Vermont, USA, 1st World Conference and Exhibition on Biomass for Energy and Industry, Sevilla, pp. 1494 -1497.
- [152] Park, C. K. and Basu, P.(1997). A model for prediction of transient response to the change of fuel feed rate to a circulating fluidized bed boiler furnace. *Chemical Engineering Science*, Vol. 52(20), pp. 3499–3509.
- [153] Pfeifer, C., Rauch, R. and Hofbauer, H.(2004): In-Bed Catalytic Tar Reduction in a Dual Fluidized Bed Biomass Steam Gasifier, *Ind. Eng. Chem. Res.*, Vol. 43, pp. 1634-1640.
- [154] Pillai, K.K.(1981): The influence of coal type on devolatilization and combustion in fluidized bed ,*J. Inst. Energy*, Vol. 54,p.142.
- [155] Prasad, B. V. R. K. and Kuester, J. L.(1988): *Ind. Eng. Chem. Res.*, Vol. 27, p.304.
- [156] Preto, F.D.S.(1986): Studies and Modelling of Atmospheric Fluidized Bed Combustion of Coal, Ph.D.-thesis, Queen's University, Kingston, Canada.
- [157] Price, B.(1998): *Electricity from Biomass*. Financial Times Business Ltd., ISBN 1 84083 0735.
- [158] Proell. T.(2004): *Potenziale der Wirbelschichtdampfvergasung fester Biomasse-Modellierung und Simulation auf Basis der Betriebserfahrungen am Biomassekraftwerk Guessing*, PhD thesis, TU Wien.
- [159] Proell, T., Rauch, R., Aichernig, C. and Hofbauer, H.(2005): Fluidized bed steam gasification of solid biomass – Analysis and optimization of plant operation using process simulation, 18th FBC conference, May 22-25, Toronto, Canada.
- [160] Pugsley, T. S., Berruti, F. and Chakma, A.(1994). Computer simulation of a novel circulating fluidized bed pressure–temperature swing adsorber for recovering carbon dioxide from fuel gases. *Chemical Engineering Science*, Vol. 49, pp. 4465–4481.
- [161] Pugsley, T. S. and Berruti, F.(1995): A core–annulus solids interchange model for circulating fluidized bed and FCC risers. In C. Laguerie and J. F. Large (Eds.), *Fluidization*, VIII (pp.829–837). New York Engineering Foundation.
- [162] Purdy, M.J., Feider, R.M. and Ferrell, J.K.(1984): *Ind. Eng. Chem. Process Des. Dev.* 23, pp. 267–293.
- [163] Pyle, D.L. and Harrison, D.(1967): An Experimental Investigation of the Two-Phase Theory of Fluidization, *Chem. Eng. Sci.*, Vol. 22, pp. 1199-1207.
- [164] Pyle, D.L.(1970): Fluidized Bed Reactors. Review, *Proc. 1st Int. Symp. Chem. React. Eng.*, Washington, D.C., pp. 106-130.
- [165] Pyne (2006): <http://www.pyne.co.uk>
- [166] Quaak, P., Knoef, H. and Stassen, H.(1999): *Energy from biomass*. World Bank technical paper no. 422. Energy series.
- [167] Rabitz, H., Kramer, M. and Dacol, D.(1983): Sensitivity Analysis in Chemical Kinetics, *Ann. Rev. Phys. Chem.*, Vol. 34, pp. 419-461.
- [168] Reed, T. B.(1981): *Biomass gasification*, Noyes Data Corporation, New Jersey.

- [169] Reid, R. C., Praussnitz, J. M. and Poling, B. E.(1986): The properties of gases and liquids, fourth Ed., McGraw-Hill Book Company, p11.10.
- [170] Reman, G.H.(1955): Chem. Ind. London, Vol. 1, p.46.
- [171] Rhodes, M.J. and Geldart, D.(1987): Powder Technol., Vol. 53, p.155.
- [172] Rhodes, M. J.(1990): Modelling the flow structure of upward-flowing gas–solid suspensions. Powder Technology, Vol. 60, pp. 27–38.
- [173] Rhodes, M., Zhou, S. and Benkreira, H.(1992): Similar profiles of solids flux in circulating fluidized-bed risers. Chemical Engineering Science, Vol. 47, pp. 1635–1643.
- [174] Roider, J.(2002): Kinetic modelling of biomass gasification with steam in a fluidized bed, Diplomarbeit, TU Wien.
- [175] Richardson, J.F.(1971): Incipient Fluidization and Particulate Systems, in Fluidization, J.F. Davidson and D. Harrison (Eds.), Academic Press, New York, pp. 26-64.
- [176] Rowe, P.N.(1963): A Theoretical Study of a Batch Reaction in a Gas-Fluidised Bed, in Fluidization, Soc. Chem. Ind. London, Vol. 42, pp. 15-31.
- [177] Rowe, P.N.(1972): Fluidised Bed Reactors, Proc. 2nd Int. Conf. Reaction Eng., Amsterdam, Netherlands, A9.1-A9.14.
- [178] Rowe, P.N.(1976): Prediction of bubble size in a gas fluidised bed, Chem. Eng. Sci., Vol. 31(4) , pp. 285–288.
- [179] Sadaka Samy S., Ghaly A. E. and Sabbah M. A.(2002): Two phase biomass air-steam gasification model for fluidized bed reactors: Part I—model development , Biomass and Bioenergy, Vol. 22(6), pp. 439-462.
- [180] Saxena, S.C. and Vogel, G.J.(1977): The Measurement of Incipient Fluidization Velocities in a Bed of Coarse Dolomite at Elevated Temperature and Pressure, Trans. Instn. Chem. Eng., Vol. 55, pp. 184-189.
- [181] Schnitzlein, M.G.(1987): Ph.D. dissertation, City University of New York.
- [182] Schuster G., Löffler G., Weigl K. and Hofbauer H.(2001): Biomass steam gasification – an extensive parametric modeling study ,Bioresource Technology, Vol. 77(1), pp. 71-79.
- [183] Shen, C.Y. and Johnstone, H.F.(1955): Gas-Solid Contact in Fluidized Beds, AIChE J., Vol. 1, pp. 349-354.
- [184] Sit, S.P. and Grace, J.R.(1978): Interphase Mass Transfer in an Aggregative Fluidized Bed, Chem. Eng. Sci, Vol. 33, pp. 1115-1122.
- [185] Smith, I.W.(1982): The combustion rates of coal chars: A review,19th symp.(int.) on combustion, The combustion institute , pp. 1045-1065.
- [186] Staub F. W., Canada G. S.(1978): Fluidization (J. F. Davidson and D. L. Keairns, Eds), Cambridge University Press, Cambridge, p.339.
- [187] Stewart, P.S.B. and Davidson, J.F.(1967): Slug Flow in Fluidised Beds, Powder Technol., Vol. 1, pp. 61-80.
- [188] Sriramulu, S., Sane, S., Agarwal, P. and Mathews, Tarek.(1996): Mathematical modelling of fluidized bed combustion: 1. Combustion of carbon in bubbling beds, Fuel, Vol. 75(12) ,pp. 1351-1480.
- [189] Takeuchi et al.(1986): In Proc. 3rd World Cong. Chem. Eng., p.477, Tokyo.
- [190] Talukdar, J., Basu, P. and Joos, E.(1993): Sensitivity Analysis of a Performance Predictive Model of Circulating Fluidized Bed Boiler Furnace, 4th Int. Conf. on Circ. Fluid. Beds, Somerset, PA, USA, pp. 541-546.
- [191] Talukdar, J. and Basu, P.(1995): Modelling of nitric oxide emission from a circulating fluidized bed combustor. In C. Laguerie and J. F. Large (Eds.), Fluidization VIII (pp. 829–837). New York: Engineering Foundation.
- [192] Talukdar, J.(1996): Coal combustion in a circulating fluidized bed. Ph.D. thesis, Technical University of Nova Scotia, Canada.
- [193] Talukdar, J. and Basu, P.(1997): The effect of fuel parameters on the performance of a circulating fluidized bed boiler. In M. Kwauk and J. Li(Eds.), Circulating fluidized bed technology (pp. 307–332). Beijing: Science Press.
- [194] The Chemical Rubber Co. (Ed.)(1977): CRC handbook of chemistry and physics, 58th Ed., CRC Press, Boca Raton/Florida.

- [195] Thiel, W.J. and Potter, O.E.(1977): Ind. Eng. Chem. Fundamentals, Vol. 16, p.242.
- [196] Thonglimp, V.(1981): Ph.D. Thesis, Institut National Polytechnique, Toulouse.
- [197] Todd, B. and Young, J. B.(2002): Thermodynamic and transport properties of gases for use in solid oxide fuel cell modelling, Journal of Power Sources , Vol. 110(1), pp. 186-200.
- [198] Toomey, R.D. and Johnstone, H.F.(1952): Gaseous Fluidization of Solid Particles, Chem. Eng. Prog., Vol. 48, pp. 220-226.
- [199] van Deemter, J.J.(1961): Mixing and Contacting in Gas-solid Fluidized Beds, Chem. Eng. Sci., Vol. 13, pp. 143-154.
- [200] van Deemter, J.J.(1967): In Fluidization, A.A.H. Drinkenburg (Ed.), Netherlands University Press, Amsterdam, Netherlands, pp. 334-347.
- [201] Van den Bleek, C.M.; Brem, G.; Grubor, B.; Johnsson, J.E.; Jones, R.F.; Langer, V.; Verwey, N. (1990): Documentation of the IEA-AFBC model, Version 1.1, G. Brem, (Ed.), TNO Apeldoorn, The Netherlands.
- [202] Van der Vaart D.R.(1985): PhD Thesis, University of Cambridge, England.
- [203] Van Swaaij, W.P-M.(1978): The Design of Gas-solids Fluid Bed and Related reactors, ACS Symp. Ser., Vol. 72, pp. 193-222.
- [204] van Swaaij, W.P.M.(1985): Chemical Reactors, in Fluidization 2nd Edition, J.F. Davidson, R. Clift and D. Harrison (Eds.), Academic Press, London, UK, pp. 595-629.
- [205] Van Swaaij, W.P.M., van den Aarsen, F.G., Bridgewater, A.V. and Heesink, A.B.M.(1994): A review of biomass gasification. Report to the Commission of the European Communities, DG XII.
- [206] VDI-GVC (Ed.) – VDI (1997): Wärmeatlas: Berechnungsblätter für den Wärmeübergang, Springer, Heidelberg.
- [207] Vilienskii, J. and Hezmalian, M.L.(1978): Energia, Vol. 11, pp. 246.
- [208] Walsh, P.M., Mayo, J.E. and Beer, J.M.(1984): Refluxing Particles in the Freeboard of a Fluidized Bed, AIChE Symp. Ser., Vol. 80(234), pp. 119-128.
- [209] Wartha, C.(1998): An experimental study on fuel nitrogen conversion to NO and N₂O and on carbon conversion under fluidized bed conditions, PhD thesis, TU Wien.
- [210] Weimer, A. and Clough, D.(1981): Modelling a low pressure steam oxygen fluidized bed coal gasifying reactor, Chem. Eng. Sci., Vol. 36(3), pp. 548-567.
- [211] Wein, J. W.(1992): Das Expansionsverhalten von Gas/Feststoff: Wirbelschichten bei höheren Geschwindigkeiten. Ph.D. thesis, TU Hamburg-Harburg, Germany.
- [212] Weinstein et al.(1986): Fluidization V, K. Ostergaard and A. Sorensen, eds., p. 329, Engineering Foundation, New York.
- [213] Wells, J.W., Culvers, M.H. and Krishnan, R.P.(1981): TVA Atmospheric Fluidized Bed Combustor Simulation, Oak Ridge National Laboratory, Tennessee, USA.
- [214] Wen, C.Y. and Chen, L.H.(1982): Fluidized Bed Freeboard Phenomena: Entrainment and Elutriation, AIChE J., Vol. 28(1), pp. 117-128.
- [215] Werther, J.(1978): Influence of the Distributor Design on Bubble Characteristics, in Fluidization, Davidson and Keairns (Eds.), Cambridge University Press, Cambridge, UK, pp. 7-12.
- [216] Werther, J.(1980a): Mathematical Modelling of Fluidized Bed Reactors, Int. Chem. Eng., Vol. 20, pp. 529-541.
- [217] Werther, J.(1980b): Modelling and Scale-Up of Industrial Fluidized Bed Reactors, Chem. Eng. Sci., Vol. 35, pp. 372-379.
- [218] Wilke, C.R.(1950): J. Chem. Phys., Vol. 18, pp. 517.
- [219] Winter, F.(1995): Single fuel particle and NO_x/N₂O emission characteristics under (circulating) fluidized bed combustor condition, PhD thesis, TU Wien.
- [220] Winter, F., Wartha, C. and Hofbauer, H.(1995): Characterization and emission of single fuel particles under FBC condition, 3rd Int. Conf. on Combustion Technologies for a Clean Environment , July 3-6, Lisbon, Portugal.
- [221] Wisecarver, K.D., Kitano, K. and Fan, L.S.(1986): Circulating Fluidized Bed Technology, P. Basu, ed., p.145, Pergamon, New York.
- [222] Yan, Hong-ming., Heidenreich, C. and Zhang, D.(1998): Mathematical modelling of a bubbling fluidised-bed coal gasifier and the significance of 'net flow' , Fuel, Vol.

77(9/10), pp. 1067-079.

- [223] Yang, W.C.(1998): 30 Years of Industrial Research on Fluidization – Bridging the Gap between Theory and Practice, Fluidization IX, L.-S. Fan and T.M. Knowlton (Eds.), Engineering Foundation, New York, pp. 31-43.
- [224] Yates, J.G.(1975): Fluidised Bed Reactors, Chem. Engineer, pp. 671-677.
- [225] Yates, J.G.(1983): Fundamentals of Fluidized-Bed Chemical Processes, Butterworths, London, UK.
- [226] Yerushalmi, J. et al. (1976): paper delivered at AIChE annual meeting.
- [227] Yerushalmi, J. and Cankurt, N.T.(1979): Further Studies of the Regimes of Fluidization, Powder Technol., Vol. 24, pp. 187- 205.
- [228] Yin, X., Xu, B.Y., Wu C. and Luo, Z.(1996): Mathematic model study on circulating fluidized bed gasifier for biomass., Acta Energiæ Solaris Sinica, Vol. 17, pp. 1–8.
- [229] Zenz, F.A. and Weil, N.A.(1958): A Theoretical-Empirical Approach to the Mechanism of Particle Entrainment from Fluidized Beds, AIChE J., Vol 4, pp. 472-479.
- [230] Zenz, F.A. and Othmer, D.F.(1960): Fluidization and Fluid-Particle Systems, Reinhold, New York.
- [231] Zhang, R., Chen, D. and Yang, G.(1985): Fluidization, Science and Technology, M. Kwauk et al., eds., p.148, Science Press, Beijing.
- [232] Zhang, M., Jin, B. and Fan, C.(1987): A Mathematical model for Coal Combustion in Pressurized Fluidized Beds, 9th Int. Conf. on Fluidized Bed Combustion, ASME, New York, USA, pp. 730-737.
- [233] Zimont, V.L. and Trushin, Y.M.(1969): Total combustion kinetics of hydrocarbon fuels. Combust, Explosion Shockwaves, Vol. 5 (4), pp. 567–573.

SYMBOLS AND ABBREVIATIONS

A	Area (cross-sectiona area)	$[m^2]$
A_a	Area of annulus	$[m^2]$
Ar	Archimedes number, $Ar = \frac{d_p^3 \rho_g (\rho_p - \rho_g) g}{\mu^2}$	$[-]$
a	Interphase surface area per unit bed volume	$[m^{-1}]$
a	Decay constant of solids load in the freeboard (Eq.6.20)	$[m^{-1}]$
$a_1, \dots a_7$	Burcat coefficient for thermodynamic calculation.	
C	Concentration	$[mol / m^3]$
C_1	Coefficient (Eq. 2.4)	$[-]$
C_2	Coefficient (Eq. 2.4)	$[-]$
$C_{A,B}$	Concentration of component A in bubble	$[mol / m^3]$
$C_{A,E}$	Concentration of component A in Emulsion	$[mol / m^3]$
C_c	Partial pressure of oxygen in core	$[bar]$
C_{CO_2}	Partial pressure of carbondioxide at char surface	$[bar]$
C_g	Partial pressure of oxygen in bulk gas	$[bar]$
C_{H_2O}	Partial pressure of steam at char surface	$[bar]$
C_p	Heat capacity	$[J / mol K]$
$C_{p,i}$	Heat capacity of component 'i'	$[J / mol K]$
C_s	Partial pressure of oxygen at char surface	$[bar]$
C_w	Coefficient	$[-]$
c_p	Heat capacity	$[J / kg K]$
CO_{ppm}	Concentration of CO in ppm	$[ppm]$
D	Diameter of Column	$[m]$
D	Molecular diffusivity	$[m^2 / s]$
$D_{A,B}$	Diffusivity of component A in component B	$[m^2 / s]$
D_{eff}	Effective diffusivity of reactant	$[m^2 / s]$
D_g	Molecular diffusivity of oxygen	$[m^2 / s]$
d	Diameter	$[m]$
d_a	Diameter of annulus	$[m]$
d_B	Bubble diameter (equivalent diameter of a sphere)	$[m]$
$d_{B,0}$	Initial bubble diameter	$[m]$
$d_{B,max}$	Maximum bubble diameter	$[m]$
d_c	Diameter of core	$[m]$
d_{char}	Mean diameter of char	$[m]$

d_p^*	dimensionless particle diameter	[-]
E_a	Activation energy	[J/mol]
E_{ap}	Apparent activation energy for char combustion	[J/mol]
\dot{E}_{in}	Energy	[J/s]
FC	Fixed carbon	[wt/wt]
ΔG^0	Standard state Gibbs Free energy	[J/mol]
ΔG_j^0	Standard state Gibbs Free energy for reaction 'j'	[J/mol]
g	Gravity	[m / s^2]
H	Height	[m]
$H(P, T)$	Enthalpy at pressure P and temperature T	[J/mole]
$\Delta H_{f,298}^0$	Enthalpy of formation at 298.15 K	[J/mole]
$H_{gas}(T)$	Enthalpy of the gas stream(mixture) at temperature T	[J/mole]
$H_i(T)$	Enthalpy of the species 'i' at temperature T	[J/mole]
$H_i^0(T)$	Standard state enthalpy of component 'i'	[J/mol]
$H_{ij}(P_i, T_i)$	Enthalpy of component 'j' at the inlet condition 'i'	[J/mole]
$H_{inorganic}(T)$	Enthalpy of the inorganic mixture (bed material) at temperature T	[J/mole]
ΔH_j^0	Standard state change in enthalpy for reaction 'j'	[J/mol]
$H_{oj}(P_o, T_o)$	Enthalpy of component 'j' at the exit condition 'o'	[J/mole]
$\Delta H_{T_o}^T$	Change in enthalpy due to change in temperature from T_o to T	[J/mole]
$\Delta H_{P_o}^P$	Change in enthalpy due to change in pressure from P_o to P	[J/mole]
H_U	Lower heating value	[J/mole]
$H_{U,gas}$	Lower heating value of gas mixture	[J/mole]
HHV	Higher heating value	[J/kg]
$h(P, T)$	Enthalpy at pressure P and temperature T	[J/kg]
$\Delta h_{f,298}^0$	Enthalpy of formation at 298.15 K	[J/kg]
$h_{inorganic}(T)$	Enthalpy of the inorganic mixture (bed material) at temperature T	[J/kg]
h_m	Mass transfer coefficient	[$kg / m^2 s bar$]
$\Delta h_{v,298}$	Latent heat of vaporization	[J/kg]
j	Reaction	
K	Constant	[s^{-1}]
K	Constant in Eq. 6.20	[$m^{1.6} s^2$]
$K_{B,E}$	Mass transfer coefficient between bubble and emulsion (Eq.6.14)	[s^{-1}]
$k_{B,E}$	Mass transfer coefficient between bubble and emulsion (Eq.6.16)	[m / s]
K'_{eqm}	Thermodynamic equilibrium constant of reaction j	[-]
$K_{j\infty}$	Elutriation rate constant	[$kg / m^2 s$]

k	Cell number	[-]
k	Reaction rate constant	[dependent]
k_0	Frequency factor in the reaction rate constant	[dependent]
$k_{char,c}$	Reaction rate constant of carbon based on core surface	[$kg / m^2 s bar^n$]
$k_{char,p}$	Reaction rate constant of carbon based on particle volume	[$kg / m^3 s bar^n$]
$k_{char,s}$	Reaction rate constant of carbon based on external surface	[$kg / m^2 s bar^n$]
k_{back}	Backward rate of reaction	[dependent]
K_{eqm}	Equilibrium rate of reaction	[]
k_{for}	Forward rate of reaction	[dependent]
LHV	Lower heating value	[J / kg]
M	Molecular weight	[kg/mol]
M_A	Molecular weight of A	[kg/mol]
M_c	Molecular weight of carbon	[kg/mol]
M_{gas}	Molecular weight of gas mixture	[kg/mol]
m	Mass	[kg]
\dot{m}	Mass flow rate	[kg/s]
m_{bed}	Mass hold up of bed material in the zone	[kg]
$\dot{m}_{bed,in}$	Mass of bed material entering the zone	[kg/s]
$\dot{m}_{bed,out}$	Mass of bed material exiting the zone	[kg/s]
$m_{bed,k}$	Mass hold up of bed material in the cell	[kg]
m_{char}	Mass hold up of char in the zone	[kg]
$\dot{m}_{char,in}$	Mass of char entering the zone	[kg/s]
$\dot{m}_{char,out}$	Mass of char exiting the zone	[kg/s]
$m_{char,k}$	Mass hold up of char in the cell	[kg]
$\dot{m}_{char,k}$	Mass of char reacted in cell k	[kg/s]
$\dot{m}_{char,react}$	Mass of char reacted in the zone	[kg/s]
m_{gas}	Mass of gas mixture	[kg]
N	Number	[-]
N	Amount of substance	[mol]
$N_{A,B}$	Amount of component A in bubble	[mol]
N_{or}	Number of orifice	[-]
n	Amount	[mol]
n	Order of reaction	[-]
\dot{n}	Mole flow rate	[mol / s]
\dot{n}_{ij}	Amount of component 'j' at inlet 'i'	[mole/s]

\dot{n}_{oj}	Amount of component 'j' at exit 'o'	[mole/s]
P	Pressure	[Pa]
ΔP	Pressure drop	[Pa]
P_i	Inlet Pressure	[Pa]
P_o	Exit pressure	[Pa]
Q	Volumetric flow rate	[m^3 / s]
Q	Energy input	[J/s]
Q	Combustion rate of carbon	[kg_{carbon} / s]
Q_a	Volumetric flow rate in annulus	[m^3 / s]
Q_B	Volumetric flow rate in bubble	[m^3 / s]
Q_c	Volumetric flow rate in core	[m^3 / s]
Q_E	Volumetric flow rate in emulsion	[m^3 / s]
q	Specific combustion rate of carbon on external surface	[$kg_{carbon} / m^2 s$]
q_{dry}	Specific dry gasification rate of carbon on external surface	[$kg_{carbon} / m^2 s$]
$q_{H,net}$	Net hydrogen released from the char external surface	[$kg_{Hydrogen} / m^2 s$]
q_{net}	Net specific reaction rate of carbon on external surface	[$kg_{carbon} / m^2 s$]
$q_{O,net}$	Net oxygen released from the char external surface	[$kg_{Oxygen} / m^2 s$]
q_{st}	Specific steam gasification rate of carbon on external surface	[$kg_{carbon} / m^2 s$]
R	Universal gas constant	[J/mol K]
Re	Renolds number, $(Re) = \frac{U d_p \rho_g}{\mu_g}$	[-]
Re_{mf}	Renolds Number based on minimum fluidization velocity	[-]
Re_t	Renolds Number based on terminal velocity	[-]
r	Radius	[m]
r_B	Radius of bubble	[m]
r_i	Rate of reaction for component 'i'	[$mol / m^3 s$]
S	Surface area	[m^2]
$S_{B,E}$	Surface area of bubble in contact with emulsion	[m^2]
S_i^0	Standard state entropy of component 'i'	[J/mol K]
ΔS_j^0	Standard state change in entropy for reaction 'j'	[J/mol K]
Sh	Sherwood Number	[-]
T	Temperature	[K]
T_i	Temperature at inlet	[K]
T_o	Temperature at Exit	[K]
t	Time	[s]

U	Velocity (superficial velocity)	[m/s]
U^*	dimensionless velocity	[-]
U_o	Superficial velocity	[m/s]
U_B	Bubble velocity	[m/s]
$U_{B\infty}$	Velocity of a single isolated bubble	[m/s]
U_c	Superficial gas velocity corresponding to the maximum pressure fluctuation amplitude	[m/s]
U_E	Emulsion velocity	[m/s]
U_k	Superficial gas velocity corresponding to levelling out of pressure fluctuation amplitude	[m/s]
U_{mb}	Minimum bubbling velocity	[m/s]
U_{mf}	Minimum fluidization velocity	[m/s]
U_{ms}	Minimum slugging velocity	[m/s]
U_t	Terminal velocity	
U_{tr}	Transport velocity	
V	Volume	[m ³]
V_B	Volume of bubble	[m ³]
V_{gas}	Volume of gas	[m ³]
VM	Volatile matter	[wt / wt]
W	Rate of work done	[J/s]
w	Weight fraction	[wt / wt]
x	Distance	[m]
x_1, \dots, x_n	Variable	[-]
Y	Correction factor for modified two phase theory	[-]
y	Mole fraction	[-]
z	Height	[m]
z_0	Reference height	[m]

Greek Letter

α	Ratio of carbon to bed hold up	[-]
β	Stoichiometric coefficient (char combustion)	[-]
δ	Fraction	[-]
δ_B	Bubble volume fraction	[-]
ε	Porosity	[-]
$\bar{\varepsilon}$	Mean porosity	
ε_0	Porosity at reference height z_0	[-]

ε_a	Porosity in annulus	[-]
ε_c	Porosity in core	[-]
ε_{mf}	Porosity at minimum fluidization condition	[-]
ε_z	Average porosity at height z	[-]
ε_∞	Porosity above TDH	[-]
ϕ	Mechanism factor for primary surface product (1 for CO_2 , 2 for CO)	[-]
ϕ_{ij}	Viscosity coefficient (Eq.5.7)	[-]
φ	Sphericity	[-]
λ	Air ratio	[-]
μ	Viscosity	[Pas]
μ_m	Viscosity of mixture	[Pas]
ρ	Density	[kg / m^3]
ρ_g	Density of gas	[kg / m^3]
ρ_p	Density of particle	[kg / m^3]
σ	Tolerance limit	[-]
σ^{rel}	Relative system response	[-]
ν	Atomic diffusion volume	[-]
ν_{ij}	Stoichiometric coefficient of species 'i' in reaction 'j'	[-]
ω	Amount of a substance	[mole]
ξ	Parameter	[-]
ξ	Stoichiometric coefficient of element	[-]
∞	Single isolated	[-]
∞	Above Transport Disengaging height	[-]
χ	Linear sensitivity coefficient	[-]
χ^{rel}	Relative sensitivity coefficient	[-]

Indices

A	species
a	Annulus
accu	Accumulation
B	specie
B	Bubble
bed	Bed Material

c	Core
c	Carbon in char
dry	Dry gasification (with CO_2)
E	Emulsion
eq	Equivalent
Ex	Exchange (mass)
g	Gas
H	Hydrogen in char
i	specie
in	Entering the system boundary
j	specie
k	Cell
m	mean
max	Maximum
mb	Minimum bubbling
mf	Minimum fluidization
ms	Minimum slugging
N	Number of cells
O	Oxygen in char
or	Orifice
out	Exiting the system boundary
out	Output
p	Particle
pr	Producer gas
pro	Produced
react	Amount reacted
st	Steam gasification
t	terminal
tar	Prescribed target value

Curriculum Vitae

Name : Priyanka Kaushal

DOB : 11.06.1978

Email : pkaushal@mail.zserv.tuwien.ac.at

Present Occupation

- Project assistant in zero emission energy technology group in Institute of Chemical Engineering, TU Wien

Working on “Modelling of the fast fluidized combustion reactor of the dual fluidized bed biomass gasification system

Educational Qualifications

- **Master of Engineering (M.E) in Chemical Engineering** from Punjab University, Chandigarh, India in 2003.
- **Bachelor of Engineering (B.E) in Chemical Engineering** from SLIET Punjab, India in 2001.

Research Project

- Vapour Liquid Equilibrium (VLE) model for binary solution of 2-Nitropropane and P-Xylene and for binary solution of 2-Nitropropane and Cumene.
- Molecular modelling of the decomposition of solid crystalline Gas hydrate (methane).
- To develop a flow improver (Plasticizer) for high crude.
- Computer aided design of Sieve Tray CO₂ Absorption Column.

Industrial Training Projects

- **Molecular modelling of the decomposition of Gas hydrate on MOLDY software.**
- **Optimization of process parameters for the up-gradation of gasoline** on computer controlled (PLC based) Pilot Plant (Xytel USA made) having **Fixed Bed Reactor** system.

Skills in Computers

- Proficient in C and C++ programming languages
- Adapted to ASPEN, MOLDY and CAD software

(Priyanka Kaushal)